Aus dem Zentralinstitut für Seelische Gesundheit
der Medizinischen Fakultät Mannheim
(Direktor: Prof. Dr. med. Andreas Meyer-Lindenberg)

Multi-Omics Analysis of Alcohol Use Disorder in Postmortem Human Brain Tissue

Inauguraldissertation
zur Erlangung des Doctor scientiarum humanarum (Dr. sc. hum.)
der
Medizinischen Fakultät Mannheim
der Ruprecht-Karls-Universität
zu
Heidelberg

vorgelegt von
Lea Sigrid Silke Zillich

aus
Heidelberg
2022

Dekan: Prof. Dr. med. Sergij Goerdt
Referentin: Priv.-Doz. Dr. Stephanie Witt

TABLE OF CONTENTS

Page

ABBREVIATIONS

ACC	Anterior Cingulate Cortex
AUD	Alcohol Use Disorder
AUDIT	Alcohol Use Disorder Identification Test
BA9	Brodmann Area 9
CHR	Chromosome
CN	Caudate nucleus
CpG	Dytosine-phosphate-guanine
CUD	Cocaine Use Disorder
DMR	Differentially methylated regions
DNAm	DNA methylation
DE	Differentially expressed
DSM	Diagnostic and Statistical Manual of Mental Disorders
eQTL	Expression quantitative trait loci
EWAS	Epigenome-wide association study
GWAS	Genome-wide association study
Kb	Kilobases
mQTL	Methylation quantitative trait loci
NAcc	Nucleus accumbens
PAU	Problematic alcohol use
PUT	Putamen
PMI	Postmortem Interval
RIN	RNA Integrity Number
snRNA-seq	single-nuclei RNA sequencing
VS	Ventral Striatum
WGCNA	Weighted Gene Correlation Network Analysis

PREAMBLE

This is a cumulative thesis consisting of two studies I was the first author on. The first *Epigenome-wide Association Study of Alcohol Use Disorder in Five Brain Regions* was published in Neuropsychopharmacology and is presented in chapter 2 of this thesis. The second study *Multi-omics Signatures of Alcohol Use Disorder in the Dorsal and Ventral Striatum* was published in Translational Psychiatry and can be found in chapter 3. I was involved in the conception of both studies. I performed the literature research, developed the analysis plan and performed all bioinformatic analyses independently and under the supervision of the co-authors. I wrote both manuscripts and revised them according to the co-authors and the reviewer's input.

Zillich, L., Frank, J., Streit, F., Friske, M. M., Foo, J. C., Sirignano, L., Heilmann-Heimbach, S., Dukal, H., Degenhardt, F., Hoffmann, P., Hansson, A. C., Nöthen, M. M., Rietschel, M., Spanagel, R., & Witt, S. H. (2022). Epigenome-wide association study of alcohol use disorder in five brain regions. Neuropsychopharmacology, 47(4), 832-839. https://doi.org/10.1038/s41386-021-01228-7

Zillich, L., Poisel, E., Frank, J., Foo, J. C., Friske, M. M., Streit, F., Sirignano, L., Heilmann-Heimbach, S., Heimbach, A., Hoffmann, P., Degenhardt, F., Hansson, A. C., Bakalkin, G., Nöthen, M. M., Rietschel, M., Spanagel, R., & Witt, S. H. (2022). Multi-omics signatures of alcohol use disorder in the dorsal and ventral striatum. Translational Psychiatry, 12(1), 190. https://doi.org/10.1038/s41398-022-01959-1

1 INTRODUCTION

1.1 Alcohol Use Disorder, Alcohol Dependence, and Alcohol Consumption

1.1.1 Defining the Constructs

Alcohol Use Disorder (AUD) is defined in the Diagnostic and Statistical Manual of Mental Disorders (DSM) 5 by a set of co-occurring symptoms, such as loss of control over alcohol intake, craving, development of tolerance, and withdrawal symptoms when alcohol consumption ceases (American Psychiatric Association, 2013).
In the history of the DSM, the diagnostic criteria and name of AUD have been changed repeatedly, reflecting both the heterogeneity as well as the societal view on of the disorder. In the DSM-5, AUD is a dimensional construct and can be mild, moderate, or severe, depending on the number of symptoms an affected person experiences. In the previous version, the DSM-IV, one of two categorical diagnoses, alcohol abuse and alcohol dependence, were given. Alcohol abuse is characterized by symptoms such as continued consumption despite negative social consequences or an increased likelihood of getting hurt when drinking. In alcohol dependence, additional symptoms such as withdrawal and tolerance are observed (American Psychiatric Association, 1994). Both diagnostic manuals observe symptoms over in a 12-month period.
Alcohol consumption is a continuous construct and is most commonly assessed by the first three items of the alcohol use disorder identification test (AUDIT), the so-called consumption scale (AUDIT-C) (Babor et al., 2001). It consists of questions regarding the frequency of alcohol consumption, the amount of alcohol consumed at a drinking event, and the frequency of binge drinking. The remaining AUDIT items form the problem scale (AUDIT-P) and inquire about problematic consequences that arrive from drinking. The problem scale is often used as a proxy for AUD. Another commonly used measure is drinks per week, which is the number of standard drinks individuals consume in a typical week.

1.1.2 Prevalence and Relevance to Global Health

The lifetime prevalence of AUD varies worldwide. The lowest prevalence is observed in North African and Middle Eastern countries (0.59%) and the highest in Eastern European countries (4.25%). This also corresponds to the prevalence of alcohol consumption in different regions of the world, which differ due to varying religious, cultural, and policy aspects (World Health Organization, 2019). Globally, AUD has a lifetime prevalence of 1.32% (Degenhardt et al., 2018). AUD contributes significantly to the global burden of disease with 5.3% of all deaths and more than 230 diseases being attributable to harmful alcohol consumption (World Health Organization, 2019). Although many individuals are affected by AUD, the current FDA-approved treatment options are limited. Currently, there are only a few medications available for the treatment of AUD. In the US, naltrexone and acamprosate can be prescribed to treat AUD, and both medications have been shown to reduce the number of drinking days

in the first few months after treatment, compared to a placebo (Donoghue et al., 2015). At the same time, not all patients benefit from these treatments, and relapse rates remain high. To offer the best possible care to patients with AUD, it is necessary to gain a deeper understanding of pathomechanisms to facilitate personalized medicine as a novel treatment option for AUD in the future (Litten et al., 2016).

1.2 Neurocircuitry of Addiction

This section presents the neurobiological perspective on the mechanisms underlying AUD. While alcohol consumption has toxic effects on the entire organism, dependence or use disorders are thought to develop in the brain (Volkow et al., 2016). The current understanding of the development of substance use disorders and AUD in particular relies on a neurocircuitry of addiction that is associated with three stages of addiction. These stages and the corresponding circuits are depicted in Figure 1.1.
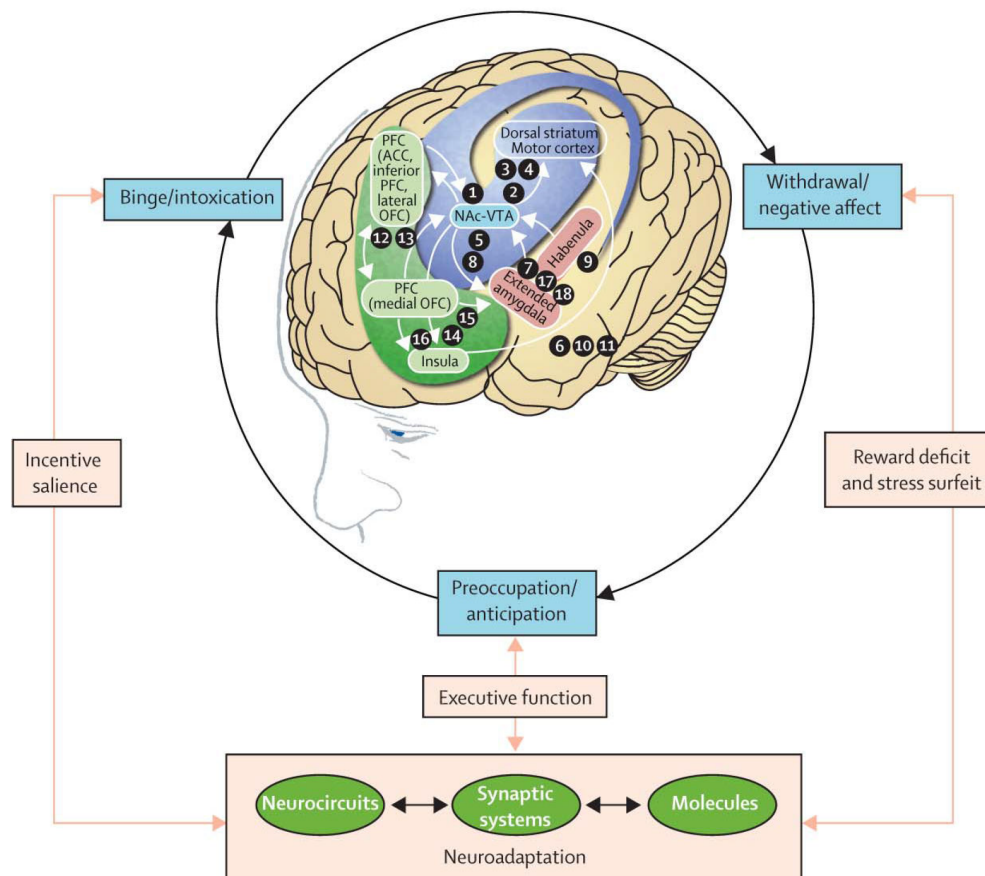

Figure 1.1. The three stages of addiction and the associated neurocircuitry, published in Koob and Volkow (2010), The Lancet Psychiatry (3) 8, 760-773, reprinted with permission from Elsevier.

1.2.1 The Three Stages of Addiction

The neurocircuitry of addiction describes signaling pathways within functionally connected brain regions that are thought to be involved in the development and maintenance of substance use disorders. According to Koob and Volkow (2010), there are three stages of addiction. The binge/intoxication stage is mainly characterized by the rewarding effects of substances, which are associated with an increase of dopamine in the mesolimbic dopamine system, in particular in the ventral tegmental area. The time course of dopamine signaling is thought to be especially important for how a reward is perceived and has an important impact on behavior (Schultz, 2007). In the second stage, the negative effect/withdrawal stage, reward thresholds are elevated, which might be due to dopamine systems being compromised from extended drug intake (Koob & Volkow, 2010). The preoccupation/anticipation stage is closely related to relapsing behavior and is characterized by an altered response to drug-associated stimuli, e.g. cue reactivity.

The three stages of addiction are associated with five major circuits: the mesolimbic dopamine system, the extended amygdala, the ventral striatum, the ventral striatum/dorsal striatum/hippocampus, and the dorsolateral frontal cortex. The latter three are further discussed in this thesis. The brain regions that play a major role in these circuits are depicted in Figure 1.1.

1.2.2 The Ventral Striatum

The ventral striatum comprises the olfactory tubercle and the nucleus accumbens (NAcc). The NAcc is activated by glutamatergic signaling from the frontal cortex, the amygdala, the hippocampus, and the thalamus (Cui et al., 2013). In addition, dopaminergic neurons of the ventral tegmental area project into the NAcc by the mesolimbic pathway, and dopamine release from these neurons into the NAcc is assumed to mediate the rewarding effect of addictive drugs (Taber et al., 2012; Volkow & Morales, 2015). In addition, an interaction of dopamine and glutamatergic signaling in the NAcc is likely (Cui et al., 2013). The NAcc is especially important in incentive learning, and the increase in dopamine in the ventral striatum is thought to mimic the effect of highly salient stimuli in conditioned learning. In drug abuse, this potentially leads to a recalibration of the dopamine-activation/reward threshold for natural reinforcers, i.e., when compared to the dopamine-activation of drugs of abuse, the activation of natural reinforcers such as food is small.

1.2.3 The Dorsal Striatum

When alcohol is consumed for its rewarding qualities, the behavior can be classified as goal-directed, meaning that the association with a desirable outcome mediates the behavior (Dickinson & Weiskrantz, 1985; O'Tousa & Grahame, 2014). Goal-directed behavior is primarily associated with earlier stages of AUD, as the disorder progresses, habit formation increasingly directs behavior. Habit formation refers to behaviors that

have been built through a lengthy reinforcement history and is characterized by an indifference to the value of the reinforcement (O'Tousa & Grahame, 2014). Habits are highly associated with a cue. For example, an alcoholic beverage after work could be consumed for the rewarding qualities. Over time, the consumption could be driven by the cue "coming home from work" rather than drinking the alcoholic beverage for reward. In the neurocircuitry of addiction, this change from goal-directed to habitual/compulsive use is associated with an inner-striatal shift of activation from the ventral to the dorsal striatum (Everitt & Robbins, 2005; Koob & Volkow, 2010). For example, in an fMRI-study, alcohol-related pictures evoked higher activation in the ventral striatum of social compared to heavy drinkers and in the dorsal striatum in heavy compared to light drinkers (Vollstädt-Klein et al., 2010). The dorsal striatum consists of the caudate nucleus (CN) and the putamen (PUT). Both regions are involved in sensorimotor processing and activation in the caudate nucleus is associated with the reinforcement learning necessary for habit formation (Galandra et al., 2018), while the putamen is mainly involved in inhibitory control and habit formation itself (Akkermans et al., 2018). For example, the duration of AUD has been associated with increased cue-related activation in the posterior putamen (Sjoerds et al., 2014). Figure 1.2 shows a section in which the VS, the CN and the PUT are highlighted.
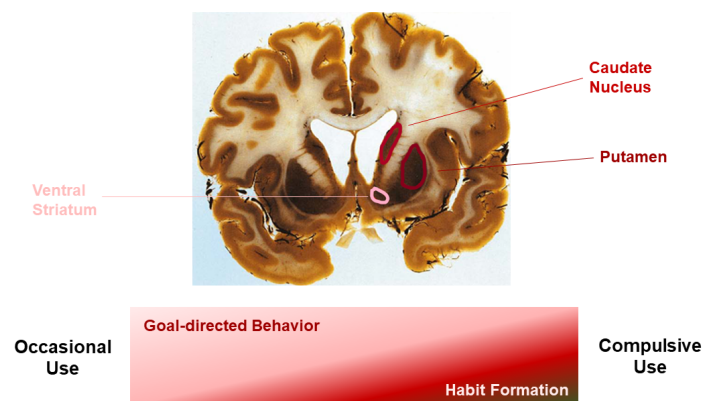
Figure 1.2. Habit formation and the corresponding brain regions in the ventral and dorsal striatum. The section from postmortem human brain tissue is published in Hagens et al. (1990) and was adapted to show ventral and dorsal striatal regions.

1.2.4 The Prefrontal Cortex

The prefrontal cortex plays a vital part, especially in sustaining substance use disorders (Goldstein & Volkow, 2011). During the preoccupation/anticipation stage of addiction, impulse control is important to resist urges and cues associated with drinking (Koob & Volkow, 2010). The dorsolateral prefrontal cortex and Brodmann Area 9 (BA9) in particular are involved in higher-order executive functioning and are an important part of the reward circuitry (Goldstein & Volkow, 2011). The anterior cingulate cortex (ACC) has been associated with attentional biases in AUD (Bach et al., 2015) and self-control (Tang et al., 2015).

1.3   Genetics of Alcohol Use Disorder

AUD is a moderately heritable disorder. Evidence from twin and adoption studies suggests a heritability of around 50% (Goldman et al., 2005; Verhulst et al., 2015), meaning that around half of the variance in the AUD phenotype could be explained by genetics. Over time, different methods have been used to study the genetics of AUD, which are highlighted in the next two paragraphs.

1.3.1   From Candidate to Genome-wide Approaches

In the early stages of molecular genetic studies on the genetic underpinnings of psychiatric disorders, candidate gene studies were used to investigate the association of variation in a single gene with a phenotype (Kwon & Goate, 2000). Genes were selected based on a biological hypothesis. In AUD research, genetic variation in genes encoding enzymes involved in alcohol metabolism were among the first candidate genes (Edenberg, 2007). Studying genetic variation in *ADH1B*, *ADH1C* and *ALDH2* is also an example of successful candidate gene studies, as the first genome-wide significant SNP associated with AUD is located between *ADH1B* and *ADH1C* (Frank et al., 2012). At the same time, it is one of the few examples of candidate genes replicating in genome-wide association studies (GWAS).

During the first ten years of candidate gene research, increasing evidence emerged that candidate gene studies do not produce replicable results and lead to false positive associations (Duncan & Keller, 2011). For example, it has been shown that a set of candidate genes is not more predictive of major depression than a set of randomly selected genes (Border et al., 2019). Candidate gene studies have thus been superseded by genome-wide approaches; not only in genetics, but also in the fields of epigenetics (Shabalin et al., 2015), and gene expression research (Kukurba & Montgomery, 2015), which are discussed in later chapters. Genome-wide approaches are often referred to as hypothesis-generating, meaning that they explore the relationship between a phenotype and a feature, i.e., a genetic variant, without a prior hypothesis about the relationship.

1.3.2   Genome-wide Association Studies of Alcohol Phenotypes

The association of a disease phenotype with common genetic variants can be investigated in GWAS. In a case-control GWAS, a logistic regression is performed for each single nucleotide polymorphism (SNP) with the abundance of the disease phenotype as an outcome and the SNP as the predictor along with covariates. To correct for multiple testing, a Bonferroni corrected p value threshold of $5*10^{-8}$ is applied. This in turn requires a large samples size to identify small effects withstanding multiple testing correction.

A recent GWAS performed a meta-analysis of DSM-5 AUD in the Million Veteran Program (Kranzler et al., 2019), DSM-IV alcohol dependence in the Psychiatric Genomics Consortium (Walters et al., 2018) and the problem-scale of the alcohol use disorder identification test (AUDIT) using the UK Biobank (Sanchez-Roige et al., 2018). The resulting GWAS of problematic alcohol use (PAU) included 435,563 participants

and identified 29 variants (Zhou et al., 2020). Among them were *ADH1B* and *ADH1C*, but also novel candidates such as *PDE4B* and *CADM2*. The Manhattan plot of the PAU GWAS with all annotated loci is shown in Figure 1.3.
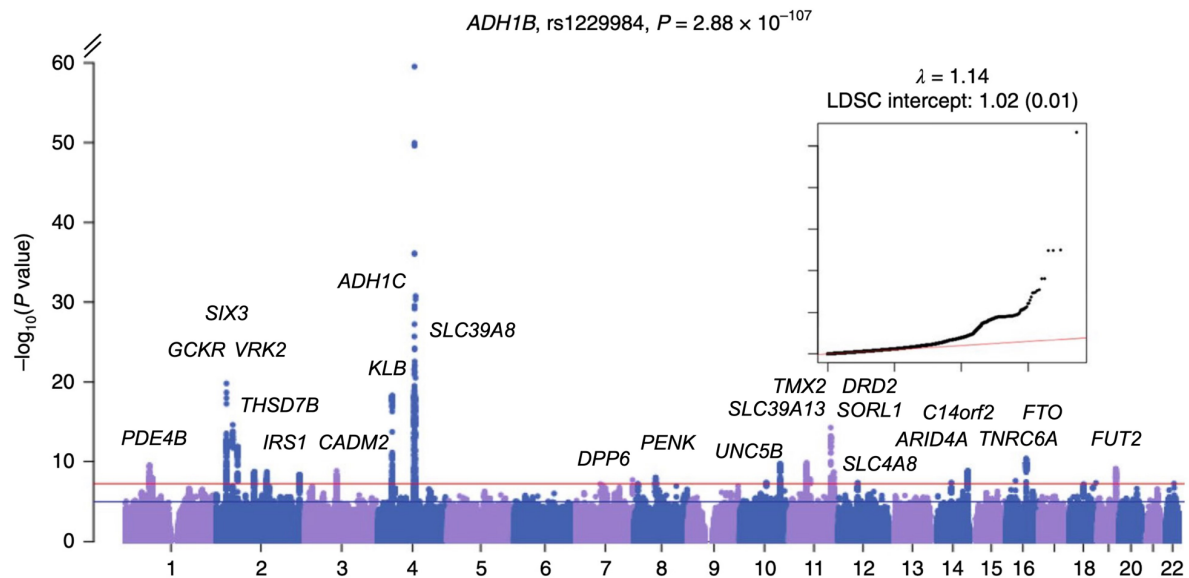
Figure 1.3. Manhattan Plot of the GWAS of Problematic Alcohol Use reprinted by permission from Springer Nature: Nature Neuroscience: Zhou et al. (2020).

The information from GWASs can be further used to create polygenic scores, to perform gene-level tests, and to carry-out enrichment analyses. Interestingly, Zhou et al. (2020) found an enrichment of genes expressed in different brain regions in PAU-related genetic variants. The strongest enrichment was shown for the NAcc, the cortex, PUT, substantia nigra, CN, BA9, and ACC (Zhou et al., 2020).

GWAS are not only useful to genetically characterize a disease phenotype, but are also valuable tools for assessing genetic determinants of treatment response. There was a recent GWAS on responsiveness to acamprosate and naltrexone treatment in AUD, which identified a single genome-wide significant SNP in *BRE* associated with time until relapse to heavy drinking (Biernacka et al., 2021). Although this GWAS was severely underpowered, investigating genetic determinants of treatment outcomes might lead to a more tailored treatment of AUD.

1.4   Epigenetics of Alcohol Use Disorder

1.4.1   Epigenetics and DNA Methylation

Epigenetics refers to the regulation of gene activity not caused by changes in the DNA sequence itself. One epigenetic mechanism is DNA methylation, i.e. the addition of a methyl-group at the 5` position of cytosines (see also Figure 1.4), which most

commonly occurs in cytosine-phosphate-guanine sites (CpG site) (Rakyan et al., 2011). A specific CpG site can either be methylated or unmethylated. DNA methylation can influence gene expression, most often through methylation levels of CpG-islands in promoter regions. CpG-islands are typically at least 200 base pairs long and contain at least 50% GC-content. About 40% of mammalian genes contain CpG islands in their promoters and exonic regions (Fatemi et al., 2005) highlighting them as important sites for gene expression regulation (Deaton & Bird, 2011).
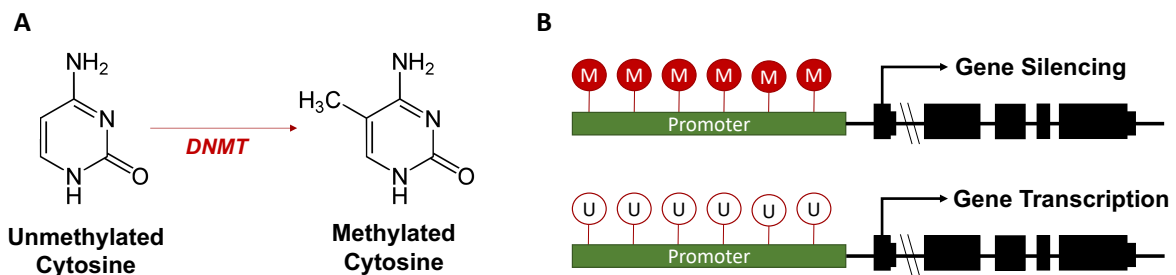
Figure 1.4. A) Addition of a methyl-group through DNA-methyltransferase (DNMT). B) influence of methylated (M) and unmethylated (U) promoters on gene transcription.

CpG sites are commonly classified based on their distance from a CpG-island. The *shore* refers to the ±0-2 kilobase (kb) region around a CpG-island and the *shelf* to the ±2-4 kb region. CpG sites not annotated to CpG-islands are referred to as *open sea*. This classification helps grade the relevance an individual CpG site might have for gene expression regulation. For example, it has been found that CpG methylation in shore regions has a stronger association with gene expression than methylation in a CpG island (Irizarry et al., 2009; Martino & Saffery, 2015).

Increased DNA methylation levels are typically associated with lower gene expression, which is likely due to impaired transcription factor binding in highly methylated regions (Gibney & Nolan, 2010). However, gene expression and protein translation are influenced by a variety of molecular mechanisms, which makes the disentangling of the effect of CpG methylation on gene expression difficult.

1.4.2   Determining DNA Methylation Levels

DNAm arrays, such as the EPIC BeadChip, depict a reliable and cost-effective alternative to expensive next-generation sequencing procedures such as whole-genome bisulfite sequencing, or methyl-binding domain sequencing, which requires years of laboratory experiences to develop suitable protocols for high CpG coverage (Aberg et al., 2020). Of the around 28 million CpG sites known to exist in the human genome (Lövkvist et al., 2016), about 870,000 are captured by the Illumina Infinium HumanMethylation EPIC BeadChip, which is well suited for high-throughput analysis of the methylome (Moran et al., 2016). CpG sites covered by the BeadChip are distributed within several regulatory features such as CpG-islands, promoter regions, open sea regions, and enhancers, but also within exonic and intergenic regions.

To analyze DNA methylation on a microarray, genomic DNA is bisulfite-converted and subsequently pipetted onto the BeadChip. The resulting data from scanning the methylation array are light intensity signals, which are bioinformatically translated to methylation values. A methylation beta-value is a percentage estimate that indicates the mean methylation of a CpG site in the sample. After quality control, these beta values are commonly logit-transformed into M-values (Du et al., 2010), which have the advantage of being more normally distributed than beta values and are thus useful for further statistical analyses.

1.4.3 Epigenome-wide Association Studies

Similar to GWAS, epigenome-wide association studies are hypothesis-generating procedures (Flanagan, 2015). Each CpG-site is tested for an association with the phenotype of interest, usually in (robust) multiple linear regression models. DNAm levels are tissue- and cell-type specific (Lokk et al., 2014). To account for this, cell type proportions are estimated for each sample based on reference data (Houseman et al., 2012) or in a reference-free approach (Houseman et al., 2014). In addition, a correction for technical effects should be applied (Lehne et al., 2015). The EPIC BeadChip contains internal control probes, which allow to capture both technical effects which can be directly observed, such as sequencing batch, as well as other effects, such as a different sensitivity in parts of the scanning systems. A common technique to capture this variation is performing a principal component analysis of the internal control probes and including the first ten resulting principal components in the linear model (Lehne et al., 2015).
In addition to cell type composition and technical effects, smoking and age are known to largely influence DNA methylation levels (Horvath, 2013; Zeilinger et al., 2013) and should therefore be included as covariates in every DNA methylation analysis.

1.4.4 DNA Methylation in Alcohol Use Disorder

1.4.4.1 DNA Methylation in Peripheral Tissues

While investigating DNAm in brain tissue is of primary importance to understand mechanisms of AUD, peripheral tissues, such as blood and saliva, are more accessible. Therefore, past research has focused mainly on these tissues.
The largest EWAS of AUD to date identified 96 CpG sites significantly associated after FDR correction in N=625 participants (Lohoff et al., 2020). Of these, 70 were replicated in in two independent cohorts: Generation Scotland (N=4301) and Grady Trauma Project (N=391). The top hit was annotated to *GAS5*, a long non-coding RNA, which also showed differential expression between AUD cases and controls in postmortem human amygdala tissue (Lohoff et al., 2020).
Because of the high multiple testing burden, sample size is a key factor in epigenome-wide association studies to identify meaningful DMPs. Therefore, many studies investigate alcohol consumption rather than AUD, because this information is usually available in larger population-based cohorts. For example, in an EWAS of alcohol

intake in the Melbourne Collaborative Cohort Study, 1414 significantly associated CpG sites were identified, 1078 of which were replicated in two independent cohort studies (Dugué et al., 2021). In the same study, a longitudinal analysis revealed evidence of changes in DNAm patterns over time dependent on alcohol intake. This is in line with findings from a clinical cohort, in which widespread changes in DNAm were observed in patients at the beginning of withdrawal treatment compared with controls (Witt et al., 2020). At the end of withdrawal treatment, DNAm patterns of patients more resembled those of controls compared to the initial timepoint.

A more recent EWAS of alcohol consumption analyzed N=8161 participants of the Generation Scotland Family Health Study (Lohoff et al., 2022), the largest EWAS to date. The top hit from this study, which was also replicated in an independent clinical cohort, was the cystine/glutamate transporter SLC7A11, providing evidence for methylation-mediated glutamate signaling alterations related to alcohol consumption (Lohoff et al., 2022). Interestingly, differential gene expression of *SLC7A11* was observed in postmortem human prefrontal cortex, suggesting a functional relevance of the differential methylation finding.

While EWAS in peripheral tissues are helpful for investigating the effects of alcohol consumption and alcohol use disorder in large cohorts and have led to drug targets such as the PCSK9 inhibitor to treat alcohol-associated liver diseases (Lohoff et al., 2018), there is a lack of knowledge about DNAm in the brain and drug targets for AUD.

1.4.4.2 DNA Methylation in Postmortem Human Brain Tissue

Postmortem human brain tissue valuable resource for research into AUD which is however very sparse. By now, several studies have investigated the association of DNAm and AUD in different brain regions. In most studies, DNAm was measured using an Illumina Methylation EPIC BeadChip. The brain region most frequently studied is the dorsolateral prefrontal cortex, specifically its subregions BA9 and BA10. For example, Wang et al. (2016) identified differentially methylated CpG sites in male, but not female individuals with alcohol dependence compared to controls. A further co-methylation analysis using WGCNA revealed modules enriched for biological processes, such as transcriptional regulation and neural development (Wang et al., 2016). Meng et al. (2021) found two DMRs in BA9 and NAcc of individuals with alcohol dependence compared to controls. Interestingly, this DMR was genotype-dependent on a variant in *DLGAP2*, which was also shown to influence alcohol consumption in a mouse model (Meng et al., 2021). In a study in BA10, differential methylation in *NR3C1* – a gene which encodes the glucocorticoid receptor – was highlighted (Gatta et al., 2021). A recent study investigated differential methylation through MBD-seq, first in 1,132 blood samples and then in postmortem BA10 tissue of N=50 individuals (Clark et al., 2022). While the postmortem brain analysis did not reveal epigenome-wide significant hits, there was a significant overlap between the monocyte- and B-cell-specific association studies in blood and hydroxy-/methylation in brain (Clark et al., 2022).

While the largest body of evidence has been accumulated for the prefrontal cortex, there are studies which have investigated other brain regions as well. For example,

Hagerty et al. (2016) utilized postmortem tissue of the precuneus and putamen and found more than 400 DMPs, which also showed enrichment for inflammation-related pathways.

The aforementioned studies were able to identify differential methylation, although often not epigenome-wide significant. This is likely because of the small sample size, which ranged between N=20-96. At the same time, the interpretation of EWAS-findings alone is difficult, because each CpG site usually has a small effect and does not necessarily influence gene expression. Therefore, evidence from multiple layers of -omics are needed to provide convergent evidence and enhance our understanding of the molecular mechanisms of AUD.

1.5   Gene Expression in Alcohol Use Disorder

1.5.1   RNA-sequencing and Differential Expression Analysis

Gene expression is a complex process involving multiple steps during the transfer of genetic information from DNA to messenger RNA (mRNA) or the transition from genotype to phenotype (Gibney & Nolan, 2010).

Next-generation sequencing technologies are the gold standard for analyzing whole-genome transcriptomics and have become increasingly cost-effective in recent years (Levy & Myers, 2016). The RNA-seq workflow is depicted in Figure 1.5. First, RNA is extracted from primary tissue and total RNA is purified for the ribonucleic acid of interest, such as mRNA or small RNAs. Afterwards, the RNA is converted to cDNA, followed by sequencing library construction and amplification. After sequencing, the resulting reads can either be aligned to the genome or transcriptome, or a pseudo-alignment can be performed. Afterwards, aligned reads are quantified in a count matrix and differential expression can be tested.

By now, RNA-sequencing is also possible at the single-cell or single-nuclei (snRNA-seq) level. snRNA-seq allows the measurement of gene expression in each nucleus analyzed, as opposed to bulk-sequencing which estimates the mean gene expression profile in a sample. Because of the high resolution, it is possible to cluster the gene expression profiles of the individual nuclei into known and novel cell-types and perform cell-type specific analyses (Lake et al., 2016).
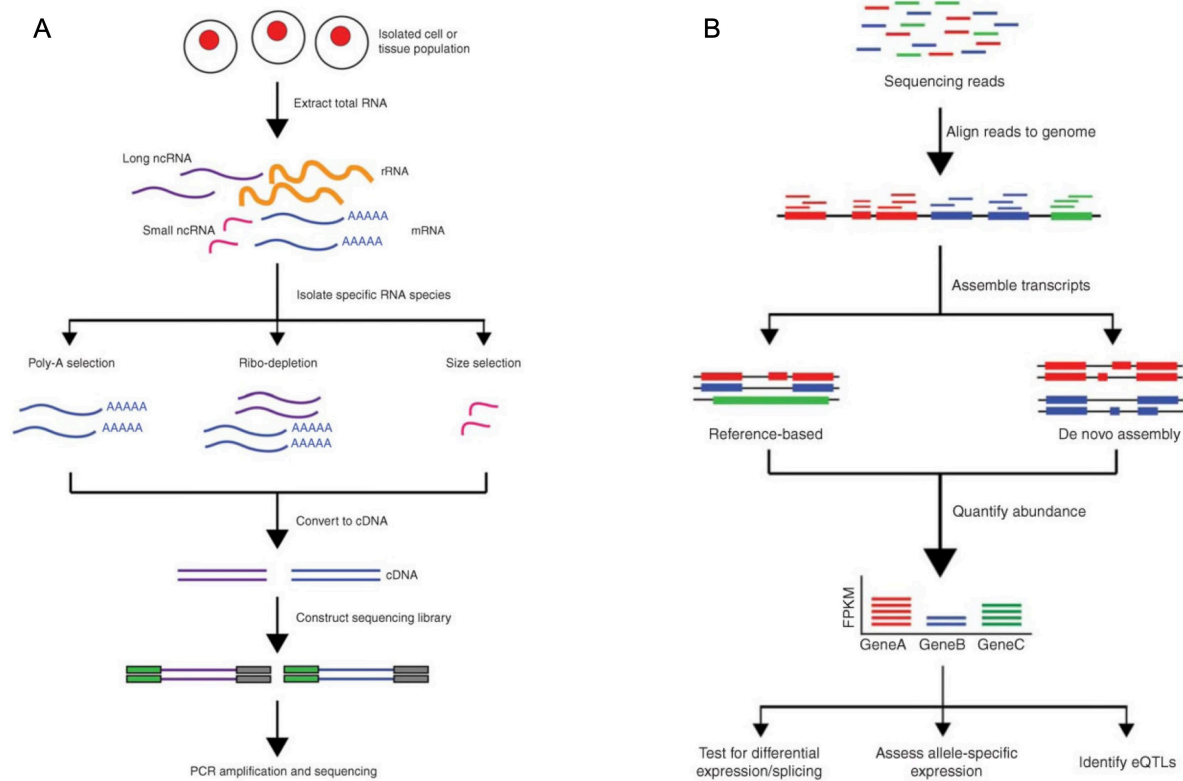
Figure 1.5. RNA-sequencing workflow, adapted from (Kukurba & Montgomery, 2015), reprinted by permission from Cold Spring Harbor Laboratories.

1.5.2 Gene Expression in Postmortem Human Brain Tissue

So far, gene expression studies in AUD have been conducted primarily in postmortem human brain tissue. In an early study that used microarray technology to measure gene expression, widespread differential expression in the central and basolateral amygdala, and the superior frontal cortex was observed, although this only reached nominal significance (Ponomarev et al., 2012). In the same study, a WGCNA analysis was conducted and the resulting modules were related to different cell types, depicting a common result of WGCNA. However, no information on the association of modules with AUD status was available (Ponomarev et al., 2012). The first study assessing gene expression in substance use disorders applied RNA-sequencing in individuals with cocaine use disorder (CUD), AUD, and controls. They observed two genes differentially expressed in the hippocampus of individuals with AUD compared to controls and eight genes which were genome-wide significant for both, AUD and CUD (Zhou et al., 2011). The strongest association for AUD was for a member of the histone H4 family.

More recent studies have investigated BA9 using next-generation sequencing technologies. Kapoor et al. (2019) found 125 genes differentially expressed in BA9 between individuals with AUD and controls. Network analyses resulted in modules enriched for calcium signaling and immune pathways (Kapoor et al., 2019). A recent study investigated microRNAs and mRNAs in eight brain regions: the amygdala, CN,

cerebellum, hippocampus, NAc, prefrontal cortex, putamen, and ventral tegmental area (Lim et al., 2021). MicroRNA and mRNA networks were also enriched for immunological pathways, such as IL-8 signaling, *CREB* signaling in neurons, and neuroinflammation signaling (Lim et al., 2021).

A snRNA-seq study in BA9 showed differential expression particularly in astrocytes, microglia and oligodendrocytes, and found that DE genes were enriched for neuroinflammation-related pathways (Brenner et al., 2020). When results from snRNA-seq were compared to those from Kapoor et al. (2019), it was shown that there was a moderate overlap between bulk results and those originating from different cell-types, but microglia displayed a very distinct gene expression pattern (Brenner et al., 2020). In summary, there is accumulating evidence of transcriptome-wide differential expression in AUD, but at the same time a lack of studies investigating striatal brain regions. Importantly, investigating a single -omic layer cannot give an accurate picture of the molecular mechanisms associated with AUD.

1.6 Multi-Omics Data Integration

Integrating multiple layers of -omics allows a deeper characterization of the functional mechanisms in AUD. Already there have been some attempts at multi-omics data integration in AUD. Two studies attempted to integrate data from GWAS with DNA methylation and/or gene expression data from postmortem human brain samples. Lin et al. (2020) investigated a potential functional relevance of GWAS-identified variants associated with AUD and comorbid psychiatric disorders, and they observed that methylation (mQTL) and expression quantitative trait loci (eQTL) were enriched in variants for these disorders. Quantitative trait loci describe genetic loci which predict biological processes, such as DNA methylation (Hormozdiari et al., 2018). Similarly, Kapoor et al. (2021) performed fine-mapping of genetic variants from a large GWAS of AUD (Kranzler et al., 2019) and two GWAS of alcohol dependence (Lai et al., 2019; Walters et al., 2018), using eQTL and mQTL data from fetal and adult dorsolateral prefrontal cortex from individuals with and without AUD. The genes prioritized in this study showed an overlap with causal genes that were previously related to neurodegenerative diseases (Kapoor et al., 2021).

While GWAS data have been followed-up in expression and methylation datasets, there is a lack of studies integrating DNA methylation and gene expression data.

1.7 Aims

The following studies aimed to identify epigenetic mechanisms associated with AUD – both on the single site and the regional level – to investigate differential gene expression associated with AUD status in the neurocircuitry of addiction, relate our results to GWAS findings, and to integrate the gene expression with DNA-methylation data using a network approach (WGCNA) in order to identify functionally relevant molecular mechanisms in AUD.

2 STUDY 1: EPIGENOME-WIDE ASSOCIATION STUDY OF ALCHOHOL USE DISORDER IN FIVE BRAIN REGIONS[1]

2.1 Abstract

Alcohol Use Disorder (AUD) is closely linked to the brain regions forming the neurocircuitry of addiction. Postmortem human brain tissue enables the direct study of the molecular pathomechanisms of AUD. This study aims to identify these mechanisms by examining differential DNA-methylation between cases with severe AUD (n=53) and controls (n=58) using a brain region-specific approach, in which sample sizes ranged between 46 and 94. Samples of the anterior cingulate cortex (ACC), Brodmann Area 9 (BA9), caudate nucleus (CN), ventral striatum (VS), and putamen (PUT) were investigated. DNA-methylation levels were determined using the Illumina HumanMethylationEPIC Beadchip. Epigenome-wide association analyses were carried out to identify differentially methylated CpG-sites and regions between cases and controls in each brain region. Weighted Correlation Network Analysis (WGCNA), gene-set and GWAS-enrichment analyses were performed. Two differentially methylated CpG-sites were associated with AUD in the CN, and 18 in VS ($q < .05$). No epigenome-wide significant CpG-sites were found in BA9, ACC, or PUT. Differentially methylated regions associated with AUD case-/control status ($q < .05$) were found in the CN (n=6), VS (n=18) and ACC (n=1). In the VS, the WGCNA-module showing the strongest association with AUD was enriched for immune-related pathways. This study is the first to analyze methylation differences between AUD cases and controls in multiple brain regions and consists of the largest sample to date. Several novel CpG-sites and regions implicated in AUD were identified, providing a first basis to explore epigenetic correlates of AUD.

2.2   Introduction

Every year, approximately 5.3% of all deaths worldwide are a result of the harmful use of alcohol and approximately 230 diseases are associated with alcohol use (World Health Organization, 2019). The lifetime prevalence of alcohol use disorder (AUD) varies globally, with North African/Middle Eastern countries having the lowest (0.59%) and Eastern European countries the highest (4.25%) prevalence. With a global prevalence of 1.32%, AUD is an important contributor to global disease burden (Degenhardt et al., 2018). AUD is a moderately heritable disease; a meta-analysis of twin studies estimated a heritability of 49% (Verhulst et al., 2015).

It has been proposed that drug-induced alterations in gene expression in the neurocircuitry of the brain contribute to addiction (Robison & Nestler, 2011). Recent evidence suggests that alterations in DNA-methylation, an epigenetic mechanism affecting gene expression, play an important role in addiction (for reviews see: Longley et al. (2021), Maze and Nestler (2011)). Differential DNA-methylation is associated with alcohol consumption and AUD both in peripheral blood and postmortem brain tissue (for an overview see: Bazov et al. (2013)). Examining alterations in DNA-methylation in epigenome-wide association studies (EWAS) allows for the investigation of inter-individual differences which are attributable to a phenotype (Rakyan et al., 2011). For example, a recent EWAS of AUD in peripheral blood suggests that networks in glucocorticoid signaling and inflammation-related genes are associated with AUD (Lohoff et al., 2020).

Human postmortem brain tissue is a sparse and valuable resource and allows a more direct characterization of AUD mechanisms than possible by analyzing peripheral blood (Edgar et al., 2017). So far, a small number of postmortem brain studies have been conducted, mostly investigating the prefrontal cortex (PFC), which, due to its role in reward regulation and higher-order executive function, is thought to be disrupted in addiction (Goldstein & Volkow, 2011). An EWAS comparing individuals with AUD with age-matched controls detected a range of differentially methylated CpG-sites in Brodmann Area 9 (BA9) in 16 pairs of males, but not in seven pairs of females (Wang et al., 2016). Another study identified AUD-associated differentially methylated CpG-sites in Brodmann Area 10, which did not remain significant after multiple testing correction (Gatta et al., 2021). However, downstream analyses implicated *NR3C1*, a gene coding for the glucocorticoid receptor, which is crucial to stress regulation and found to be functionally relevant in AUD. The increased DNA-methylation in individuals with AUD was also associated with reduced *NR3C1* mRNA and protein expression levels (Gatta et al., 2021).

Investigating DNA-methylation in the wider addiction neurocircuitry may give deeper insights into the pathophysiological mechanisms of AUD, and may reveal potential targets for treatment or prevention (Koob & Volkow, 2010; Noori et al., 2012). Dysfunction in the addiction neurocircuitry, which comprises areas involved in cognitive control such as the dorsolateral PFC, the anterior cingulate cortex (ACC), and regions in the basal ganglia, can have impairing consequences associated with disrupted reward-related decision-making, alcohol craving, and compulsive alcohol consumption (Goldstein & Volkow, 2011; Park et al., 2010). Of particular interest is the striatum,

which is divided into ventral and dorsal subdivisions based on function and connectivity. The ventral striatum (VS), comprises the nucleus accumbens (NAcc) and olfactory tubercle while the dorsal striatum contains the caudate nucleus (CN) and putamen (PUT) (Volkow & Morales, 2015). The NAcc is thought to be important in addiction due to its role in processing motivation, more precisely aversion and reward (Volkow & Morales, 2015). The caudate nucleus and putamen both influence motor function; in addition, the caudate is involved in goal-directed action, executive functioning and cognitive control, while the putamen is implicated in various types of learning, including reinforcement learning and habit formation (Galandra et al., 2018). In a study investigating DNA-methylation in PFC and NAcc, CpG-sites in *DLGAP2* emerged as differentially methylated between 39 male AUD cases and 47 controls in both brain regions; the differences were genotype-dependent (Meng et al., 2021).

In the present study, we aimed to identify epigenetic mechanisms associated with AUD, in five brain regions previously implicated in the neurocircuitry of addiction (Volkow & Morales, 2015). Brain-region specific EWAS of AUD were performed in the BA9, ACC, VS, CN and PUT.

2.3   Materials and Methods

2.3.1   Samples

In total, 395 human postmortem brain samples from 111 subjects (53 AUD, 58 controls) were obtained from the New South Wales Tissue Resource Center (University of Sydney, Australia) under study reference number 2009-238N-MA by the Ethics Committee II of the Medical Faculty Mannheim. AUD and control subjects were matched by age and sex. All individuals met the following inclusion criteria, which were determined by next-of-kin interviews: age >18, no history of severe psychiatric, neurodevelopmental, or other substance use disorders (except nicotine use disorder), and Western European ancestry. Individuals with AUD were classified according to DSM-IV criteria and had consumed at least 80g alcohol daily, whereas controls had consumed less than 20g. Methylation data was generated in two batches and each batch was analyzed separately. The first batch comprised 220 samples of BA9, ACC, CN, and VS from 28 cases and 27 controls. In the second batch, 175 samples from 56 additional individuals from the CN, VS, and PUT were analyzed. Material from one to five brain regions was available for each individual. Therefore, the sample composition varies between the brain region-specific analyses. A sample description can be found in Table 2.1. Table 2.2 shows the number of samples for each brain region and each batch. Additional phenotype information, such as cause of death and detailed exclusion criteria can be found in the Supplementary Information (Table 2.S1 and Text 2.S1).

2.3.2 Epigenome-wide Methylation

DNA was extracted from bulk brain tissue using the DNeasy extraction kit from Qiagen (Qiagen, Hilden, Germany). The genomic DNA samples were stored at -20°C. For the microarray analysis, the samples were randomized based on AUD case/control status and sex, and pipetted on processing plates. Due to the sample and different group sizes, samples from each brain region were processed on separate plates. Epigenome-wide methylation levels were determined using the Illumina HumanMethylationEPIC Beadchip and Illumina HiScan array scanning systems (Illumina, San Diego, CA).

Table 2.1
Descriptive statistics of demographic data.

Characteristic	Cases	Controls	*p*
N	53	58	
Age, years	56.72 (10.81)	56.69 (10.29)	0.989
Sex (M/F)	34/19	40/18	0.737
pH-value	6.5 (0.28)	6.57 (0.32)	0.189
PMI (hours)	35.46 (16.1)	28.17 (15.29)	0.038*
Estimated Smoking	0.72 (0.26)	0.51 (0.31)	> .001*
Blood Alcohol level (N)	8	0	
Blood Alcohol Level (g/100ml)	0.211 (0.179)		
Number of Brain Regions			
5	19 (35.8%)	19 (32.8%)	
4	9 (17.0%)	8 (13.8%)	
3	18 (34.0%)	21 (36.2%)	
2	0 (0%)	3 (5.1%)	
1	7 (13.2%)	7 (12.1%)	

Data are presented as count (n/n; n (%)) or mean (±SD), PMI: post-mortem interval, pH: pH-value of the brain, p: p-value of t-Test comparing cases and controls, estimated smoking is the likelihood of smoking estimated based on the methylation data.
significant difference between cases and controls

2.3.3 Data preprocessing, Quality Control, and Filtering

All data preprocessing and analysis steps were performed using the R statistical environment, version 3.6.1. An updated version of the CPACOR-pipeline published by Lehne et al. (2015) was used to extract methylation data from raw intensity data and perform quality control. Samples were removed if (i) DNA quality was not sufficient (missing rate > 0.10) or (ii) a discrepancy between methylation-based and phenotypic sex emerged. Probes were removed when (i) the call-rate was insufficient (< 0.95), (ii) SNPs with a minor allele frequency > 0.10 were located in the probe sequence, (iii) the probes were located on the X or Y chromosome (chr). After quality control 381 samples

remained. Depending on the brain region, 657 593 – 694 791 sites were available for analysis after filtering. Detailed descriptions of sample size, the number of sites remaining after QC, and the inflation coefficient lambda for each model can be found in Table 2.2.

Table 2.2.
Sample Overview.

Brain Region	Total N	Case Batch I	Case Batch II	Control Batch I	Control Batch II	# of CpG sites	Genomic Inflation
Anterior Cingulate Cortex	54	28		26		657 593	0.958
Brodmann Area 9	46	25		21		657 593	0.942
Putamen	94		44		50	694 572	0.963
Caudate Nucleus	94	28	17	27	22	694 790	0.919
Ventral Striatum	93	28	18	26	21	694 790	0.962

Number of individuals per brain region after quality control. # of CpG-sites refers to the number of sites remaining after quality control, for VS and CN union of the two batches.

2.3.4 Statistical Analysis

Methylation values were log-transformed (base 2) and included as dependent variables in the association analyses, as recommended by Du et al. (2010). Control for batch effects and technical quality was applied by extracting signals of the internal control probes of the EPIC array, performing principal component analysis (PCA), and extracting the first ten principal components. These were included as covariates in all association tests. To control for cell-type heterogeneity, cell counts were estimated using the method by Houseman et al. (2012), with the dorsolateral prefrontal cortex reference data (Jaffe & Kaminsky, 2018). This approach results in two estimates, one for neurons and one for other cell types. These were standardized so that the sum of both counts added up to one. The estimate for neurons was included as a covariate in all analyses.

Data on smoking was not available for all participants (missing for n=11, 10.81%). Smoking status was therefore estimated based on a validated set of sites (Maas et al., 2019). Estimated smoking was included as a continuous covariate. 86% of current smokers were correctly classified; according to the regression model their likelihood of smoking was >50%.

2.3.4.1 Epigenome-wide Association Analysis

Tests of methylation differences between individuals with AUD and control subjects were performed with linear models, adjusting for sex, age, postmortem interval (PMI), pH-value, estimated smoking, standardized neuronal cell count, and the first ten principal components of the internal control probes. Each region and each batch was analyzed separately. The summary statistics for CN and VS were then meta-analyzed based on effect estimates and standard errors using METAL (Willer et al., 2010). P-values were corrected for multiple testing using the Benjamini-Hochberg (FDR) correction (Benjamini & Hochberg, 1995); resulting values are reported as q-values. CpG-sites were annotated using the manufacturer's manifest (http://webdata.illumina.com.s3-website-us-east-1.amazonaws.com/downloads/productfiles/methylationEPIC/infinium-methylationepic-v-1-0-b4-manifest-file-csv.zip; downloaded on 10th of August 2018). Regression coefficients of differential methylation for the epigenome-wide significant CpG-sites were summarized for each brain region. As each brain region was processed on a separate plate, no inferential statistical procedure was applied to compare DNA-methylation levels between brain regions (due to confounding of batch and regions). Test statistics from all epigenome-wide significant CpG-sites were reported for each brain region and also for an independent EWAS in peripheral blood, in which DNA-methylation levels of male patients with AUD, who had just entered withdrawal treatment were compared with healthy controls (Witt et al., 2020). As the cause of death of two control subjects from the second batch was "toxicity", a sensitivity analysis excluding these subjects was performed in CN, VS, and PUT.

2.3.4.2 Differentially Methylated Regions (DMRs)

DMRs were identified using the comb-p algorithm (Pedersen et al., 2012), which accounts for autocorrelation between tests of adjacent methylation sites and combines these sites to regions of enrichment, in a given window. The following settings were used: Seed-p value < 0.01, minimum of 2 probes, sliding window 500 bp. The Šidák correction as implemented in comb-p was applied to correct for multiple testing. Comb-p was applied to the result statistics for all brain regions.

2.3.4.3 Pyrosequencing and TaqMan Assay

The DMR in *DDAH2* was replicated by pyrosequencing and gene expression levels were determined using a TaqMan Assay (for details see Supplementary Text 2.S3).

2.3.4.4 Gene-Ontology (GO) over-representation analysis.

Functional analysis to identify gene pathways targeted by differentially methylated CpG-sites was performed for sites with a threshold of $p_{nominal}$ < 0.001 using missMethyl (Phipson et al., 2016). missMethyl controls for probe number bias, the increased likelihood of a gene to be differentially methylated, if more probes cover the gene and multi-gene bias, and the fact that probes can be annotated to more than one gene.

GWAS-Enrichment-Analysis. Gene-sets were created consisting of the genes to which the differentially methylated CpG-sites were annotated. Two gene-sets were created for each of the CN and VS results, one for genes implicated by epigenome-wide significant CpG-sites, and one for genes implicated by nominally significant CpG-sites, giving a total of four gene-sets. Multi-marker Analysis of GenoMic Annotation (MAGMA)(de Leeuw et al., 2015) was used to test enrichment of those gene-sets in the results of a genome-wide association study (GWAS) of AUD (Zhou et al., 2020).

2.3.4.5 Weighted Correlation Network Analysis (WGCNA)

The WGCNA R package (Langfelder & Horvath, 2008) was used to generate co-methylated modules and relate those to AUD case-/control status. For each brain region the quantile-normalized beta values of CpG-sites nominally associated ($p < 0.05$) with AUD status were used as input. Soft power thresholds were picked according to the criterion of approximate scale-free topology ($R_{signed}^2 > 0.90$). The number of CpG-sites and the soft power thresholds picked can be found in Supplementary Table 2.S2. Unassigned CpG-sites were clustered in the "grey" module, which was not taken into account for further analyses. For each brain region, the module of correlated CpG-sites with the highest association with AUD was identified. A GO analysis with the CpG-sites comprising the module was performed using missMethyl (Phipson et al., 2016).

2.3.4.6 GWAS ATLAS

The PheWAS tool from the publicly available database GWAS ATLAS (Watanabe et al., 2019) [https://atlas.ctglab.nl/] was used to identify genome-wide significant associations of the genes implied by the top hits in the EWAS.

2.4 Results

2.4.1.1 Epigenome-wide Association Analysis

In the CN, two CpG-sites were epigenome-wide significantly hypomethylated in AUD cases compared to controls. The two sites were annotated to the genes *IREB2* (cg04214706) and *HMGCR* (cg26685658). cg04214706 was also differentially methylated in the ACC ($p_{nominal} = 0.005$).

In the VS, 18 CpG-sites were epigenome-wide significantly associated with AUD. Nine CpG-sites were hyper- and nine hypomethylated. The top three hits were annotated to *SLC30A8, FAM20B,* and *PCAT29*. Of the epigenome-wide significant CpG-sites, cg12049992 in *PIEZO2* and cg16767842 in *GLANT9* were also differentially methylated in CN ($p_{nominal} \leq 0.023$). Additionally, cg1354575 in *TCL1A* was differentially methylated in PUT ($p_{nominal} = 0.035$) and cg02849689 (intergenic) in ACC ($p_{nominal} = 0.012$). Three of the epigenome-wide significant CpG-sites showed nominally significant associations in an EWAS of AUD in peripheral blood, namely cg27512762 in *PCAT29,* cg06427508 in *KLHL6* (effect in opposite direction), and cg02849689,

which was not annotated to a nearby gene. In ACC, BA9, and PUT no epigenome-wide significant differentially methylated CpG-sites were identified ($q \geq 0.57$). Epigenome-wide significant CpG-sites can be found in Table 2.3 and the top 100 associations for each brain region, together with more detailed information on location and annotation to enhancers, in supplementary tables (2.S3a–2.S3e). All coefficients of CpG-sites with $q < 0.05$ for each brain region and in peripheral blood are summarized in Supplementary Table 2.S4. Manhattan plots for EWAS in the ACC, CN, and VS are depicted in Figure 2.1.

Post-hoc power analyses using the web app EPIC Array Power Calculations (https://epigenetics.essex.ac.uk/shiny/EPICDNAmPowerCalcs/) were conducted for sample sizes of n=46 and n=94, to adequately reflect our sample sizes and the additional settings 2% mean difference and significance threshold 1×10^{-7}, which was closest to the FDR corrected thresholds in the present study. This resulted in 11% of CpG-sites having a power larger than 90% to detect mean methylation differences of 2% for a sample size of 94 and 3.18% for a sample size of 46 (see also Supplementary Figure 2.S1). It has to be noted, that the power calculations assumed equal distributions between cases and controls, which was not the case for all analyses. The sensitivity analyses did not reveal major differences between the EWAS in the complete sample and the reduced sample, in which control subjects who died of toxicity were excluded. The effect sizes of the nominally significant CpG-sites in each of the brain regions were highly correlated ($r_{CN} = 0.99$, $r_{VS} = 0.98$, $r_{PUT} = 0.99$, all $p < 0.001$). Scatterplots of the effect sizes for nominally significant CpG-sites in both analyses are depicted in Supplementary Figure 2.S2.

Table 2.3.

Epigenome-wide significant CpG-sites associated with AUD.

Caudate Nucleus

Chr	Position	CG	Gene	Effect	Std Err	P	Direction	FDR
15	78729669	cg04214706	*IREB2*	-0.393	0.073	7.58E-08	+-	0.03
5	74633012	cg26685658	*HMGCR*	-5.92	1.105	8.53E-08	--	0.03

Ventral Striatum

Chr	Position	CG	Gene	Effect	Std Err	P	Direction	FDR
8	117961971	cg17163967	*SLC30A8*	0.504	0.0882	1.09E-08	++	0.007
1	178998656	cg23933289	*FAM20B*	0.269	0.0482	2.36E-08	++	0.008
15	69908472	cg27512762	*PCAT29*	0.17	0.032	6.80E-08	-+	0.016
7	1008720	cg02028351	*COX19*	0.18	0.034	1.28E-07	++	0.017
16	68563886	cg02941431		-0.251	0.047	1.27E-07	--	0.017
3	183274235	cg06427508	*KLHL6*	0.379	0.072	1.44E-07	++	0.017
12	132882652	cg16767842	*GALNT9*	0.239	0.046	1.74E-07	-+	0.017
16	4901809	cg02741291	*UBN1*	0.579	0.113	2.61E-07	?+	0.023
16	1946176	cg10824492		-0.147	0.029	3.35E-07	--	0.026
19	35168316	cg18564234	*SCGB1B2P; ZNF302*	-0.776	0.153	4.13E-07	--	0.029
13	73687406	cg06630619		-0.43	0.085	4.76E-07	--	0.03
11	1215457	cg23618269	*MUC5AC*	-0.432	0.086	5.25E-07	--	0.03
14	96177134	cg13545750	*TCL1A*	-0.226	0.046	7.21E-07	--	0.039
5	79331052	cg04360099	*THBS4*	0.303	0.062	1.03E-06	++	0.048
6	29400397	cg26754552		0.277	0.057	9.88E-06	++	0.048
11	59390857	cg02849689		-0.298	0.061	1.24E-06	--	0.048
18	11147785	cg12049992	*PIEZO2*	-0.28	0.058	1.20E-06	+-	0.048
17	18210650	cg16021181	*TOP3A*	-0.307	0.063	1.11E-06	--	0.048

Chr: chromosome, Direction: (+) hypermethylated, (-) hypomethylated, (?) CpGs not available in one batch. FDR: false discovery rate corrected p-value.
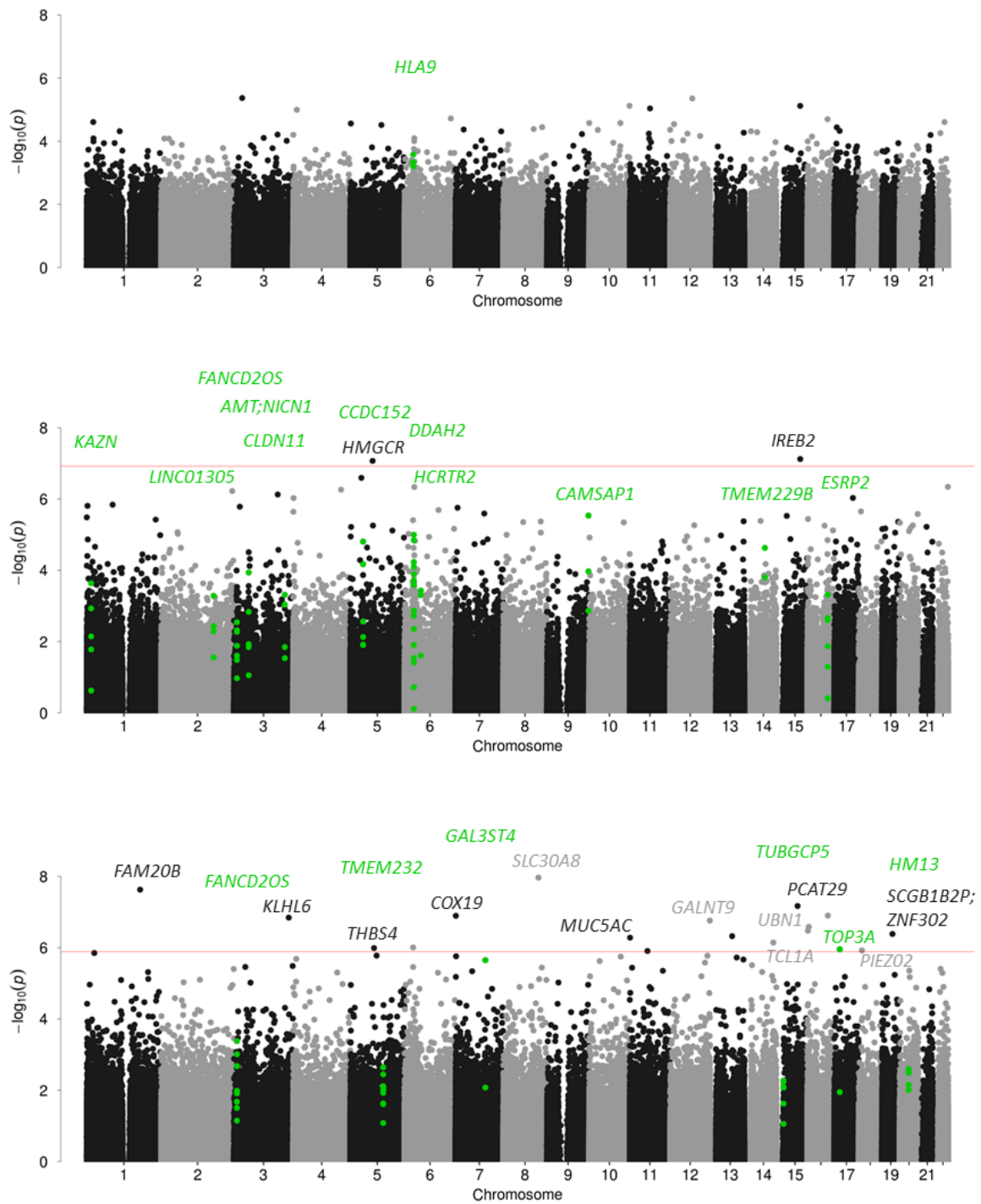
Figure 2.1. Manhattan plots of association of methylation values with AUD in (A) anterior cingulate cortex; (B) caudate nucleus; (C) ventral striatum. Highlighted CpG-sites represent differentially methylated regions. Genes implicated by CpGs (light and dark grey) and DMRs (green) are specified in the figures. Red line indicates FDR-corrected significance.

2.4.1.2 Differentially Methylated Regions

In the CN, 10 DMRs were associated with AUD. The top three regions were annotated to the genes *DDAH2, CCDC152,* and *CAMSAP1.* Six DMRs were associated with AUD ($q < 0.05$) in the VS, with the three most strongly associated regions in *TMEM232, FANCD2OS,* and *HM13.* All significant DMRs for CN and VS are highlighted in Figure 2.1 and can be found in supplementary tables 2.S5a and 2.S5b. In the ACC, one region in *HLA9* was differentially methylated (p Šidák -corrected $= 3.25*10^{-6}$). No epigenome-wide significant DMRs were observed in BA9 and PUT.
The DMR in *DDAH2* was replicated by pyrosequencing (cg04074004: $t(76.77)= 2.39$, $p = 0.019$). Differential expression was not observed (all $p > 0.136$). For details see Supplementary Text 3.S3.

2.4.1.3 Gene-Ontology Analysis

The strongest overrepresentation in the CN was for the biological process "homophilic cell adhesion via plasma membrane adhesion molecules" ($p = 5.37*10^{-6}$, $q = 0.12$) and "cell-cell adhesion via plasma-membrane adhesion molecules" ($p = 1.68*10^{-5}$, $q = 0.187$). In the VS, the cellular "Lsm1-7-Pat1 complex" showed the strongest overrepresentation ($p = 6.49*10^{-5}$, $q \approx 1$). Both associations did not remain significant after correction for multiple testing. The ten GO-terms showing the strongest overrepresentation can be found in Supplementary Tables 2.S6a and 2.S6b.

2.4.1.4 GWAS Enrichment Analysis

No significant enrichment was observed in any of the regions and gene-sets tested (all $p \geq 0.277$).

2.4.1.5 Weighted Correlation Network Analysis (WGCNA)

For the caudate nucleus, 15 modules were identified consisting of 49-10,330 CpG-sites (*Median* = 965). The strongest association with AUD was observed for module "black", which showed the strongest enrichment for the cellular component "PML body" ($p = 0.001$) and the molecular function "G-rich strand telomeric DNA binding" ($p = 0.001$). For CpG-sites nominally associated with AUD status in the VS 14 modules were identified, consisting of 38-12,721 CpG-sites (*Median* = 611). Module "purple" showed the strongest association with AUD and was enriched for a variety of immune-related GO-terms, such as the biological processes "regulation of T-cell proliferation" ($p = 4.32e^{-6}$) and "regulation of leukocyte cell-cell adhesion" ($p = 6.83e^{-6}$). For caudate nucleus module "black" and ventral striatum module "purple" the correlations of the gene significance (GS), which reflects the biological significance of a CpG-site with an external trait (here AUD) and the module membership (MM), which reflects the correlation of each CpG-site with the module, were calculated and are displayed in Figure 2.2a and 2.2b. The top enriched GO-terms for these modules can be found in Supplementary Tables 2.S7a and 2.S7b. Results for ACC, BA9, and putamen are described in the Supplementary Information (Text 2.S2, Figure 2.S3).

A)

B)
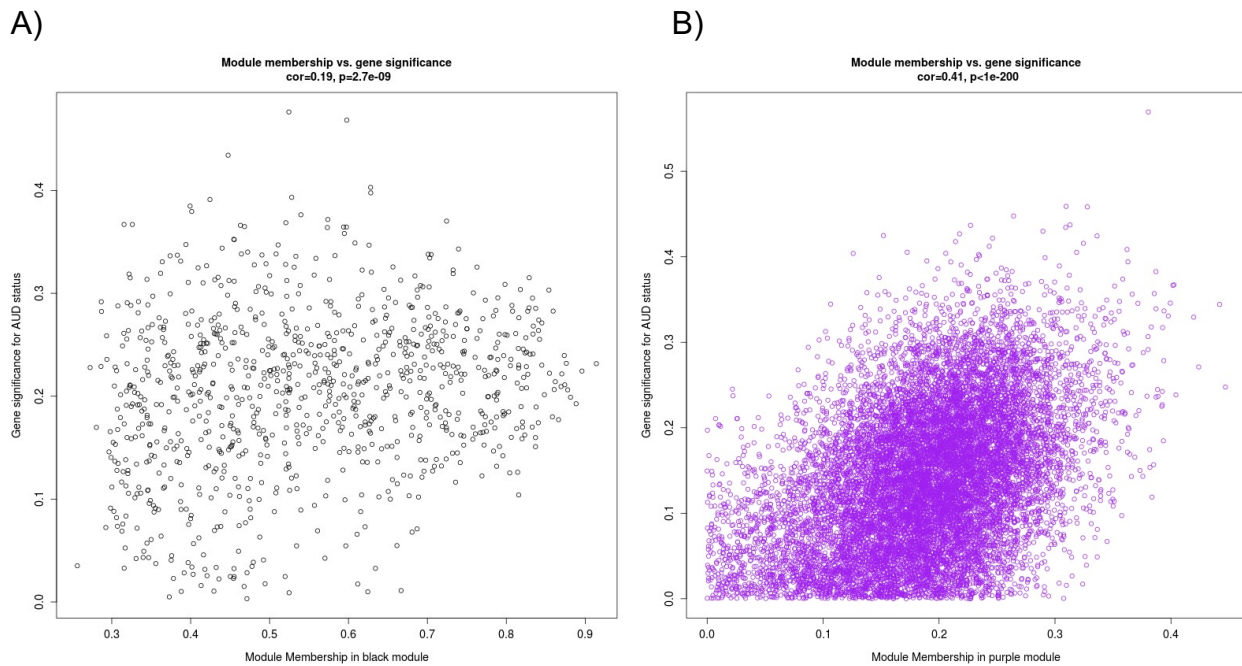
Figure 2.2. Association of gene significance for AUD status with module membership, for the modules A) "black" in caudate nucleus, and B) "purple" in ventral striatum.

2.4.1.6 GWAS ATLAS

GWAS ATLAS results for the genes implicated by the most strongly associated site and region both in the CN and VS can be found in Supplementary Tables 2.S8a-2.S8d. In brief, *IREB2* has previously been associated with smoking phenotypes (e.g., number of cigarettes a day, numbers of cigarettes previously smoked daily), parental illnesses such as lung cancer and chronic bronchitis, and psychiatric disorders like schizophrenia and bipolar disorder (Furberg et al., 2010; Ruderfer et al., 2018; Watanabe et al., 2019). Genome-wide significant associations of *DDAH2* with phenotypes from a variety of domains, e.g., immunological, metabolic, respiratory, and psychiatric have been found. In the psychiatric domain, *DDAH2* has been associated with schizophrenia and bipolar disorder e.g. (Pardiñas et al., 2018; Ruderfer et al., 2018). *SLC30A8* has been implied in blood sugar levels (Kanai et al., 2018) and *TMEM232* in allergic rhinitis and asthma (Watanabe et al., 2019).

2.5 Discussion

The present study examined DNA-methylation associated with AUD in regions of the addiction neurocircuitry using an epigenome-wide methylation analysis approach employed in human postmortem brain tissue. The largest of its kind to date and first to examine five brain regions, this study identified several novel differentially methylated CpG-sites as well as DMRs associated with AUD, providing potential insight into underlying mechanisms.

We found significant differentially methylated CpG-sites in two striatal regions. In the caudate nucleus, two epigenome-wide significant CpG-sites in *IREB2* and *HMGCR,* were identified*. IREB2* is a gene encoding iron regulatory protein 2, which is an RNA-binding protein that is involved in the regulation of cellular iron metabolism [https://www.genecards.org/cgi-bin/carddisp.pl?gene=IREB2]. Iron overload in the brain has previously been associated with cognitive decline in AUD (Listabarth et al., 2020). Neurodegeneration has been reported in two subjects with bi-allelic loss of function variants in *IREB2* (Cooper et al., 2019; Costain et al., 2019). *IREB2* has also been associated with smoking phenotypes (Watanabe et al., 2019). The association with smoking, which strongly affects DNA methylation (Sugden et al., 2019; Zeilinger et al., 2013), may be linked to the relevance of the gene to addiction phenotypes. In the present study, the *IREB2*-CpG-site was also differentially methylated in the anterior cingulate cortex (nominal significance), which might reflect a relevance in addiction phenotypes in multiple brain regions.

In the ventral striatum, 18 CpG-sites were epigenome-wide significantly associated with AUD. The strongest association was observed in a CpG-site in *SLC30A8*, which encodes a zinc efflux transporter that is involved in the accumulation of zinc in the intracellular vesicles. Zinc is a structure-building element in alcohol dehydrogenase (ADH) and thereby important for the proper function of ADH, which is needed to break down alcohol (Baj et al., 2020). Differential methylation in *SCL30A8* may lead to altered Zinc availability and indirectly impact ADH function, and thus alcohol metabolism. *SLC30A8* has also been implicated in type 1 and type 2 diabetes (Sladek et al., 2007). In both types epigenetic and transcriptomic levels of SLC30A8 have shown to be altered (Gu, 2017). Heavy alcohol consumption is also an established risk factor for type 2 diabetes on the phenotypic level (Baliunas et al., 2009). Three of the epigenome-wide significant CpG-sites were also previously differentially methylated in an independent EWAS of AUD (Witt et al., 2020); these convergent results might point towards a cross-tissue effect of these sites.

Significant regional methylation differences were observed in the anterior cingulate cortex, caudate nucleus, and ventral striatum. One differentially methylated region was observed in the anterior cingulate cortex and that region was annotated to HLA complex group 9, a non-coding RNA in the major histocompatibility complex (MHC). HLA antigens play a role in AUD and alcohol-associated liver disease (Shigeta et al., 1980). In the caudate nucleus, the DMR showing the strongest association with AUD was annotated to *DDAH2*, encoding for dimethylarginine dimethylaminohydrolase, which is involved in the formation of nitric oxide by indirect inhibition of nitric oxide synthase (NOS) [https://www.genecards.org/cgi-bin/carddisp.pl?gene=DDAH2]. Nitric oxide has previously been associated with sleep disturbances, as part of the sleep-wake state controlling metabolites (Cespuglio et al., 2012). Sleep disorders and disturbances, such as decreased total sleep time and decreased sleep efficiency, are common in individuals during periods of alcohol consumption and prolonged withdrawal (Koob & Colrain, 2020; Thakkar et al., 2015). In rodent studies, alcohol exposure influenced NOS expression in the brain (Davis & Syapin, 2005) and the knockout of neuronal NOS was associated with increased consumption of highly concentrated alcohol solutions (Spanagel et al., 2002). Although the DMR in *DDAH2*

was replicated by pyrosequencing, we did not observe differential gene expression between AUD cases and controls. It has to be noted, that differential gene expression is only partly explained by DNA-methylation differences. For example, in postmortem brain samples of individuals with schizophrenia and controls, 204 of 71,753 tested CpG gene pairs were significantly correlated (Chen et al., 2014). A potential functional relevance of the DMR in *DDAH2* requires further investigation, for instance in relation to contact frequency maps (chromosomal architecture/Hi-C), which can be simultaneously studied with the methylome in single-cell experiments (Li et al., 2019).

Of the six DMRs identified in the ventral striatum, a region in *TMEM232* showed the strongest association. *TMEM232* has previously been associated with respiratory traits, such as seasonal allergic rhinitis (Ramasamy et al., 2011). Another significant CpG-site was annotated to *HM13*. This gene encodes for minor histocompatibility antigen H13. In general, minor histocompatibility antigens function in the immune system by recognizing T cells (Robertson et al., 2007). No studies have investigated direct associations between AUD and H13 expression changes yet, but it is known that the immune system is downregulated in patients with AUD (Erickson et al., 2019).
GO-term analyses investigating molecular functions associated with differentially methylated CpG-sites did not yield significant results after multiple testing correction, which is most likely attributable to the limited statistical power. No significant enrichment was observed for each of the gene-sets in GWAS signals for AUD, which could indicate that differential methylation in the newly identified CpG-sites is more sensitive to environmental factors than genetic effects.
In the WGCNA analysis in VS a module enriched for immune-processes was most strongly associated with AUD, which are known to be influenced by alcohol abuse (Pasala et al., 2015).
In this brain region-specific analysis, comparing individuals with AUD and controls, we focused beside prefrontal areas on striatal regions, as previous studies have indicated that AUD may be associated with a striatal shift in activation from ventral to dorsal, as drug intake changes from goal-directed to habitual (DePoy et al., 2013; Vollstädt-Klein et al., 2010). These studies focus on changes in neurotransmitter release and functional connectivity but it is not known how epigenetic changes impact this functional striatal shift. Our epigenome-wide results provide a first basis to explore epigenetic contributions to functional striatal changes.
This study has several limitations. The first is PMI, which can influence the tissue quality. The longer the individual has been deceased before the tissue was extracted from the body, the further along are degradation processes (Glausier et al., 2019). While we corrected for this in our analyses our results may have been affected by postmortem degradation processes nevertheless. Second, we cannot infer whether the observed differences in DNA-methylation are a result of addiction or long-term alcohol consumption, which affects multiple organ systems. Third, the methylation array used in the present study combined with the bisulfite conversion does not distinguish between methylation and hydroxymethylation. Therefore, no conclusions can be drawn regarding methylation type specific effects. Also, for several CpG-sites the effect in the meta-analysis was driven by a large effect in one, but not the other

batch and in some of the cases this went hand-in-hand with a change in direction. For example, cg04214706 had a small positive effect, which was statistically not different from zero in the first batch, and a large negative effect in the second. Further samples are needed to validate these findings. Due to the sparse availability of human postmortem brain tissue, our sample size is small compared to EWAS in peripheral blood, which results in limited statistical power, especially taking into account the high multiple testing correction burden. However, EWAS analysis of peripheral blood allows to reveal only limited conclusions about differential methylation in the brain, whereas studies that examine multiple brain sites in a comparative fashion point to region-specific functional changes. Lastly, the correlational design of this analysis does not allow conclusions about the causality of the findings. DNA-methylation differences both be a result of AUD and be present in individuals before onset of the disorder.

Here, we identified novel associations of differential DNA-methylation between AUD cases and controls, which are prominent in alcohol-related pathways and diseases linked with AUD. To confirm these observations, larger samples are needed from the respective brain regions. Human postmortem brain tissue is difficult to obtain and very few brain banks focus on substance use disorders. Combining existing datasets, generating a larger amount of DNA-methylation data, and integrating multi-omics data, could lead to more conclusive results that may help to understand the molecular changes due to substance abuse in the brain and eventually to the identification of drug targets for more effective treatment of substance use disorders.

2.6   Funding and Disclosures

2.7   Acknowledgments

2.8 Author Contributions

SHW, MR, RS, MMN, and ACH planned the investigation. MMF and ACH performed the DNA and RNA extraction and SHH, PH, FD and MMN were responsible for generating genome-wide methylation data. LZ, JF, JCF and FS developed the analysis plan. LZ and JF performed all statistical analyses. HD, ACH and MMF performed replication and validation experiments. LZ, MMF, JCF, LS, MR, FS, and SHW reviewed the literature for the paper. LZ, MMF, FS and SHW drafted the manuscript. All authors contributed, revised, and edited the final manuscript critically. All authors agreed to the publication of the final version of the manuscript.

2.9   Supplementary Information

2.9.1   Supplementary Texts

Supplementary Text 2.S1. Detailed description of obtained postmortem human brain samples.

All tissue samples were obtained from the New South Wales Tissue Resource Centre (University of Sydney, Australia). Tissues were collected as described in Harper et al. (2003, Progress in Neuro-Psychopharmacology & Biological Psychiatry 27: 951– 961), where cases with prolonged agonal life support, cases with a history of cerebral infarction, head injury, or neurodegenerative disease (e.g., Alzheimer's disease) were excluded. Further exclusion criteria were cases with developmental disorder, head injury at time of death, recent cerebral stroke, neurological disorder, history of intravenous drug use, brain on gross examination showing obvious abnormalities, and cases with a history of other psychiatric disorders (e.g. autism, attention deficit-hyperactivity disorder, schizophrenia). We further excluded cases with reported anxiety or mood disorders or suicides have been excluded as well as cases with significant amounts of psychiatric medication (e.g., opioids, benzodiazepines; concentration <0.1 mg/L).

Supplementary Text 2.S2. WGCNA results for Anterior Cingulate Cortex, Brodmann Area 9, and Putamen.

Weighted correlation network analysis for Anterior Cingulate Cortex resulted in 10 modules consisting of 34–11,588 CpG-sites (Md = 606.5). The highest correlation with AUD was observed for module "green" (r = .44, p = 8.54e-04), which was enriched for the molecular functions "ligand-gated sodium channel activity" (p = 0.0003), "sodium channel activity" (p = 0.0004), and the biological process "noradrenergic neuron differentiation" (p = 0.0007). In Brodmann Area 9 20 modules, with a median sizes of 287 CpG-sites per module (range: 38-7,960) were constructed. Module "blue" showed the highest correlation with AUD (r = -.55, p = 4e^{-05}). GO-analysis revealed enrichment for the cellular components "actomyosin", (p = 0.0001), "stress fiber" (p = 0.0007), and "contractile actin filament bundle" (p = 0.0007). Eight modules were constructed for putamen, which consisted of 78-13,091 CpG-site with a median size of 2,020. Module "yellow" had the highest correlation with AUD (r = -.52, p = 8.13e^{-08}). This module was enriched for the biological processes "response to immune response of other organism involved in symbiotic interaction", (p = 0.0004), "response to host immune response" (p = 0.0004), and "ventral spinal cord interneuron fate commitment" (p = 0.001). Scatterplots showing the association of gene significance and module membership for the three modules can be found in Supplementary Figure 2.S2.

Supplementary Text 2.S3. Methods and results for replication by pyrosequencing and functional validation for *DDAH2*.

Samples

For a subsample of n=87 sufficient material for Pyrosequencing and the TaqMan Assay was available.

Pyrosequencing

The CpG site cg04074004 was analyzed by pyrosequencing, using the commercially available PyroMark CpG assay Hs_DDAH2_03_PM (Qiagen, Hilden, Germany). All samples (n=87) were carefully randomized on positions on sequencing plates. DNA (500ng) was bisulfite-treated using the EpiTect Fast 96 Kit (Qiagen, Hilden, Germany). We controlled for bisulfite conversion reaction, PCR amplification, and pyrosequencing reaction by including unmethylated and methylated DNA (EpiTect PCR Control DNA Set, Qiagen, Hilden, Germany).

The DNA fragment was amplified by PCR (PyroMark PCR Kit, Qiagen, Hilden, Germany) from 2 µl of bisulfite-treated DNA in a PCR volume of 25 µl. Successful amplification and the specificity of the PCR product (137 base pairs) was checked on an agarose gel. To ensure equal amplification in the CpG assay an additional mixture of DNA with a 50% DNA methylation level was prepared from unmethylated, converted and methylated, converted DNA (EpiTect PCR Control DNA Set, Qiagen, Hilden, Germany). Then, 8 µL of PCR product was processed for pyrosequencing analysis with following manufacturer´s recommendations (PyroMark Gold Q24 reagents, Qiagen, Hilden, Germany), sequenced with the sequencing primer Hs_DDAH2_03_PM (Qiagen, Hilden, Germany) with the PyroMark Q24 instrument (Qiagen, Hilden, Germany). The percentage of methylation was quantified using the PyroMark Q24 software version 2.0.8 Build 3 (Qiagen, Hilden, Germany). The sequencing was performed in triplicates.

TaqMan Assay

RNA was extracted from caudate nucleus samples using the RNeay microKit (Qiagen, Hilden, Germany). The analysis was performed on triplicates of each gene and sample using the PCR Master Mix and FAM dye-labeled TaqMan MGB probes from ThermoFisher Scientific (Massachusetts, US). The following primers have been used for the human DDAH2 gene: Forward primer sequence 1: 5-CAAAAGGCTGTCCGGGCAATGGCAG-3, position 854 on cDNA, RefSeq NM-013974.3, TaqMan assay ID Hs00967863_g1, 60 bp amplicon; forward primer sequence 2: 5- GCTCGTAGGCCAGAGGTCGATGGAG-3, position 560 on cDNA, RefSeq NM-013974.3, TaqMan assay ID Hs00967860_g1, 81 bp amplicon). As housekeeping genes the human 18S RNA (TaqMan assay ID Hs99999901_s1, 187 bp amplicon) and human Gapdh (TaqMan assay ID Hs02786624_g1, 157 bp amplicon) were used. SDS 2.2.2 software (ABI) was employed to analyze fluorescence intensity and calculation of the theoretical cycle number when a defined threshold was reached (Ct-value).

Statistical Analysis

R version 3.6.1 was used for quality control filtering and statistical analyses of the pyrosequencing results (http://www.r-project.org). We removed measurements marked as unreliable by the PyroMark software. Triplicate measurements were averaged after the removal of outliers (values deviating more than 3% for Pyrosequencing and more than 5% for TaqMan Assay). For expression of DDAH2, delta scores between the primer pairs and the housekeeping genes were calculated. We calculated student's t-Tests to compare DNA methylation of cg04074004 and delta-scores of gene expression between AUD cases and controls, as well as an ANCOVA with the same covariates as in the EWAS.

2.9.2 Supplementary Tables

Supplementary Tables 2.S3a-2.S3e have been reduced to show the top 25 findings without information on phantom4 and phantom5 enhancers, the full summary statistics showing all ~670.000 CpG sites are available under
https://www.nature.com/articles/s41386-021-01228-7

Supplementary Table 2.S1. Additional Phenotype information

Characteristic	Cases	Controls	p
Cell counts by region			
Anterior Cingulate Cortex	0.30 (0.17)	0.27 (0.17)	0.584
Brodmann Area 9	0.38 (0.05)	0.40 (0.10)	0.381
Putamen	0.21 (0.06)	0.21 (0.05)	0.857
Caudate Nucleus	0.23 (0.05)	0.23 (0.05)	0.84
Ventral Striatum	0.26 (0.07)	0.25 (0.07)	0.37
Cause of death			
Cardiac	14	23	
Cardiovascular	4	18	
Vascular	2	2	
Hepatic	6		
Infection	5	1	
COPD	1	1	
Cardiovascular / Respiratory	1		
Respiratory	1	1	
Toxicity	6	2	
Hepatic/Infection	1		
Blood loss	1		
Pancreatic	1		
Carcinoma		1	
Suicide		1	
Missing	10	8	

Data are presented as count (n) or mean (±SD), p: p-value of t-Test comparing cases and controls.

Supplementary Table 2.S2. WGCNA input

Brain Region	# CpG-Sites	Soft Power Threshold
ACC	29059	3
BA9	24157	5
Caudate Nucleus	34943	4
Ventral Striatum	35007	4
Putamen	28624	2

Supplementary Table 2.S3a Associations between top 25 CpG sites and AUD case/control status in ACC

Chr	Position	CG	Gene	Std Err	Beta	P	N_for_probe	mean M	FDR	Relation to UCSC CpG Island
3	27766382	cg02391509	NA	0.147	-0.794	4.26E-06	54	-3.024	1	S_Shore
12	74416010	cg14637885	NA	0.119	-0.643	4.40E-06	54	1.107	1	
10	134886108	cg04319990	NA	0.089	0.465	7.54E-06	54	1.851	1	S_Shore
15	78591482	cg09197434	WDR61	0.137	-0.715	7.56E-06	54	-4.148	1	
11	67929299	cg07140176	KMT5B	0.126	-0.652	9.09E-06	54	3.100	1	
4	12411504	cg01343876	NA	0.094	-0.483	1.00E-05	54	0.912	1	
6	155281917	cg05964510	NA	0.087	0.430	1.89E-05	54	2.854	1	
16	67587126	cg26536319	NA	0.106	0.520	2.00E-05	54	3.900	1	
1	22290005	cg27522078	NA	0.082	0.395	2.46E-05	54	1.001	1	
22	39003825	cg25398307	FAM227A	0.110	0.534	2.46E-05	54	2.585	1	
10	104263600	cg13071996	ACTR1A;SUFU	0.072	0.345	2.65E-05	54	-3.666	1	S_Shore
10	228801	cg21662081	ZMYND11	0.088	0.425	2.65E-05	54	2.618	1	
5	1933187	cg17143073	NA	0.116	-0.556	2.73E-05	54	3.579	1	S_Shore
12	13153637	cg21878074	HEBP1;HTR7P1	0.068	0.325	2.87E-05	54	-3.373	1	Island
5	103942397	cg11319477	NA	0.077	0.367	3.05E-05	54	3.091	1	
8	130426887	cg23468312	CCDC26	0.155	0.732	3.56E-05	54	1.295	1	
17	8301697	cg02311588	RNF222	0.079	0.370	3.63E-05	54	2.937	1	
8	101956521	cg13231392	YWHAZ	0.082	0.383	4.09E-05	54	1.187	1	
7	27190849	cg03547218	HOXA-AS3	0.118	-0.548	4.24E-05	54	-2.675	1	Island
12	308158	cg06569830	SLC6A12	0.092	0.430	4.31E-05	54	2.655	1	
10	28955341	cg05705492	NA	0.103	0.480	4.37E-05	54	2.145	1	
17	17794917	cg10145540	TOM1L2	0.067	-0.311	4.68E-05	54	1.878	1	
14	21539025	cg03907077	NDRG2;ARHGEF40	0.046	0.215	4.81E-05	54	-2.325	1	S_Shore
1	110693757	cg05949020	SLC6A17	0.060	0.279	4.81E-05	54	-3.639	1	Island
7	152564298	cg08429023	NA	0.108	0.496	4.85E-05	54	4.636	1	

Supplementary Table 2.S3b Associations between top 25 CpG sites and AUD case/control status in BA9

Chr	Position	CG	Gene	Beta	Std Err	P	N probe	mean M	FDR	Relation to UCSC CpG Island
5	96479253	cg15234096	*LIX1*	-0.659	0.117	4.02E-06	48	1.979	1	Island
19	50083579	cg18665943	*NOSIP;PRRG2*	0.694	0.127	6.43E-06	48	-4.280	1	Island
7	25892407	cg09284066	*NA*	1.272	0.243	1.21E-05	48	-2.823	1	
11	73471141	cg26725471	*RAB6A*	1.120	0.215	1.28E-05	48	-5.853	1	N_Shore
16	72614268	cg10745876	*LINC01572*	-0.614	0.121	1.85E-05	48	3.097	1	S_Shore
14	105451561	cg23541019	*C14orf79*	0.937	0.185	1.91E-05	48	5.518	1	
3	127642152	cg09104003	*KBTBD12*	0.610	0.120	1.92E-05	48	2.875	1	Island
3	113546933	cg23719571	*NA*	-0.760	0.152	2.26E-05	48	3.724	1	Island
18	35146393	cg01273679	*CELF4*	0.635	0.130	3.37E-05	48	-4.325	1	Island
8	3233041	cg18390727	*CSMD1*	-0.626	0.129	3.67E-05	48	2.284	1	
12	52396665	cg03693462	*NA*	0.417	0.086	3.88E-05	48	1.850	1	Island
18	13290021	cg08728128	*LDLRAD4*	-0.761	0.159	4.14E-05	48	2.720	1	
2	37384523	cg16795804	*EIF2AK2*	-0.622	0.132	5.13E-05	48	-1.850	1	N_Shelf
10	48369027	cg11944118	*ZNF488*	-0.544	0.116	5.66E-05	48	2.901	1	N_Shore
17	47841577	cg00749852	*FAM117A*	-0.549	0.117	5.69E-05	48	-3.853	1	Island
15	99456342	cg05920405	*IGF1R*	0.650	0.139	5.85E-05	48	3.864	1	Island
11	75114506	cg13857569	*RPS3;SNORD15B*	0.765	0.164	5.86E-05	48	3.182	1	Island
17	73451921	cg04160100	*TMEM94*	-0.864	0.187	6.57E-05	48	-1.552	1	
12	124443576	cg09805030	*CCDC92*	0.496	0.107	6.74E-05	48	3.449	1	
4	77997194	cg17818025	*CCNI*	6.877	1.493	7.06E-05	48	-9.713	1	
6	31862943	cg20208853	*EHMT2*	-0.912	0.198	7.07E-05	48	2.843	1	S_Shore
4	738199	cg23486923	*PCGF3*	-0.682	0.148	7.07E-05	48	2.259	1	N_Shore
20	57556688	cg04474326	*NELFCD*	-0.317	0.069	7.09E-05	48	-3.712	1	Island
1	16476252	cg04987201	*EPHA2*	-0.556	0.121	7.50E-05	48	2.956	1	Island
1	228345490	cg08521967	*GJC2*	-0.676	0.148	7.62E-05	48	1.720	1	

Supplementary Table 2.S3c Associations between top 25 CpG sites and AUD case/control status in PUT

Chr	Position	CG	Gene	Std Err	Beta	P	N	FDR	meanM	Relation to UCSC CpG Island
2	24163024	cg11763458	UBXN2A	0.030	-0.156	1.59E-06	94	0.57780	-4.019	N_Shore
13	109329092	cg22775535	MYO16	0.034	-0.176	1.66E-06	94	0.57780	2.502	
8	132446137	cg02547011	NA	0.070	0.350	3.52E-06	94	0.64936	3.290	
2	225267119	cg09826622	FAM124B	0.059	-0.298	3.74E-06	92	0.64936	NA	
3	44498615	cg26555960	ZNF445	0.050	-0.240	8.30E-06	94	0.86089	3.562	
7	92100819	cg10898776	ERVW-1	0.159	-0.756	9.99E-06	94	0.86089	1.931	
13	49668377	cg03071917	FNDC3A	0.089	0.422	1.02E-05	93	0.86089	NA	
17	37071381	cg16778811	LASP1	0.031	0.145	1.07E-05	94	0.86089	2.120	N_Shelf
10	76914008	cg06832364	SAMD8	0.095	0.449	1.12E-05	94	0.86089	3.100	
2	58265673	cg08018809	VRK2;	0.085	0.396	1.45E-05	94	0.98373	3.190	
1	40349894	cg22691587	TRIT1	0.043	-0.199	1.56E-05	94	0.98373	1.774	S_Shore
5	143505292	cg22936990	NA	0.058	-0.264	2.06E-05	94	1	2.962	
7	41084954	cg05969441	NA	0.085	0.384	2.16E-05	94	1	3.456	
4	111533509	cg05722981	NA	0.054	0.242	2.45E-05	94	1	-2.439	S_Shore
17	5347650	cg07377891	DHX33	0.053	0.240	2.46E-05	94	1	3.032	Island
20	62401049	cg00215103	ZBTB46	0.074	-0.326	3.38E-05	94	1	3.566	N_Shore
4	23781082	cg22151856	NA	0.046	0.200	3.74E-05	94	1	3.021	
11	106423863	cg16567688	NA	0.040	-0.173	4.08E-05	94	1	2.846	
17	74074118	cg24181662	ZACN	0.030	0.132	4.31E-05	94	1	0.767	S_Shore
7	5424177	cg23676269	TNRC18	0.069	0.300	4.52E-05	94	1	2.503	N_Shelf
16	422157	cg04507446	TMEM8A	0.082	0.352	5.07E-05	94	1	4.110	N_Shore
17	36890321	cg23901967	CISD3;PCGF2	0.036	0.154	5.13E-05	94	1	-0.102	S_Shelf
2	59401418	cg02110909	NA	0.105	0.452	5.34E-05	93	1	NA	
19	18700260	cg15899199	C19orf60	0.043	-0.182	5.51E-05	94	1	-3.986	Island
22	23856505	cg20933483	NA	0.030	-0.126	5.55E-05	94	1	2.322	

Supplementary Table 2.S3d Associations between top 25 CpG sites and AUD case/control status in CN

Chr	Position	CG	Gene	Std Err	Beta	P	Direction	Het ISq	Het ChiSq	Het Df	Het PVal	FDR	Relation to UCSC CpG Island
15	78729669	cg04214706	IREB2	-0.393	0.073	7.58E-08	+-	89.9	9.865	1	0.0017	0.0296	N_Shore
5	74633012	cg26685658	HMGCR	-5.919	1.105	8.53E-08	--	59.1	2.447	1	0.1178	0.0296	Island
5	37059055	cg20043301	NIPBL	0.586	0.114	2.55E-07	++	83.6	6.102	1	0.0135	0.0591	
22	50120053	cg20197706	NA	0.269	0.053	4.56E-07	++	63.9	2.772	1	0.0959	0.0595	S_Shore
6	33156463	cg21509966	COL11A2	0.271	0.054	4.63E-07	++	0	0.305	1	0.5807	0.0595	N_Shelf
4	160266334	cg04696208	RAPGEF2	0.553	0.110	5.49E-07	?+	0	0	0	1.0000	0.0595	
2	237416620	cg03182782	IQCA1	0.217	0.044	5.99E-07	++	0	0.481	1	0.4880	0.0595	S_Shore
3	146498234	cg15285975	NA	0.287	0.058	7.49E-07	++	0	0.232	1	0.6302	0.0650	
17	62076318	cg20433906	PRR29-AS1;PRR29	-0.231	0.047	9.34E-07	--	0	0.405	1	0.5244	0.0654	
4	1379690	cg09691317	UVSSA	-0.235	0.048	9.41E-07	--	0	0.172	1	0.6782	0.0654	
1	87035652	cg19555551	CLCA4	0.418	0.087	1.45E-06	++	0	0.874	1	0.3498	0.0875	
1	3111280	cg21836418	PRDM16	0.566	0.118	1.56E-06	++	0	0.26	1	0.6099	0.0875	N_Shore
3	19752610	cg25650360	NA	0.281	0.059	1.65E-06	++	59.8	2.486	1	0.1148	0.0875	
7	6738977	cg01982507	ZNF12	0.328	0.069	1.76E-06	++	0	0.622	1	0.4301	0.0875	
6	114287784	cg02425558	HDAC2	-0.921	0.194	2.04E-06	?-	0	0	0	1.0000	0.0934	N_Shelf
18	7857178	cg02206983	PTPRM	0.167	0.035	2.24E-06	++	9.8	1.109	1	0.2922	0.0934	
4	717989	cg18760467	PCGF3	-0.318	0.067	2.29E-06	--	0	0.198	1	0.6567	0.0934	S_Shore
7	95959582	cg14044096	NA	-0.361	0.077	2.56E-06	--	0	0.46	1	0.4976	0.0965	
20	60553835	cg00845415	TAF4	-0.420	0.089	2.64E-06	--	82.4	5.688	1	0.0171	0.0965	S_Shore
9	138800390	cg25200616	CAMSAP1	-0.229	0.049	2.91E-06	--	0	0.028	1	0.8670	0.0985	S_Shore
15	33757726	cg04093322	RYR3	0.291	0.062	2.98E-06	++	0	0.312	1	0.5765	0.0985	S_Shore
1	753223	cg15979415	FAM87B	-0.110	0.024	3.28E-06	--	0	0.288	1	0.5916	0.1008	
16	2301626	cg08968904	ECI1	-0.850	0.184	3.65E-06	+-	0	0.914	1	0.3391	0.1008	Island
1	231004326	cg10333268	C1orf198	5.417	1.172	3.80E-06	++	0	0.358	1	0.5496	0.1008	Island
6	29003627	cg23836449	LOC-100129636	-0.381	0.083	3.93E-06	--	0	0.11	1	0.7404	0.1008	

Supplementary Table 2.S3e Associations between top 25 CpG sites and AUD case/control status in VS

Chr	Position	CG	Gene	Std Err	Beta	P	Direction	Het ISq	Het ChiSq	Het Df	Het PVal	FDR	Relation to UCSC CpG Island
8	117961971	cg17163967	SLC30A8	0.504	0.088	1.09E-08	++	0	0.527	1	0.46790	0.00757	
1	178998656	cg23933289	FAM20B	0.269	0.048	2.36E-08	++	19.5	1.242	1	0.26500	0.00821	S_Shelf
15	69908472	cg27512762	PCAT29	0.170	0.032	6.80E-08	-+	67.3	3.058	1	0.08036	0.01575	Island
16	68563886	cg02941431	NA	-0.251	0.047	1.27E-07	--	65	2.859	1	0.09087	0.01666	S_Shore
7	1008720	cg02028351	COX19	0.180	0.034	1.28E-07	++	0	0.052	1	0.82030	0.01666	S_Shore
3	183274235	cg06427508	KLHL6	0.379	0.072	1.44E-07	++	0	0.075	1	0.78370	0.01666	
12	132882652	cg16767842	GALNT9	0.239	0.046	1.74E-07	-+	87.5	8.032	1	0.00460	0.01731	S_Shore
16	4901809	cg02741291	UBN1	0.579	0.113	2.61E-07	?+	0	0	0	1.00000	0.02265	S_Shelf
16	1946176	cg10824492	NA	-0.147	0.029	3.35E-07	--	18.9	1.233	1	0.26690	0.02585	
19	35168316	cg18564234	SCGB1B2P; ZNF302	-0.776	0.153	4.13E-07	--	75.7	4.109	1	0.04266	0.02869	Island
13	7687406	cg06630619	NA	-0.430	0.085	4.76E-07	--	80.5	5.132	1	0.02349	0.03008	
11	1215457	cg23618269	MUC5AC	-0.432	0.086	5.25E-07	--	42.9	1.752	1	0.18560	0.03041	Island
14	96177134	cg13545750	TCL1A	-0.226	0.046	7.21E-07	--	0	0.047	1	0.82910	0.03855	N_Shelf
6	29400397	cg26754552	NA	0.277	0.057	9.88E-07	++	21.8	1.279	1	0.25820	0.04762	
5	79331052	cg04360099	THBS4	0.303	0.062	1.03E-06	++	0	0.058	1	0.80960	0.04762	Island
17	18210650	cg16021181	TOP3A	-0.307	0.063	1.11E-06	--	0	0.015	1	0.90280	0.04790	
18	11147785	cg12049992	PIEZO2	-0.280	0.058	1.20E-06	+-	68.8	3.205	1	0.07342	0.04790	N_Shore
11	59390857	cg02849689	NA	-0.298	0.061	1.24E-06	--	2.4	1.025	1	0.31140	0.04790	
1	25869937	cg09261020	LDLRAP1	0.303	0.063	1.42E-06	-+	62.7	2.684	1	0.10140	0.05178	Island
5	87899754	cg02752121	LINC00461	0.390	0.081	1.67E-06	++	0	0.478	1	0.48930	0.05395	S_Shore
12	124710353	cg11858667	ZNF664RFLNA	-0.329	0.069	1.69E-06	?-	0	0	0	1.00000	0.05395	
7	1847567	cg04244307	NA	0.160	0.034	1.75E-06	-+	50.5	2.019	1	0.15540	0.05395	
10	105519992	cg09926728	SH3PXD2A	-0.308	0.064	1.79E-06	--	83.7	6.141	1	0.01321	0.05395	
13	88869717	cg03258300	LOC105370306	-0.518	0.109	1.90E-06	?-	0	0	0	1.00000	0.05495	
4	10519217	cg04802946	CLNK	0.385	0.081	2.07E-06	?+	0	0	0	1.00000	0.05742	

Supplementary Table 2.S4. Regression coefficients for the epigenome-wide significant CpG-sites in other brain regions and in peripheral blood.

CpG-Site	Anterior Cingulate Cortex		Brodmann Area 9		Putamen		Caudate Nucleus		Ventral Striatum		Peripheral Blood	
	Effect	P	Effect	P	Effect	P	Effect	P	Effect	P	Effect	P
cg02028351	0.061	0.635	-0.077	0.627	-0.088	0.165	-0.036	0.594	0.18	**1.28E-07**	0.012	0.808
cg02741291					0.046	0.567	0.02	0.901	0.579	**2.61E-07**	0.014	0.860
cg02849689	0.387	**0.012**	-0.029	0.877	0.043	0.542	-0.161	0.174	-0.298	**1.24E-06**	-0.070	**0.045**
cg02941431	-0.016	0.894	-0.128	0.368	-0.015	0.729	-0.056	0.383	-0.251	**1.27E-07**	0.057	0.232
cg04214706	-0.381	**0.005**	0.172	0.4	-0.064	0.434	-0.393	**7.58E-08**	-0.093	0.348	-0.139	0.082
cg04360099	-0.061	0.648	0.036	0.874	0.037	0.706	0.078	0.408	0.303	**1.03E-06**	0.096	0.183
cg06427508	-0.054	0.74	0.081	0.685	-0.016	0.777	0.025	0.683	0.379	**1.44E-07**	-0.111	**0.024**
cg06630619	0.166	0.465	0.064	0.79	-0.181	0.101	0.024	0.847	-0.43	**4.76E-07**	-0.041	0.525
cg10824492	-0.084	0.354	-0.227	0.148	0.02	0.62	-0.084	0.123	-0.147	**3.35E-07**	-0.025	0.662
cg12049992	0.327	0.121	0.166	0.653	-0.051	0.409	-0.19	**0.023**	-0.28	**1.20E-06**	0.085	0.296
cg13545750	0.045	0.654	0.006	0.958	-0.104	**0.035**	-0.011	0.878	-0.226	**7.21E-07**	-0.018	0.628
cg16021181	0.053	0.635	0.259	0.248	0.155	0.15	0.01	0.926	-0.307	**1.11E-06**	-0.023	0.822
cg16767842	0.073	0.537	0.022	0.893	0.079	0.194	0.166	**0.02**	0.239	**1.74E-07**	0.054	0.623
cg17163967	-0.014	0.93	0.03	0.882	0.077	0.221	-0.114	0.171	0.504	**1.09E-08**	0.034	0.693
cg18564234	-0.187	0.276	0.242	0.116	-0.076	0.33	-0.006	0.966	-0.776	**4.13E-07**	0.012	0.851
cg23618269	-0.147	0.617	-0.104	0.657	-0.04	0.704	0.011	0.936	-0.432	**5.25E-07**	-0.099	0.349
cg23933289	0.13	0.313	-0.067	0.696	-0.024	0.708	-0.043	0.564	0.269	**2.36E-08**	-0.042	0.455
cg26685658	0.891	0.626	0.976	0.381	-1.943	0.089	-5.919	**8.53E-08**	0.632	0.629	-0.392	0.263
cg26754552	-0.144	0.394	-0.079	0.589	-0.044	0.543	0.05	0.591	0.277	**9.88E-07**	-0.063	0.173
cg27512762	-0.085	0.358	-0.072	0.568	-0.032	0.518	0.088	0.065	0.17	**6.80E-08**	0.115	**0.002**

Supplementary Table 2.S5a. Results of comparison between AUD cases and controls (epigenome-wide significant regions) in the caudate nucleus.

Chr	Start	End	Min_p	N_probes	z_p	z_sidak_p	CG	Gene
6	31696063	31696520	1.12E-17	17	1.85E-20	2.81E-17	cg08550588	DDAH2
5	42756786	42757024	9.81E-07	6	3.11E-11	9.08E-08	cg18472410	CCDC152
9	138800324	138800391	8.93E-06	3	2.83E-10	2.93E-06	cg00022024	CAMSAP1
6	55039232	55039383	0.0002647	4	1.14E-08	5.26E-05	cg10725720	HCRTR2
3	10149974	10150225	0.0005157	7	1.56E-07	0.0004319	cg00166722	FANCD2OS
3	49459909	49460058	1.85E-05	5	1.57E-07	0.0007315	cg21926782	AMT;NICN1
3	170136766	170136921	0.005362	4	4.40E-07	0.00197	cg02241055	CLDN11
2	175190675	175190822	0.005362	4	5.10E-07	0.002406	cg02216981	LINC01305
1	15272238	15272384	0.00151	5	5.86E-07	0.002783	cg11648522	KAZN
14	67940414	67940426	0.001105	2	5.73E-08	0.003311	cg06215536	TMEM229B
16	68270252	68270388	0.005186	6	7.70E-07	0.003925	cg04513006	ESRP2

Supplementary Table 2.S5b. Results of comparison between AUD cases and controls (epigenome-wide significant regions) in the ventral striatum.

Chr	Start	End	Min_p	N_probes	z_p	z_sidak_p	CG	Gene
5	110062343	110062730	0.0001288	11	4.04E-11	7.25E-08	cg23279021	TMEM232
3	10149963	10150225	0.0001288	8	8.40E-10	2.23E-06	cg10729496	FANCD2OS
20	30135144	30135292	0.0003445	5	3.61E-08	0.0001692	cg15815607	HM13
15	22833149	22833309	0.003964	6	5.16E-07	0.002237	cg07959104	TUBGCP5
17	18210638	18210651	0.009594	2	6.08E-07	0.03195	cg03540694	TOP3A
7	99765805	99765819	0.00969	2	6.81E-07	0.03323	cg18810646	GAL3ST4

Supplementary Table 2.S6a. Top 10 associated GO-terms for the AUD case/control comparison in the caudate nucleus.

Term	Ont	N	DE	P.DE	FDR
homophilic cell adhesion via plasma membrane adhesion molecules	BP	153	28	5.37E-06	0.1197854
cell-cell adhesion via plasma-membrane adhesion molecules	BP	234	34	1.68E-05	0.1869303
dodecenoyl-CoA delta-isomerase activity	MF	3	3	6.74E-05	0.5008741
carbon-oxygen lyase activity	MF	67	12	0.0001516	0.6269051
protein localization to chromosome	BP	74	13	0.000175	0.6269051
hydro-lyase activity	MF	50	10	0.0001764	0.6269051
protein localization to chromatin	BP	22	7	0.0002047	0.6269051
peptidyl-lysine dimethylation	BP	15	6	0.000225	0.6269051
establishment of protein localization to chromatin	BP	8	4	0.0003527	0.8735079
regulation of dendrite development	BP	126	21	0.0005592	1

Supplementary Table 2.S6b. Top 10 associated GO-terms for the AUD case/control comparison in the ventral striatum.

Term	Ont	N	DE	P.DE	FDR
Lsm1-7-Pat1 complex	CC	5	4	6.49E-05	1
T cell proliferation	BP	167	20	0.0001892	1
receptor signaling complex scaffold activity	MF	24	8	0.0003144	1
negative regulation of transcription from RNA polymerase II promoter in response to stress	BP	12	5	0.0003586	1
regulation of T cell proliferation	BP	144	17	0.0003979	1
organelle part	CC	8811	553	0.0004222	1
AP-1 adaptor complex	CC	7	4	0.000459	1
negative regulation of endoplasmic reticulum unfolded protein response	BP	12	5	0.0005909	1
positive regulation of male gonad development	BP	7	4	0.0006815	1
RNA polymerase binding	MF	70	11	0.0008278	1

Supplementary Table 2.S7a. Top 10 associated GO-terms for the WGCNA-module "black" (caudate nucleus).

Term	Ont	N	DE	P.DE	FDR
PML body	CC	70	12	.0012	1
G-rich strand telomeric DNA binding	MF	6	3	.0014	1
sperm mitochondrion organization	BP	2	2	.0017	1
presynapse assembly	BP	26	7	.0017	1
ventricular system development	BP	20	6	.0017	1
cardiac ventricle development	BP	96	15	.0017	1
ventricular septum development	BP	55	11	.0018	1
type I transforming growth factor beta receptor binding	MF	10	4	.0018	1
regulation of presynapse organization	BP	20	6	.0020	1
regulation of presynapse assembly	BP	20	6	.0020	1

Supplementary Table 2.S7b. Top 10 associated GO-terms for the WGCNA-module "purple" (ventral striatum).

Term	Ont	N	DE	P.DE	FDR
regulation of T cell proliferation	BP	86	9	4.32E-06	.0715
regulation of leukocyte cell-cell adhesion	BP	187	13	6.83E-06	.0715
regulation of T cell activation	BP	197	13	1.26E-05	.0881
leukocyte cell-cell adhesion	BP	205	13	1.78E-05	.0932
T cell proliferation	BP	103	9	2.38E-05	.0998
regulation of cell-cell adhesion	BP	263	15	2.92E-05	.1019
regulation of lymphocyte proliferation	BP	119	9	7.03E-05	.1725
negative regulation of T cell proliferation	BP	30	5	7.33E-05	.1725
regulation of mononuclear cell proliferation	BP	120	9	7.47E-05	.1725
regulation of leukocyte proliferation	BP	123	9	8.97E-05	.1879

Supplementary Table 2.S8a. GWAS ATLAS results for *IREB2* [retrieved 12.01.2021].

atlas ID	PMID	Year	Domain	Trait	P-value	N
4315	30643251	2019	Psychiatric	Cigarettes per day	3.86E-82	263954
3353	31427789	2019	Psychiatric	Number of cigarettes previously smoked daily	6.32E-54	90143
3335	31427789	2019	Psychiatric	Light smokers, at least 100 smokes in lifetime	6.36E-21	105610
20	20418890	2010	Psychiatric	Number of cigarettes smoked per day	4.04E-17	38181
3630	31427789	2019	Environment	Illnesses of father: Lung cancer	2.80E-14	355137
3632	31427789	2019	Environment	Illnesses of father: Chronic bronchitis/emphysema	1.93E-13	355137
4278	30804560	2019	Respiratory	FEV1	3.78E-13	400102
3640	31427789	2019	Environment	Illnesses of mother: Lung cancer	2.98E-12	367939
3278	31427789	2019	Mortality	Father still alive	1.08E-11	375841
4282	30804560	2019	Respiratory	FEV1	1.68E-11	321047
3355	31427789	2019	Psychiatric	Ever stopped smoking for 6+ months	5.73E-11	93871
3279	31427789	2019	Mortality	Father's age at death	9.02E-11	283990
3643	31427789	2019	Environment	Illnesses of mother: Chronic bronchitis/emphysema	9.62E-11	367939
4040	29906448	2018	Psychiatric	Schizophrenia/Bipolar disorder	8.75E-10	107620
3277	31427789	2019	Environment	Maternal smoking around birth	2.70E-09	331862
1227	28748955	2017	Mortality	Life span	5.50E-09	116279
4279	30804560	2019	Respiratory	FVC	1.99E-08	400102
4316	30643251	2019	Psychiatric	Smoking cessation	2.14E-08	312821
3982	29483656	2018	Psychiatric	Schizophrenia	3.85E-08	105318
4280	30804560	2019	Respiratory	FEV1/FVC ratio	4.00E-08	400102
11	25056061	2014	Psychiatric	Schizophrenia	1.05E-07	82315
13	24280982	2014	Psychiatric	Schizophrenia vs Bipolar disorder	1.05E-07	16381
3549	31427789	2019	Body Structures	Mouth/teeth dental problems: Dentures	1.27E-07	385026
3887	27863252	2016	Immunological	Mean corpuscular hemoglobin (three-way meta)	4.60E-07	172332
3194	31427789	2019	Environment	Number of vehicles in household	5.73E-07	383893
4283	30804560	2019	Respiratory	FVC	6.77E-07	321047
4284	30804560	2019	Respiratory	FEV1/FVC ratio	8.06E-07	321047

Supplementary Table 2.S8b. GWAS ATLAS results for *SLC30A8* [retrieved 12.01.2021].

atlas ID	PMID	Year	Domain	Trait	P-value	N
4102	29403010	2018	Metabolic	Blood sugar	1.73E-08	93146
4045	30054458	2018	Endocrine	Type 2 Diabetes	1.40E-07	659256
4086	30297969	2018	Endocrine	Type 2 Diabetes (adjusted for BMI)	1.67E-07	898130
4085	30297969	2018	Endocrine	Type 2 Diabetes	5.48E-07	898130
4176	30718926	2019	Endocrine	Type 2 Diabetes	6.10E-07	191764
3469	31427789	2019	Metabolic	Impedance measures - Trunk fat mass	9.85E-07	379578

Supplementary Table 2.S8c. GWAS ATLAS results for *DDAH2* [retrieved 20.01.2021].[1]

| atlas ID	PMID	Year	Domain	Trait	P-value	N
1204	24390342	2014	Connective Tissue	Rheumatoid Arthritis	2.0378E-69	103638
1203	24390342	2014	Connective Tissue	Rheumatoid Arthritis	3.6883E-63	58284
2037	27723758	2016	Immunological	Immunoglobulin A deficiency	6.6948E-47	6487
2034	27992413	2017	Gastrointestinal	Primary sclerosing cholangitis	3.6534E-42	14890
4226	31015401	2019	Environmental	Thyroid preparations	1.7121E-31	305582
3904	27863252	2016	Immunological	White blood cell count (three-way meta)	9.8206E-26	172435
3820	21980299	2011	Endocrine	Type 1 Diabetes	1E-25	26890
3187	31427789	2019	Skeletal	Standing height	1.9189E-25	385748
3602	31427789	2019	Endocrine	Non-cancer illness code, self-reported: hypothyroidism/myxoedema	1.1414E-19	289307
3470	31427789	2019	Metabolic	Impedance measures - Trunk fat-free mass	1.8719E-18	379507
3471	31427789	2019	Metabolic	Impedance measures - Trunk predicted mass	2.9617E-18	379469
3412	31427789	2019	Skeletal	Sitting height	5.972E-18	385393
3868	27863252	2016	Immunological	White blood cell count (two-way meta)	2.2674E-17	131969
3892	27863252	2016	Immunological	Myeloid white cell count (three-way meta)	6.5552E-17	169219
3444	31427789	2019	Metabolic	Impedance measures - Whole body water mass	1.8341E-16	379835
3443	31427789	2019	Metabolic	Impedance measures - Whole body fat-free mass	2.5875E-16	379804
4217	31015401	2019	Environmental	Drugs used in diabetes	6.1046E-16	305913
3884	27863252	2016	Immunological	Lymphocyte count (three-way meta)	9.033E-16	171643
3893	27863252	2016	Immunological	Sum neutrophil eosinophil count (three-way meta)	2.3227E-15	170384
3877	27863252	2016	Immunological	Granulocyte count (three-way meta)	2.3317E-15	169822
3328	31427789	2019	Endocrine	Diabetes (diagnosed by doctor)	1.1639E-14	385420
3872	27863252	2016	Immunological	Sum basophil neutrophil count (three-way meta)	1.279E-14	170143
3895	27863252	2016	Immunological	Neutrophil count (three-way meta)	1.3421E-14	170702
3466	31427789	2019	Metabolic	Impedance measures - Arm fat-free mass (left)	2.5438E-14	379653
3446	31427789	2019	Metabolic	Impedance measures - Basal metabolic rate	2.7498E-14	379821
3889	27863252	2016	Immunological	Monocyte count (three-way meta)	2.8299E-14	170721
3467	31427789	2019	Metabolic	Impedance measures - Arm predicted mass (left)	3.1302E-14	379638
3455	31427789	2019	Metabolic	Impedance measures - Leg predicted mass (right)	3.7464E-14	379793
3454	31427789	2019	Metabolic	Impedance measures - Leg fat-free mass (right)	3.8806E-14	379793
3271	31427789	2019	Skeletal	Comparative height size at age 10	4.5248E-14	380167

[1] The table was reduced to show the first 30 findings. The full table is retrievable under:
https://www.nature.com/articles/s41386-021-01228-7

Supplementary Table 2.S8d. GWAS ATLAS results for *TMEM232* [retrieved 12.01.2021].

atlas ID	PMID	Year	Domain	Trait	P-value	N
3553	31427789	2019	Respiratory	Blood clot, DVT, bronchitis, emphysema, asthma, rhinitis, eczema, allergy diagnosed by doctor: Hayfever, allergic rhinitis or eczema	8.61E-13	385822
3552	31427789	2019	Respiratory	Blood clot, DVT, bronchitis, emphysema, asthma, rhinitis, eczema, allergy diagnosed by doctor: Asthma	7.39E-09	385822
3599	31427789	2019	Respiratory	Non-cancer illness code, self-reported: asthma	6.67E-08	289307
4266	30929738	2019	Respiratory	Asthma (child-onset)	1.54E-07	314633

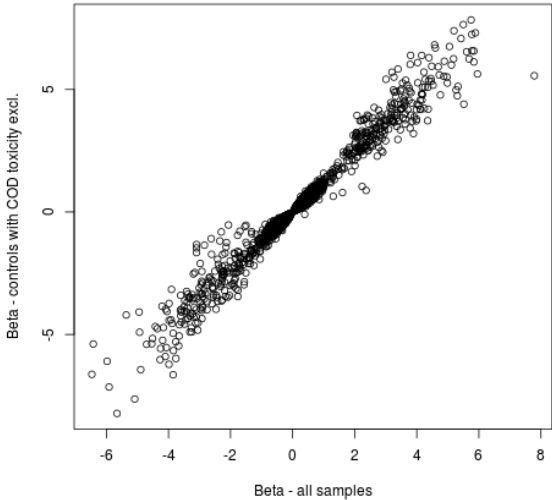### 2.9.3 Supplementary Figures

A)
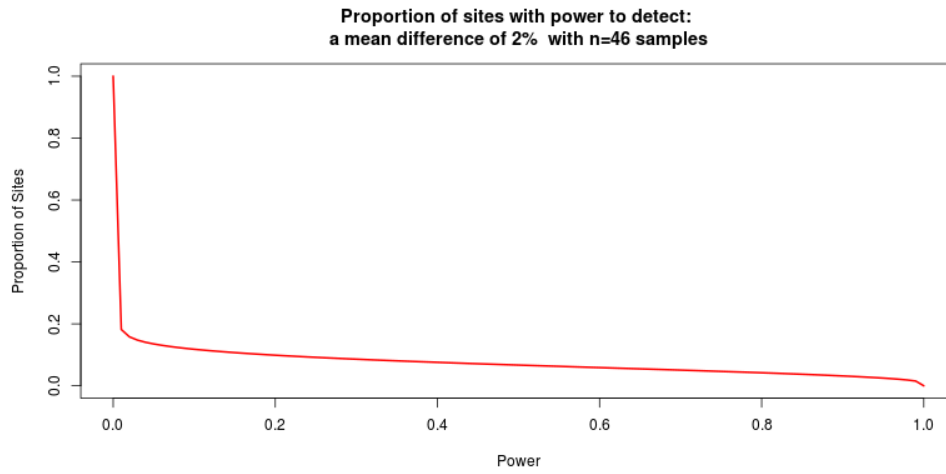
B)
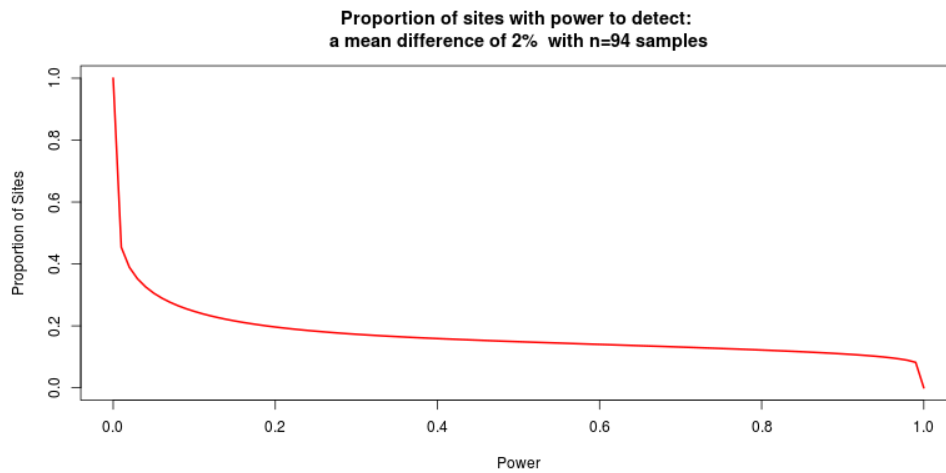
Supplementary Figure 2.S1. Power curve showing the proportion of CpG-sites on the EPIC array with sufficient power to detect a mean methylation difference of 2% for a p-value threshold of 1×10^{-7} and a sample size of A) 94 and B) 46.
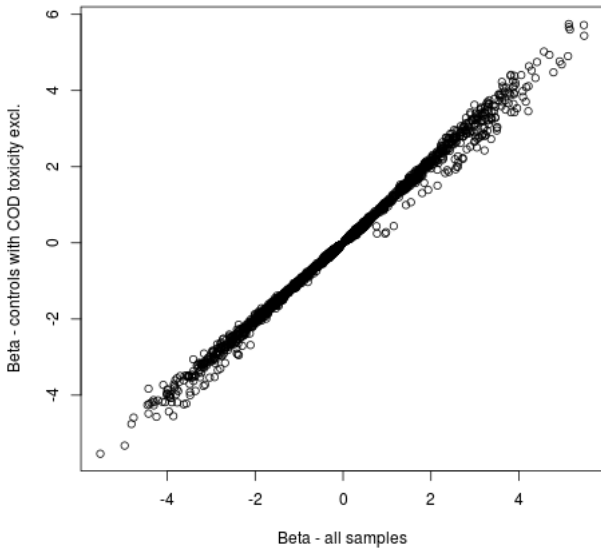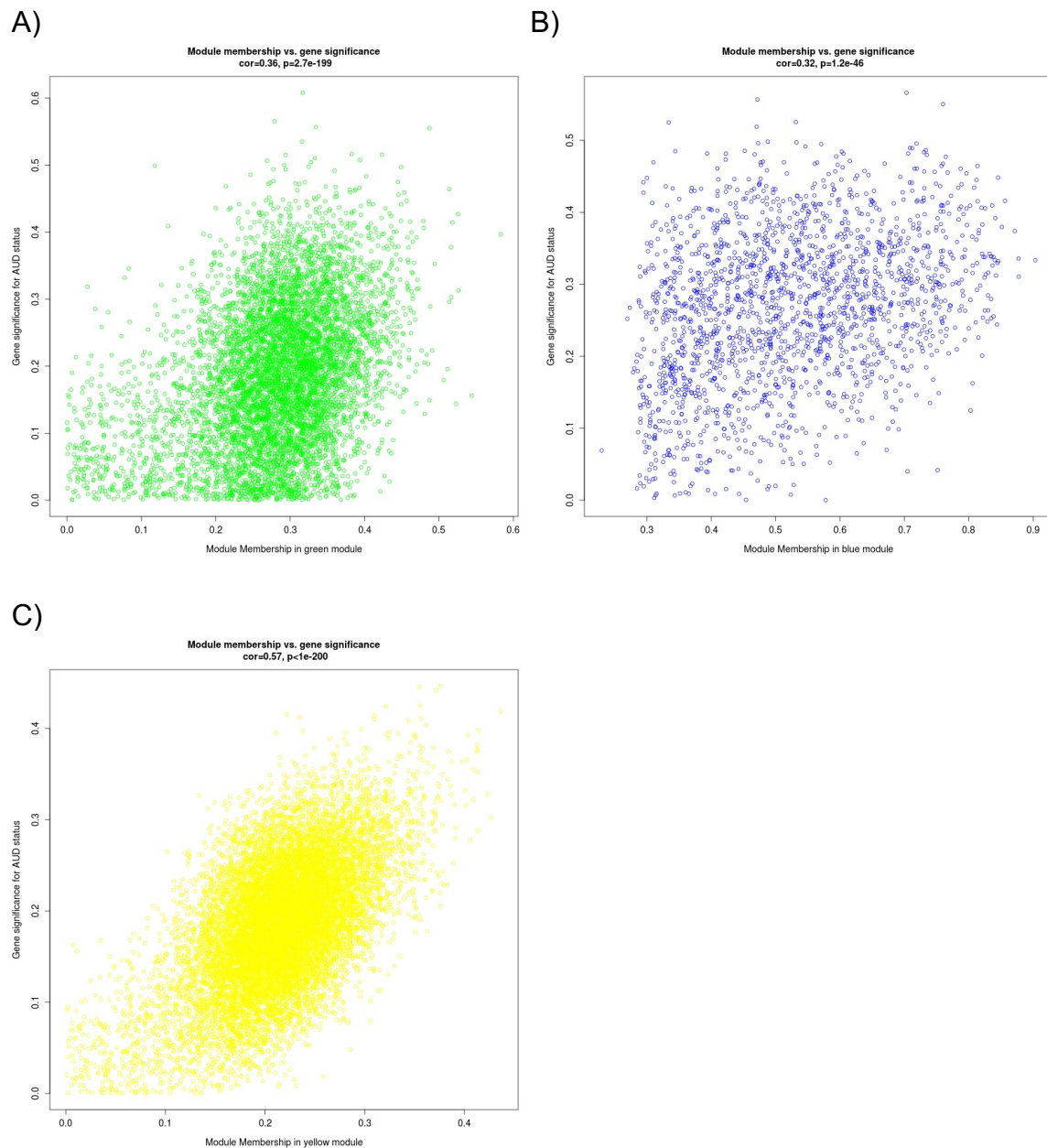
A) Caudate Nucleus
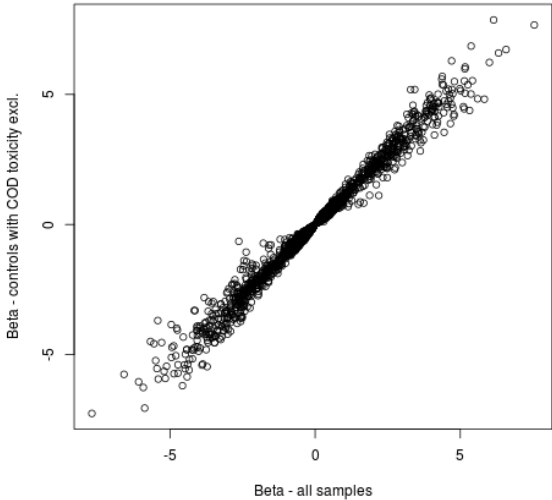
B) Ventral Striatum

C) Putamen

Supplementary Figure 2.S2. Scatterplots of effects for nominally associated CpG-sites from the EWAS in all samples, and from the sensitivity analysis for which control subjects with cause of death toxicity were excluded.

A)

B)

C)

Supplementary Figure 2.S3. Scatterplots of CpG-site significance and module membership, of WGCNA modules most strongly associated with AUD in A) anterior cingulate cortex, B) Brodmann Area 9, and C) Putamen.

3 STUDY 2: MULTI-OMICS SIGNATURES OF ALCOHOL USE DISORDER IN THE DORSAL AND VENTRAL STRIATUM[2]

3.1 Abstract

Alcohol Use Disorder (AUD) is a major contributor to global mortality and morbidity. Postmortem human brain tissue enables the investigation of molecular mechanisms of AUD in the neurocircuitry of addiction. We aimed to identify differentially expressed (DE) genes in the ventral and dorsal striatum between individuals with AUD and controls, and to integrate the results with findings from genome- and epigenome-wide association studies (GWAS/EWAS) to identify functionally relevant molecular mechanisms of AUD. DNA-methylation and gene expression (RNA-seq) data was generated from postmortem brain samples of 48 individuals with AUD and 51 controls from the ventral striatum (VS) and the dorsal striatal regions caudate nucleus (CN) and putamen (PUT). We identified DE genes using DESeq2, performed gene-set enrichment analysis (GSEA), and tested enrichment of DE genes in results of GWASs using MAGMA. Weighted correlation network analysis (WGCNA) was performed for DNA-methylation and gene expression data and gene overlap was tested. Differential gene expression was observed in the dorsal (FDR<0.05), but not the ventral striatum of AUD cases. In the VS, DE genes at FDR<0.25 were overrepresented in a recent GWAS of problematic alcohol use. The *ARHGEF15* gene was upregulated in all three brain regions. GSEA in CN and VS pointed towards cell-structure associated GO-terms and in PUT towards immune pathways. The WGCNA modules most strongly associated with AUD showed strong enrichment for immune response and inflammation pathways. Our integrated analysis of multi-omics data sets provides further evidence for the importance of immune-and inflammation-related processes in AUD.

3.2 Introduction

Alcohol Use Disorder (AUD) is a major contributor to the global disease burden, with a prevalence of ~17% among 12-month alcohol users in the US (Grant et al., 2017; World Health Organization, 2019) and an estimated heritability of 49% (Verhulst et al., 2015). Knowledge about the molecular mechanisms can foster understanding of causes and promote prevention. Recent genome-wide association studies (GWASs) have identified 29 genetic loci associated with Problematic Alcohol Use (PAU), a proxy of AUD (Zhou et al., 2020). While GWASs identify increasing numbers of disease-associated loci, the functional interpretation of many of these findings remains inconclusive. Analyzing the transcriptome can extend the understanding of the molecular mechanisms underlying AUD, by identifying associated gene expression patterns. Findings can in turn be integrated with results from GWASs and epigenome-wide association studies (EWASs) to identify the pathomechanisms underlying disease.

Processes in the central nervous system are considered to play a major role in the etiology of addiction, and the transition from chronic alcohol consumption to AUD (Volkow et al., 2016). Therefore, it is of particular interest to examine molecular changes associated with addiction in brain tissue. So far, only few studies have been conducted in postmortem human brain tissue to identify transcriptional changes associated with AUD (Farris et al., 2015; Liu et al., 2004; Ponomarev et al., 2012). These studies mainly focused on the prefrontal cortex (PFC) one important part of the neurocircuitry of addiction (Koob & Volkow, 2010; Noori et al., 2012). The first transcriptome-wide study in the PFC found DE genes implicated in neuronal processes, such as myelination, neurogenesis, and neural diseases, as well as cellular processes, such as cell adhesion and apoptosis (Liu et al., 2006). In Brodmann Area 9 downregulation of calcium signaling pathways has been observed in individuals with AUD compared to controls (Kapoor et al., 2019). In the same study, a weighted gene co-expression analysis (WGCNA) pointed towards modules associated with AUD case/control status, which were enriched for nicotine and opioid signaling, as well as immune processes. Another study in the PFC (Brodmann Area 8) showed that co-expression networks associated with lifetime alcohol consumption were enriched for GWAS signals of alcohol dependence (Farris et al., 2015).

Despite the importance of striatal regions in addiction processes, genome-wide human omics studies of these brain regions are still missing. The striatum is divided into the ventral striatum (VS), consisting of the nucleus accumbens and olfactory tubercle; and the dorsal striatum, comprising the caudate nucleus (CN) and putamen (PUT) (Volkow & Morales, 2015). The nucleus accumbens is involved in mediating motivational processes such as aversion and reward, which play a significant role in the development and maintenance of substance use disorders (SUD) (Volkow & Morales, 2015). In addition to regulating motor function, the CN and PUT are involved in cognitive processes relevant for addiction, such as executive functioning and cognitive control, reinforcement learning and habit formation (Galandra et al., 2018). Analyses of omics data from striatal regions could complement the knowledge on global molecular changes in the neurocircuitry of addiction in AUD.

In a recent EWAS of AUD in postmortem brain tissue, we identified differentially methylated CpG-sites and regions in the ventral and dorsal striatum (Zillich et al., 2022). Previous studies have shown the utility of integrating epigenetic and transcriptomic data in postmortem brain tissue of SUDs using weighted correlation network analysis (WGCNA) (Langfelder & Horvath, 2008). WGCNA clusters genes or CpG-sites into co-expressed or co-methylated modules based on correlation matrices. By relating modules to each other, WGCNA can be used for data integration, providing more insights than descriptive overlap. For example, whereas a descriptive comparison of histone H3 lysine 4 trimethylation (H3K4me3) and mRNA expression in individuals with AUD and cocaine use disorder revealed no consistent overlap between H3K4me3 trimethylation and gene expression (Zhou et al., 2011), a network analysis identified overlapping modules pointing towards co-expressed genes associated with H3K4me3 trimethylation (Farris et al., 2015). Modules associated with AUD were enriched for CNS functions, such as synaptic transmission and regulation of neurogenesis (Farris et al., 2015). WGCNA has also been used for integrating epigenetic and transcriptomic data and investigating their association with opioid use disorder (OUD) in postmortem human brain, identifying immune-related transcriptional regulation to be enriched in co-expressed and co-methylated modules (Liu et al., 2021).

The aim of the present study was to investigate differential gene expression associated with AUD status in the ventral and dorsal striatum, relate these to GWAS findings, and to integrate the findings with DNA-methylation data using a network approach (WGCNA) in order to identify functionally relevant molecular mechanisms in AUD.

3.3   Materials and Methods

3.3.1   Samples

Postmortem human brain tissue from CN, PUT and VS of a total of 48 individuals with AUD and 51 control individuals (68% male) was obtained from the New South Wales Tissue Resource Centre at the University of Sydney. The Ethics Committee II of the University of Heidelberg approved the study (reference number 2021-681). After quality control (QC), the total sample sizes for each brain region were $N_{CN} = 71$, $N_{PUT} = 77$ and $N_{VS} = 63$. Phenotypic information was assessed by next-of-kin interviews. Inclusion criteria for this study were: age>18 years, Western European Ancestry, no history of severe psychiatric or neurodevelopmental disorders, or SUDs other than AUD and nicotine use disorder or smoking. AUD was defined as meeting DSM-IV criteria for alcohol dependence and consuming 80g of alcohol a day or more (control group: <20g/day). Descriptive information can be found in Table 3.1 and Supplementary Table 3.S1.

Table 3.1.
Descriptive statistics of demographic data.

Characteristic	Cases	Controls	*p*
N	48	51	
Age, years	55.58 (10.62)	57 (10.64)	0.51
Sex (M/F)	31/17	37/14	
pH-value	6.53 (0.26)	6.65 (0.25)	0.026*
PMI (hours)	37.07 (15.79)	30.7 (15.57)	0.047*
Blood Alcohol level (N)	7	0	
Blood Alcohol Level (g/100ml)	0.21 (0.21)		
Smoking (yes/%)	32 (66.7%)	12 (23.5%)	<0.001*
Samples per Brain Region			
Caudate Nucleus	36	37	
Putamen	35	42	
Ventral Striatum	31	32	

Data are presented as count (n/n; n (%)) or mean (±SD), PMI: post-mortem interval, pH: pH-value of the brain, p: p-value of t-Test/Chi-squared test comparing cases and controls.

*significant difference between cases and controls

3.3.2 RNA extraction and -sequencing

RNA was extracted from frozen tissue according to the manufacturer´s protocol using the Qiagen RNeasy microKit (Qiagen, Hilden, Germany). The RNA Integrity Number (RIN) of all samples was determined using a TapeStation 4200 (Agilent, Santa Clara, CA). RIN values of 273 samples were larger than 5.5, for which libraries were prepared using the TruSeq Stranded Total RNA Library Prep Kit (Illumina, San Diego, CA). RNA sequencing was performed on the NovaSeq 6000 (Illumina) at the Life & Brain Center in Bonn, Germany with read lengths of 2x100bp and a sequencing depth of 62.5 M read pairs per sample on average. Technical replicates were sequenced for all but four samples.

3.3.3 DNA extraction and Methylation Profiling

DNA extraction, methylation profiling, and QC was performed as described in Zillich et al. (2022). In brief, DNA was extracted using the DNeasy extraction kit (Qiagen, Hilden, Germany); the Illumina HumanMethylation EPIC BeadChip and the Illumina HiScan array scanning system (Illumina, San Diego, CA) were used to determine DNA-methylation levels. We used an updated and customized version of the CPACOR pipeline to extract beta values from raw intensities (Lehne et al., 2015). Criteria for the removal of samples and probes can be found in Zillich et al. (2022). In the present analyses, DNA methylation data was included from all subjects from whom gene expression data was available after QC.

3.3.4 Statistical Analyses

All analyses apart from QC and read mapping were performed using R version 3.6.1 (Team, 2013). An overview of the analysis workflow can be found in Figure 3.1. The Benjamini-Hochberg (FDR) (Benjamini & Hochberg, 1995) procedure was used to correct for multiple testing. Differentially expressed genes were considered statistically significant at FDR<0.05. All downstream analyses were performed using genes significantly differentially expressed at FDR<0.25.
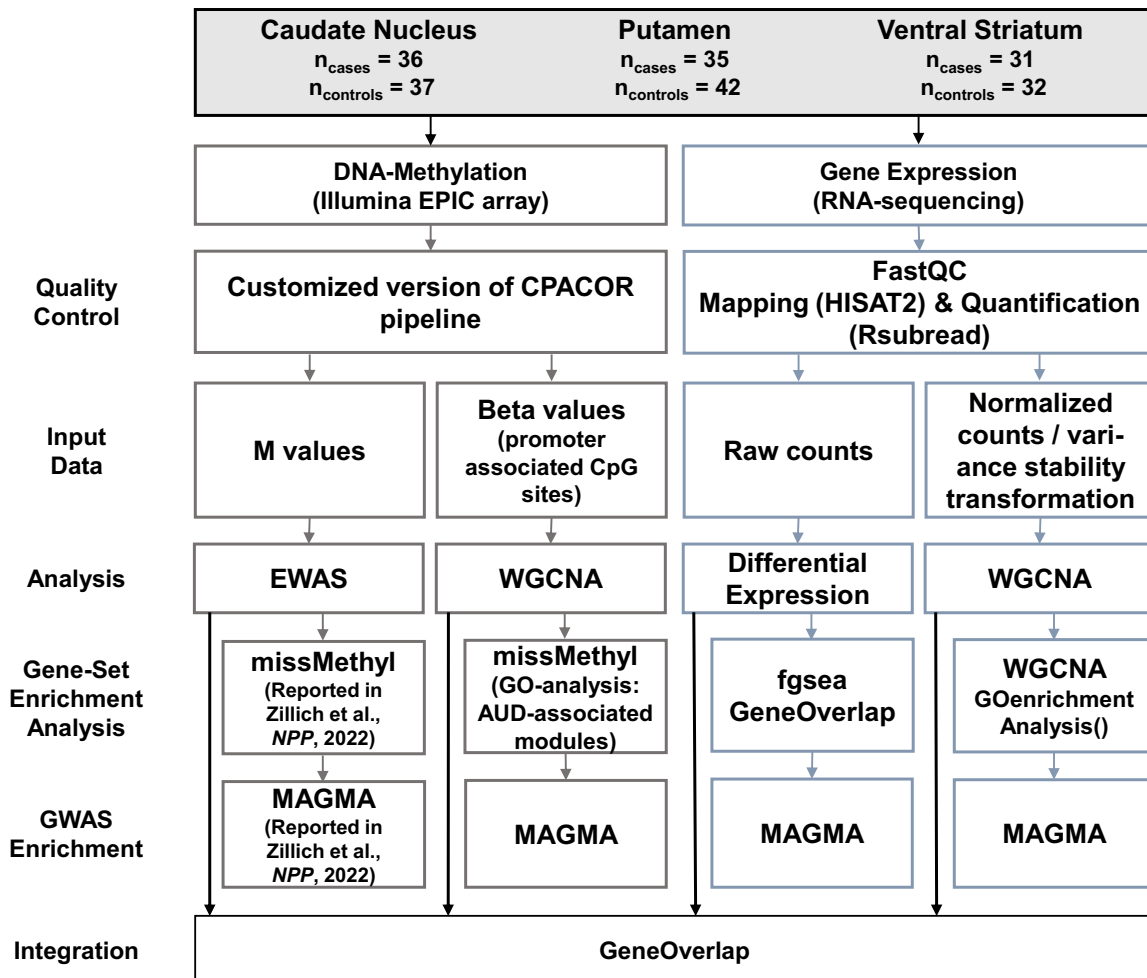

Figure 3.1. Analysis workflow of the present study.

3.3.4.1 Mapping and Quantification

Sequencing quality was determined using FastQC (Andrews, 2010) and 24 samples (11 cases and 13 controls) were excluded due to insufficient sequencing quality (e.g. strong overrepresentation of sequences, GC distribution). Raw reads were mapped to the human genome (hg38) using HISAT2 (v.2.1.0) (Kim et al., 2019). Quantification was performed with the featureCounts function of the Rsubread package (v.2.0.1) (Liao et al., 2019), with hg38 annotation.

3.3.4.2 Differential Gene Expression Analysis

Differential gene expression was determined using DESeq2 (v.1.26.0) (Love et al., 2014). Minimal pre-filtering was applied, removing genes with normalized counts <10 for more than two samples. Technical replicates were merged prior to differential expression analysis using the collapseReplicates function as implemented in DESeq2. For the differential gene expression analysis, we included age, sex, RIN, pH-value of the brain, and postmortem interval (PMI) as covariates, because of their known influence on gene expression (Birdsill et al., 2011; Durrenberger et al., 2010; Trabzuni et al., 2011). To assess residual bias after adjustment for covariates, we generated Q-Q plots and calculated genomic inflation factors (Supplementary Figure 3.S1). We further conducted a variance partition analysis using the variancePartition() function of the corresponding R package (Hoffman & Schadt, 2016), which confirmed the covariates. Results of this analysis can be found in Supplementary Figure 3.S2. Results were filtered for differentially expressed (DE) genes with an absolute log2 fold change larger than 0.02. Volcano plots displaying up- and downregulation of genes for each brain region are shown in Supplementary Figure 3.S3.

3.3.4.3 Gene-Set Enrichment Analysis

Gene-set enrichment analysis was performed using the R package fgsea (v.1.12.0) (Sergushichev, 2016), for which DE genes were ranked according to p-value. Enrichment analysis was performed for Gene-Ontology (GO) terms (Ashburner et al., 2000) and Hallmark gene sets (Liberzon et al., 2015) and the results were adjusted using FDR correction.

3.3.4.4 Cell Type Enrichment Analysis

To identify cell type specific expression signatures, we performed cell type enrichment analysis using DE genes (FDR<0.25) from the three brain regions. As a reference gene set for brain cell types, we used the "top ranked cell type-enriched genes based on human data" as provided by McKenzie et al. (2018). These contain the 1000 most enriched genes in a cell type and cover astrocytes, endothelial cells, microglia, neurons, and oligodendrocytes. Using the R package GeneOverlap (v.1.22.0) (Shen, 2021) , we assessed the overlap of AUD-status associated DE genes with markers from the different cell populations. Results were adjusted for multiple testing using the Benjamini-Hochberg method as implemented in GeneOverlap.

3.3.4.5 Differential Methylation Analysis

Effect sizes and p values for CpG sites were used from the EWAS results as presented in the original publication (Zillich et al., 2022). In brief, the EWAS model was based on methylation M-values as the dependent variable and AUD status as the predictor. As covariates, sex, age, postmortem interval (PMI), pH-value, estimated smoking, standardized neuronal cell count, and the first ten principal components of the EPIC array internal control probes were included.

3.3.4.6 WGCNA

Weighted correlation network analyses (WGCNA, v.1.70-3) (Langfelder & Horvath, 2008) were performed to identify modules of co-expressed genes and co-methylated CpG-sites. We assessed the relationship of these modules with AUD case/control status and tested the overlap between associated modules. WGCNA clusters the input matrix according to a dynamic tree cutting algorithm, using a soft power threshold that approximates the criterion of scale-free topology ($R_{signed}^2 > 0.80$). Resulting soft power thresholds for expression networks were 6 for CN, 5 for PUT, and 14 for VS; for methylation networks, all power thresholds were 2.

To identify methylation networks associated with gene expression, beta values from normalized intensities of all samples from which gene expression data were available were filtered for promoter-associated CpG-sites based on the manufacturer's manifest (Illumina, San Diego, CA). The resulting 105 796 CpG-sites were used as input.

For the RNA-seq data, count matrices were normalized using the DESeq2 function normalizeCounts and variance stability transformation was applied.

Networks were constructed using following settings: minimum module size=30, mergeCutHeight=0.25, maxBlockSize=36 000. In WGCNA, modules are labeled using colors. In the results section modules are labeled according to type of data, brain region, and color assigned in the analysis, e.g. "e-VS-pink" for module "pink" from the WGCNA analysis of gene expression data in the ventral striatum. For each module, its eigengene was calculated and correlated with AUD status. Association of modules with AUD status and covariates is shown in Supplementary Figure 3.S4. For modules associated with AUD status, we performed enrichment analysis using the GOenrichmentAnalysis function implemented in the WGCNA package for expression data and the R package missMethyl (v.1.20.4) (Phipson et al., 2016) for methylation modules. Further, we extracted hub genes of AUD associated WGCNA expression modules by calculating the product of module membership and gene significance for each gene of a module. Based on this score, the 10% of highest ranking genes were defined as module hub genes. To investigate the biological relevance of hub genes, protein-protein interaction networks were generated using the *Search Tool for the Retrieval of Interacting Genes/Proteins* (STRING, v.11.5) (Szklarczyk et al., 2021). Graphical representation of gene networks was restricted to high confidence interactions (interaction score threshold 0.7).

3.3.4.7 Expression and Methylation Data Integration

To identify genes both DE and differentially methylated, we analyzed the overlap of DE genes (FDR<0.25) with the results of an EWAS (p<0.001) in the same sample(Zillich et al., 2022). We prioritized CpG-sites based on their functional relevance in gene expression regulation. Thus, promoter-associated CpG-sites were used in the analysis.

At the module level, gene-set overlap tests were performed using the R package GeneOverlap (v.1.22.0) (Shen, 2021). Here, Fisher's exact test is used to identify significant overlap. For each brain region, the overlap of the AUD-associated co-expression and co-methylation modules was tested.

3.3.4.8 GWAS Enrichment Analysis

We analyzed enrichment of DE genes with an FDR<0.25, and genes in AUD-associated WGCNA modules in GWAS summary statistics using Multi-marker Analysis of GenoMic Annotation (MAGMA, v.1.08b) (de Leeuw et al., 2015). We performed GWAS enrichment analysis for several SUDs, such as alcohol use disorder and problematic alcohol use (Zhou et al., 2020), cannabis use disorder (Johnson et al., 2020), and a recent GWAS comparing individuals with opioid use disorder with unexposed controls (Polimanti et al., 2020). Bonferroni correction (n=4 tests per gene set) of p values was applied to adjust for multiple testing.

3.4 Results

3.4.1 Differential Gene Expression

Gene expression analysis of postmortem brain tissue from AUD cases and controls revealed DE genes at FDR<0.05 in both dorsal striatal regions. In the caudate nucleus, 49 DE genes were identified at FDR<0.05 (39 up- and 10 downregulated). Tubulin Tyrosine Ligase Like 4 (*TTLL4*, log2FC=0.11, p=$2.3*10^{-8}$) and GATA Binding Protein 2 (*GATA2*, log2FC=-0.27, p=$8.6*10^{-7}$) were the most significantly upregulated and downregulated genes, respectively. Top up- and downregulated genes in the putamen were found to be Transcription Elongation Factor A Like 2 (*TCEAL2*, log2FC=0.09, p=$5.8*10^{-5}$) and Desmin (*DES*, log2FC=-0.86, p=$2.6*10^{-6}$), the latter being the only significant gene after correction for multiple testing. Nine genes were downregulated in both dorsal striatal regions, with *HLA-DOB* having the highest log2FC in both regions. In the ventral striatum, no DE genes were detected at FDR<0.05. The most significant differential gene expression in the ventral striatum was observed for Ankyrin Repeat And Ubiquitin Domain Containing 1 (*ANKUB1*) which was upregulated in AUD cases (log2FC=1.35, p=$5.8*10^{-5}$). In the VS of AUD cases Caseinolytic Mitochondrial Matrix Peptidase Chaperone Subunit B (*CLPB*, log2FC=-0.11, p=$5.2*10^{-6}$) was the most significantly downregulated gene.

None of the DE genes at FDR<0.05 overlapped between multiple brain regions. Therefore, the less conservative significance threshold of FDR<0.25, which was also used for downstream analyses, was applied to compare the overlap of DE genes. At FDR<0.25 the cardiomyopathy associated 5 (*CMYA5*) gene showed an upregulation in both caudate nucleus and putamen. *ARHGEF15* (Rho Guanine Nucleotide Exchange Factor 15) was upregulated in all three brain regions at FDR<0.25. The Top 5 DE genes from each brain region are listed in Table 3.2; complete summary statistics are listed in Supplementary Table 3.S2 (CN), 3.S3 (PUT), and 3.S4 (VS). Overlap between DE genes in the different brain regions is shown in Figure 3.2A.
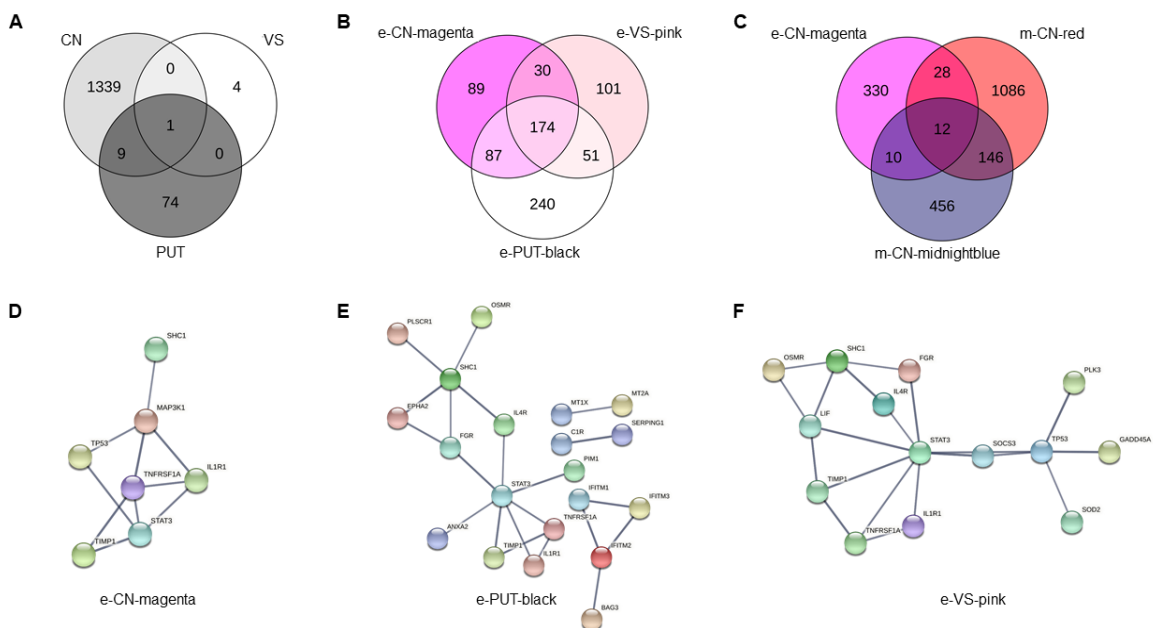

Figure 3.2. Venn Diagrams of gene overlap of A) DE genes at FDR < 0.25 in caudate nucleus (CN), putamen (PUT), and ventral striatum (VS), B) genes forming WGCNA expression-modules showing the strongest association with AUD status for CN, PUT, and VS, C) genes forming WGCNA expression-module "e-CN-magenta" and those forming the methylation-modules "m-CN-red" and "m-CN-midnightblue". Network plots depicting the WGCNA gene expression modules showing the strongest association with AUD: D) module magenta from caudate nucleus, E) module black from putamen and F) module pink from ventral striatum.

3.4.2 Gene-set Enrichment Analysis

Pathway analysis using a pre-ranked enrichment analysis revealed significant enrichment of dorsal striatum DE genes for several GO terms and Hallmark gene-sets. Genes in the CN were found to be related to cilia- and microtubule-associated GO-terms, while none of the Hallmark gene-sets was significantly enriched. GO-term and Hallmark gene-set analysis in PUT samples showed enrichment for immune processes, such as "acute inflammatory response to antigenic stimuli" (p_{FDR}=0.006) and "adaptive immune response" (p_{FDR} =0.006). In the VS the most significantly enriched GO-terms were also related to cilia and microtubules, as well as antigen

processing. All GO-terms and Hallmark gene-set with FDR <0.10 are listed in Supplementary Tables 3.S5 (CN), 3.S6 (PUT), and 3.S7 (VS).

Table 3.2.

Entrez Gene ID	Gene Name	baseMean	log2(FC)	lfcSE	Stat	P-Value	FDR
Caudate Nucleus							
9654	TTLL4	1125.89	0.11	0.02	5.59	$2.33*10^{-8}$	0.0005
2624	GATA2	51.17	-0.27	0.05	-4.92	$8.58*10^{-7}$	0.0091
25904	CNOT10	695.68	0.06	0.01	4.84	$1.27*10^{-6}$	0.0091
222256	CDHR3	1483.68	0.19	0.04	4.75	$1.99*10^{-6}$	0.0106
375611	SLC26A5	63.80	0.28	0.06	4.62	$3.81*10^{-6}$	0.0163
Putamen							
1674	DES	22.06	-0.86	0.18	-4.70	$2.64*10^{-6}$	0.0486
2050	EPHB4	118.04	-0.19	0.05	-4.19	$2.78*10^{-5}$	0.0939
9144	SYNGR2	499.84	-0.20	0.05	-4.19	$2.76*10^{-5}$	0.0939
55741	EDEM2	348.56	-0.07	0.02	-4.23	$2.30*10^{-5}$	0.0939
84245	MRI1	662.19	-0.13	0.03	-4.13	$3.57*10^{-5}$	0.0939
Ventral Striatum							
81570	CLPB	1188.85	-0.11	0.02	-4.56	$5.16*10^{-6}$	0.0653
22899	ARHGEF15	54.23	-0.26	0.06	-4.49	$7.04*10^{-6}$	0.0653
55584	CHRNA9	5.58	-1.17	0.26	-4.44	$9.14*10^{-6}$	0.0653
100463488	MTRNR2L10	4.91	-2.07	0.50	-4.16	$3.23*10^{-5}$	0.1730
389161	ANKUB1	30.26	1.35	0.34	4.02	$5.79*10^{-5}$	0.2480

Top 5 differentially expressed genes in caudate nucleus, putamen and ventral striatum.

3.4.3 Cell Type Enrichment Analysis

In the CN, upregulated DE genes were significantly enriched for astrocytic markers (p_{FDR} =$7*10^{-6}$), whereas an enrichment for endothelial cell marker genes was detected among downregulated genes (p_{FDR} =$2*10^{-7}$). No significant cell-type enrichment of DE genes was found in the putamen and the ventral striatum. GeneOverlap heatmap visualizations for the three brain regions are displayed in Supplementary Figure S3.5.

3.4.4 WGCNA

3.4.4.1 Expression

In the CN, 21 modules with a median size of 352 genes (range: 64-7 259) were identified. Module "e-CN-magenta", consisting of 328 genes, showed the strongest positive association with AUD status (r=0.42, p=$2.89*10^{-4}$). In the PUT, of the 25 modules (median size 249 genes, range: 33-5 381) identified, module "e-PUT-black"

was most strongly correlated with AUD with a positive direction of effect (r=0.41, p=2.31*10^{-4}). For expression data from the ventral striatum, 16 modules with a median size of 429 genes (range: 35-9 708) were identified; module "e-VS-pink" had the strongest positive association with AUD (r=0.41, p=0.009). Interestingly, in a GO-term analysis the three AUD associated modules were all enriched for immune processes, such as "defense response" and "inflammation response". Gene network representation of hub genes in modules "e-CN-magenta", "e-VS-pink", and "e-PUT-black" revealed the signal transducer and activator of transcription 3 (*STAT3*) gene as a conserved hub node in all three brain regions (Figure 3.2D-2F). There was also a wide overlap of the genes in the three modules: 174 (22.54%) were partially shared between all three modules corresponding to the three brain regions, while another 21.76% were shared between at least two modules (Figure 3.2B). A gene network analysis of the 174 shared genes between regions identified *STAT3*, *TP53*, *ICAM1*, *MYC*, and *NFKBIA* as the top 5 hub nodes of the network. A visualization of the network is depicted in Figure 3.3.

3.4.4.2 Methylation

In the CN, WGCNA resulted in 36 modules with a median size of 346 CpG-sites (range: 66-41 423). Module "m-CN-red", consisting of 2 117 CpG-sites, showed the strongest association with AUD case control status (r=-0.27, p=0.021). This module was most highly enriched for the biological processes "cell activation" (p=1.52*10^{-5}) and "leukocyte activation" (p=2.09*10^{-5}). In PUT 177 modules were identified (median size=57 CpG-sites, range: 30-42 248). Module "m-PUT-plum" consisted of 70 CpG-sites and was significantly associated with AUD case/control status (r=-0.29, p=0.023) and enriched for the biological processes "positive regulation of I-κB kinase/NF-κB signaling" (p=0.002) and "regulation of I-κB kinase/NF-κB signaling" (p=0.005). WGCNA in the VS methylation data resulted in 85 modules (median size=178 CpG-sites, range: 35-30 370). The module with the strongest association with AUD was "m-VS-lavender" (r=-0.29, p=0.023), which consisted of 117 CpG-sites and was enriched for the molecular function "natural killer cell lectin-like receptor binding" (p=3.43*10^{-4}) and the biological process "susceptibility to natural killer cell mediated cytotoxicity" (p=3.65*10^{-4}). The top 10 enriched GO-terms for all AUD-associated modules can be found in Supplementary Tables 3.S8-S10.

3.4.5 Expression and Methylation Data Integration

In the CN, 12 genes showed both differential methylation and differential gene expression. DE statistics, EWAS summary statistics and functional annotation for these genes are provided in Supplementary Table 3.S11. No overlap was observed in the VS and PUT. At the module-level, co-expression module "e-CN-magenta" showed significant overlap with the methylation modules "m-CN-red" (p=0.003) and "m-CN-midnightblue" (p=0.014) (Figure 3.2C), while expression module "e-CN-purple" did not show significant overlap with the methylation modules in CN. Of the 3 AUD-associated expression modules in the VS, only "e-VS-salmon" showed significant overlap with the

methylation module "m-VS-turquoise" (p=0.003), but not "m-VS-lavender". No overlap was observed for gene expression and DNA-methylation in PUT.

3.4.6 GWAS Enrichment Analysis of DE Genes and WGCNA modules

In the VS, but not in the dorsal striatum, we observed enrichment of DE genes in the GWAS signal of PAU (p=0.045). In the putamen DE genes were enriched for GWAS signal from a study comparing individuals with OUD to unexposed controls (p=0.025). None of the DE genes in any of the brain regions showed enrichment for signals from a GWAS of Cannabis Use Disorder or AUD.

From the WGCNA modules showing the strongest association with AUD, only module e-VS-pink showed significant enrichment for GWAS signals of CUD (p=0.043). None of the findings remained statistically significant after multiple testing correction. Results from the respective analyses are depicted in Supplementary Figure 3.S6 and enrichment p values as well as the number of overlapping genes are displayed in Supplementary Table 3.S12.

Figure 3.3. Network plot of genes, co-expressed between the WGCNA modules e-CN-magenta, e-PUT-black and e-VS-pink.

3.5 Discussion

In the present study, we identified DE genes, co-expression networks, and pathways associated with AUD in the dorsal and ventral striatum. The results were integrated with DNA-methylation data and results from GWASs of SUDs.

We discovered that one gene (*ARHGEF15*) was consistently upregulated in all investigated brain regions of AUD cases compared to controls. *ARHGEF15* encodes a specific guanine nucleotide exchange factor for the activation of Ras homolog family member A (RhoA), a GTPase, which has been linked to higher blood pressure and hypertension over the Rho/ROCK signaling cascade (Wirth, 2010). It is postulated that the Rho Guanine Nucleotide Exchange Factor 15 negatively regulates excitatory synapse development by suppressing the synapse-promoting activity of EPHB2 (Margolis et al., 2010). EPHB2 deficiency has been linked to depression-like behaviors and memory impairments in animal studies (Zhen et al., 2018). In line with this, genetic variation within *ARHGEF15* has been associated with hematocrit, red blood cell count, and hemoglobin concentration (Astle et al., 2016), but also with psychiatric traits, such as neuroticism and worries(Nagel et al., 2018) as well as bipolar disorder (Ikeda et al., 2018).

Among the genes that were downregulated in both dorsal striatal regions, *HLA-DOB* displayed the highest fold change. HLAs of the Major Histocompatibility Class II are an essential part of the acquired immune system presenting antigens to T-lymphocytes (for review: Howell et al. (2010)). The most significantly downregulated gene in the VS is *CLPB*, a mitochondrial chaperone, which has been associated with progressive brain atrophy (Saunders et al., 2015) and with the cellular response to alcohol-induced stress (Tóth et al., 2014). In a recent GWAS, *CLPB* was associated with the amount of alcohol consumed on a typical day ($p=9.67*10^{-5}$, N=116 163) (Watanabe et al., 2019).

DE genes in the ventral striatum were enriched for GWAS signals of PAU, but not AUD. This could be a result of the larger sample size of the PAU GWAS, but also point towards differences in genetic variation as responsible for differential expression.

Our results from the pathway and network analyses further underline immune-related effects of chronic alcohol exposure; the pathway and network modules most strongly associated with AUD case-control status were also enriched for immune system and inflammation processes. This was observed for all three brain regions, and both in expression and methylation data, providing further evidence for the important role of immune processes in AUD.

Gene networks derived from WGCNA hub genes similarly revealed genes related to inflammatory processes as strongly connected network nodes. Here, *STAT3* represents a conserved network hub node in all three brain regions. *STAT3* is a member of the JAK/STAT pathway and acts as a transcription factor upon activation by cytokines, hormones and growth factors (Nicolas et al., 2013). Interestingly, a recent study assessing expression signatures of alcohol withdrawal in rats discovered a very similar gene network in the hippocampus with *STAT3* as a hub node surrounded by a network of downstream targets (Chen et al., 2021). The authors also discovered increased levels of STAT3 and its neuroinflammation-related target genes in

postmortem brain tissue of subjects with AUD. Activation of the *STAT3* gene network was found to be primarily restricted to astrocytes. This supports the results of the cell type enrichment analyses, where enrichment of astrocytic expression signatures was detected for upregulated DE genes in the CN.

These results strongly reflect the well-described effect of chronic alcohol exposure on different aspects of the innate and acquired immune systems (Szabo & Saha, 2015). Chronic alcohol exposure accelerates the inflammatory response and reduces anti-inflammatory cytokines (Szabo & Saha, 2015). An activated immune response in response to chronic alcohol exposure has been shown on the cell level (McClintick et al., 2019), as well as on the transcription (McClintick et al., 2019), and protein levels (Donnadieu-Rigole et al., 2016; Yen et al., 2017). In a previous EWAS, we found strong enrichment of immune processes in differentially methylated CpG-sites associated with alcohol withdrawal (Witt et al., 2020). Neuroinflammation has been repeatedly associated with AUD and both the glutamate excitotoxicity and the production of acetaldehyde, key processes in AUD metabolism, have been suggested to produce an inflammatory response in the brain (de Timary et al., 2017). On a phenotypic level, there is also widespread overlap between symptoms of inflammation and of SUDs, such as anhedonia, depression, and decreased cognitive functioning(Crews et al., 2017). In addition, in candidate gene studies in postmortem human PFC, hippocampus, and orbitofrontal cortex, increased mRNA levels of *HMGB1*, which encodes a proinflammatory cytokine and toll-like receptor genes have been associated with alcohol consumption in AUD cases, providing evidence for chronic neuroinflammation in response to alcohol (Coleman et al., 2017; Crews et al., 2013; Vetreno et al., 2021). Notably, there is an overlap of findings not only on the single-gene level but also on the level of pathways and networks/modules. This overlap underlines that alcohol consumption has common biological effects in different brain regions, i.e., most prominently, effects on immune and inflammation processes.

Several limitations apply to our study. First, we cannot distinguish between effects being a consequence of chronic alcohol consumption or addiction. Second, although we corrected for PMI, which can influence tissue quality as a confounding factor, it cannot be ruled out that other characteristics not easily accounted for, such as cause of death, or blood alcohol level for which the majority of individuals have missing data, influenced gene expression. Third, although the sample size is comparatively large for postmortem brain studies in the addiction field, the small number of differentially expressed genes is likely attributable to limited power. Lastly, analyzing bulk tissue does not adequately reflect the diversity of cell types across different brain regions and future studies on single-cell level are needed to investigate cell-type specific transcriptional changes associated with AUD.

It has to be noted that besides DNA methylation, epigenetic mechanisms such as histone and chromatin modifications, or microRNA expression profiles can influence gene expression and are especially important in addiction research (Robison & Nestler, 2011). Future studies should therefore expand the epigenetic profiling of AUD to include these mechanisms.

In summary, the present study provides further evidence from multi-omics data sets for the importance of immune-and inflammation-related processes in AUD. Notably,

drugs that reduce neuroinflammation to reduce drinking, such as phosphodiesterases, may be promising approaches for novel treatment options for AUD. Recently published randomized controlled trials suggest that a phosphodiesterase inhibitor reduces heavy drinking whereas an antibiotic compound was not effective (Grodin et al., 2021; Petrakis et al., 2019). A deeper understanding of the underlying mechanisms will enhance the discovery of drug targets and drive forward the development of precision medicine within in this field.

3.6 Acknowledgments

The authors have nothing to disclose.

Supplementary information is available at TP's website.

Raw data and analysis code are available from the corresponding author upon reasonable request.

3.7 Author Contributions

LZ, SHW, MR, RS, MMN, GB, and ACH planned the investigation. MMF and ACH performed the DNA and RNA extraction and SHH, PH, FD, AH and MMN were responsible for generating genome-wide methylation and gene expression data. LZ, EP, JF, JCF and FS developed the analysis plan. LZ and EP performed all statistical analyses. LZ, EP, MMF, JCF, LS, MR, FS, and SHW reviewed the literature for the paper. LZ, EP and SHW drafted the manuscript. All authors contributed, revised, and edited the final manuscript critically. All authors agreed to the publication of the final version of the manuscript.

3.8   Supplementary Material

3.8.1   Supplementary Tables

Supplementary Table 3.S1.

Characteristic	Cases	Controls
Cause of death		
Cardiac	12	16
Cardiovascular	4	17
Vascular	2	2
Hepatic	3	0
Infection	3	0
COPD	1	1
Cardiovascular / Respiratory	2	0
Respiratory	0	1
Toxicity	7	1
Hepatic/Blood Loss	2	0
Suicide	0	1
Pancreatic	1	0
Carcinoma	0	2
Missing	11	10

Causes of death for cases and controls, numbers represent absolute values.

Supplementary Table 3.S2.
Top 25 Differentially Expressed Genes in the Caudate Nucleus

Entrez Gene ID	Gene Name	baseMean	log2FoldChange	lfcSE	stat	pvalue	padj
9654	TTLL4	1125,891862	0,111755104	0,02000906	5,58522643	2,33E-08	0,00049944
2624	GATA2	51,17294178	-0,269462816	0,05474884	-4,9217997	8,58E-07	0,00907485
25904	CNOT10	695,6780636	0,064432003	0,01330129	4,84404291	1,27E-06	0,00907485
222256	CDHR3	1483,68364	0,191116379	0,04019607	4,7546035	1,99E-06	0,01063724
375611	SLC26A5	63,80153241	0,277247116	0,05999272	4,62134595	3,81E-06	0,0163171
431705	ASTL	35,52340071	1,01347103	0,22522525	4,4998108	6,80E-06	0,02425718
3310	HSPA6	209,4175483	0,977380563	0,22006303	4,4413665	8,94E-06	0,02732634
59352	LGR6	38,23788111	0,638618413	0,14558469	4,38657662	1,15E-05	0,03080082
51162	EGFL7	568,0722962	-0,218359266	0,05122967	-4,2623596	2,02E-05	0,03684511
134701	RIPPLY2	116,9339722	-0,149412838	0,03509307	-4,2576168	2,07E-05	0,03684511
101867536	PRNCR1	132,4166313	0,170196403	0,03987104	4,26867206	1,97E-05	0,03684511
2622	GAS8	664,4667851	0,137176392	0,03322177	4,12911133	3,64E-05	0,0382092
7840	ALMS1	6645,454067	0,086182074	0,02086885	4,12969855	3,63E-05	0,0382092
9967	THRAP3	4583,466442	0,060927516	0,01469992	4,14475169	3,40E-05	0,0382092
29072	SETD2	4881,352101	0,055691472	0,01350151	4,12483417	3,71E-05	0,0382092
55092	TMEM51	103,9427389	-0,158275004	0,03742252	-4,2294052	2,34E-05	0,0382092
55628	ZNF407	2298,323712	0,060322839	0,01454639	4,14692733	3,37E-05	0,0382092
115509	ZNF689	364,5177545	-0,074383898	0,01790833	-4,1535914	3,27E-05	0,0382092
79867	TCTN2	1029,73874	0,156598151	0,03818038	4,10153445	4,10E-05	0,03992075
54856	GON4L	3179,487875	0,060061526	0,01468106	4,09109017	4,29E-05	0,03994636
3603	IL16	528,6574541	0,180791094	0,04482857	4,03296202	5,51E-05	0,04015051
4867	NPHP1	701,3950445	0,192740817	0,04789235	4,024445949	5,71E-05	0,04015051
5450	POU2AF1	19,75195055	0,509069076	0,12806086	3,97521205	7,03E-05	0,04015051
11064	CNTRL	1857,990581	0,122630536	0,03089709	3,96900011	7,22E-05	0,04015051
64800	EFCAB6	879,8762055	0,178827565	0,04425116	4,0411951	5,32E-05	0,04015051

Supplementary Table 3.S3.
Top 25 Differentially Expressed Genes in the Putamen

Entrez Gene ID	Gene Name	baseMean	log2FoldChange	lfcSE	stat	pvalue	padj
1674	DES	22,0608224	-0,862912427	0,18371299	-4,697068	2,64E-06	0,04859343
2050	EPHB4	118,03543	-0,188700441	0,04502869	-4,1906709	2,78E-05	0,09390869
9144	SYNGR2	499,843631	-0,202370954	0,04827128	-4,192368	2,76E-05	0,09390869
55741	EDEM2	348,564163	-0,065696082	0,01551941	-4,2331556	2,30E-05	0,09390869
84245	MRI1	662,191957	-0,12897457	0,03120104	-4,133662	3,57E-05	0,09390869
92270	ATP6AP1L	501,698199	-0,132261385	0,03058535	-4,3243375	1,53E-05	0,09390869
152273	FGD5	255,795077	-0,125497157	0,03017119	-4,1595026	3,19E-05	0,09390869
2115	ETV1	2320,84941	0,145232611	0,03611574	4,02131048	5,79E-05	0,0986564
22899	ARHGEF15	68,442381	-0,194283369	0,04806433	-4,0421528	5,30E-05	0,0986564
140597	TCEAL2	2072,05142	0,091907566	0,02285025	4,02216968	5,77E-05	0,0986564
202333	CMYA5	1361,48167	0,100593218	0,02504181	4,01701116	5,89E-05	0,0986564
9217	VAPB	3953,45536	0,068768616	0,01724865	3,9868984	6,69E-05	0,10271238
1329	COX5B	1850,30076	0,078791664	0,01986342	3,96667218	7,29E-05	0,10322494
3588	IL10RB	278,571227	-0,112304057	0,02918966	-3,8473921	0,00011938	0,10466945
7045	TGFBI	165,958964	-0,375945603	0,09574903	-3,9263647	8,62E-05	0,10466945
9182	RASSF9	37,4944692	-0,546029704	0,14030081	-3,89185	9,95E-05	0,10466945
29941	PKN3	57,7205695	-0,195332477	0,05064146	-3,8571653	0,00011471	0,10466945
79135	APOO	414,633951	0,064231097	0,01658828	3,87207651	0,00010791	0,10466945
170384	FUT11	331,617013	-0,077259543	0,01982709	-3,8966657	9,75E-05	0,10466945
201292	TRIM65	349,331305	-0,1409807	0,03617676	-3,8969958	9,74E-05	0,10466945
284119	CAVIN1	1038,55312	-0,161126009	0,04176002	-3,8583796	0,00011414	0,10466945
2990	GUSB	345,334976	-0,077734139	0,02041603	-3,8075058	0,00014038	0,11748149
3112	HLA-DOB	22,1572893	-0,527114558	0,13942469	-3,7806399	0,00015643	0,12000463
4719	NDUFS1	5942,86838	0,057049934	0,01508876	3,78095572	0,00015623	0,12000463
1349	COX7B	1549,54622	0,063216209	0,0169427	3,73117712	0,00019059	0,12125479

Supplementary Table 3.S4.
Top 25 Differentially Expressed Genes in the Ventral Striatum

Entrez Gene ID	Gene Name	baseMean	log2FoldChange	lfcSE	stat	pvalue	padj
22899	ARHGEF15	54,23120878	-0,257109941	0,05723018	-4,49255893	7,04E-06	0,06531986
55584	CHRNA9	5,576775509	-1,173410131	0,26448584	-4,43657072	9,14E-06	0,06531986
81570	CLPB	1188,847201	-0,107637579	0,02361417	-4,55817836	5,16E-06	0,06531986
100463488	MTRNR2L10	4,912348321	-2,066583414	0,49716691	-4,1567195	3,23E-05	0,17303947
389161	ANKUB1	30,2564	1,354927799	0,33692831	4,02141279	5,79E-05	0,24804977
29775	CARD10	52,45034651	-0,249663234	0,06321502	-3,94942919	7,83E-05	0,27991395
4804	NGFR	508,7276223	-1,068018715	0,28654913	-3,72717484	0,000193638	0,37740072
92270	ATP6AP1L	436,1068645	-0,13284904	0,03527724	-3,76585728	0,000165979	0,37740072
284467	TAFA3	7,359598966	-1,190808827	0,31091277	-3,83004158	0,000128122	0,37740072
353088	ZNF429	489,0094538	-0,105238948	0,02771536	-3,79713505	0,000146378	0,37740072
5507	PPP1R3C	2957,267186	0,237817076	0,06588432	3,60961591	0,000306651	0,47594041
6581	SLC22A3	124,6933081	0,216288623	0,05997803	3,60613084	0,000310796	0,47594041
554251	FBXO48	73,28271516	-0,140266881	0,03881036	-3,61416114	0,000301322	0,47594041
56955	MEPE	252,0116981	-1,23591192	0,34602805	-3,57171026	0,000354658	0,47801732
5768	QSOX1	995,4951343	-0,090000669	0,02551914	-3,52679091	0,000420629	0,53046241
100874123	ZNRF3-AS1	65,71734633	0,209783544	0,05982894	3,50638926	0,00045423	0,54101365
10990	LILRB5	18,92162101	-0,313452326	0,09116856	-3,43816262	0,000585676	0,59791927
728763	CROCC2	57,18529249	1,044535883	0,30348826	3,44176699	0,000577928	0,59791927
1896	EDA	86,27093229	-0,141207175	0,04154743	-3,39869793	0,000677075	0,61852993
2028	ENPEP	151,8256639	0,380836191	0,11298853	3,37057387	0,000750118	0,61852993
3040	HBA2	1516,023957	0,380466644	0,112436	3,38385063	0,000714769	0,61852993
3957	LGALS2	11,74597877	-0,368083156	0,10851276	-3,39207254	0,000693661	0,61852993
3039	HBA1	1219,925941	0,363550186	0,10971245	3,31366403	0,000920821	0,62832127
3043	HBB	2237,167026	0,391190605	0,11768005	3,32418804	0,000886764	0,62832127
3671	ISLR	85,53784437	-0,368683136	0,11148004	-3,30716717	0,000942446	0,62832127

Supplementary Table 3.S5
Top 10 associated GO terms in the caudate nucleus.

Pathway	P-Value	FDR	ES	NES	nMore Extreme	size
Gene-Ontology Terms						
GOBP_AXONEMAL_DYNEIN_COMPLEX_ASSEMBLY	0,0001	0,013	0,778	1,783	0	31
GOBP_AXONEME_ASSEMBLY	1,00E-04	0,013	0,768	1,855	0	70
GOBP_CILIARY_BASAL_BODY_PLASMA_MEMBRANE_DOCKING	1,00E-04	0,013	0,603	1,488	0	108
GOBP_CILIUM_MOVEMENT	1,00E-04	0,013	0,696	1,738	0	146
GOBP_CILIUM_OR_FLAGELLUM_DEPENDENT_CELL_MOTILITY	1,00E-04	0,013	0,665	1,645	0	113
GOBP_CILIUM_ORGANIZATION	1,00E-04	0,013	0,637	1,633	0	418
GOBP_EMBRYONIC_HEART_TUBE_DEVELOPMENT	1,00E-04	0,013	0,614	1,477	0	63
GOBP_EMBRYONIC_ORGAN_DEVELOPMENT	1,00E-04	0,013	0,481	1,229	0	364
GOBP_EMBRYONIC_ORGAN_MORPHOGENESIS	1,00E-04	0,013	0,499	1,262	0	226
GOBP_EXTRACELLULAR_TRANSPORT	1,00E-04	0,013	0,826	1,912	0	35

Supplementary Table 3.S6.
Top 10 associated GO terms in the putamen.

Pathway	P-Value	FDR	ES	NES	nMore Extreme	size
Gene-Ontology Terms						
GOBP_ACUTE_INFLAMMATORY_RESPONSE_TO_ANTIGENIC_STIMULUS	0,00010045	0,006	0,791	1,806	0	20
GOBP_ADAPTIVE_IMMUNE_RESPONSE	1,00E-04	0,006	0,525	1,406	0	484
GOBP_ADAPTIVE_IMMUNE_RESPONSE_BASED_ON_SOMATIC_RECOMBINATION_OF_IMMUNE_RECEPTORS_BUILT_FROM_IMMUNOGLOBULIN_SUPERFAMILY_DOMAINS	1,00E-04	0,006	0,479	1,267	0	293
GOBP_AEROBIC_RESPIRATION	1,00E-04	0,006	0,618	1,566	0	83
GOBP_AMEBOIDAL_TYPE_CELL_MIGRATION	1,00E-04	0,006	0,461	1,230	0	386
GOBP_ANTIBACTERIAL_HUMORAL_RESPONSE	1,00E-04	0,006	0,745	1,794	0	36
GOBP_ANTIGEN_PROCESSING_AND_PRESENTATION	1,00E-04	0,006	0,527	1,402	0	357
GOBP_ANTIGEN_PROCESSING_AND_PRESENTATION_OF_ENDOGENOUS_PEPTIDE_ANTIGEN	1,00E-04	0,006	0,596	1,507	0	77
GOBP_ANTIGEN_PROCESSING_AND_PRESENTATION_OF_EXOGENOUS_PEPTIDE_ANTIGEN_VIA_MHC_CLASS_I	1,00E-04	0,006	0,539	1,400	0	143

Supplementary Table 3.S7.
Top 10 associated GO terms in the ventral striatum.

Pathway	P-Value	FDR	ES	NES	nMore Extreme	size
Gene-Ontology Terms						
GOBP_AXONEME_ASSEMBLY	1,00E-04	0,030	0,629	1,612	0	72
GOBP_CELLULAR_RESPONSE_TO_DSRNA	0,0001	0,030	0,750	1,803	0	29
GOBP_CELLULAR_RESPONSE_TO_EXOGENOUS_DSRNA	0,0001	0,030	0,791	1,876	0	25
GOBP_CILIUM_MOVEMENT	1,00E-04	0,030	0,575	1,526	0	147
GOBP_CILIUM_OR_FLAGELLUM_DEPENDENT_CELL_MOTILITY	1,00E-04	0,030	0,560	1,470	0	114
GOBP_CILIUM_ORGANIZATION	1,00E-04	0,030	0,484	1,320	0	422
GOBP_MICROTUBULE_BASED_MOVEMENT	1,00E-04	0,030	0,479	1,304	0	362
GOBP_MICROTUBULE_BUNDLE_FORMATION	1,00E-04	0,030	0,576	1,504	0	102
GOBP_NEGATIVE_REGULATION_OF_ANTIGEN_PROCESSING AND_PRESENTATION	0,0001	0,030	0,841	1,987	0	24

Supplementary Table 3.S8.
Enrichment of GO-terms for WGCNA modules in caudate nucleus.

module	enrichmentP	P adjusted	nModGenesInTerm	N	Term Ontology	termName
e-CN-magenta	4,21E-35	7,65E-31	107	1349	BP	defense response
e-CN-magenta	1,33E-29	2,42E-25	68	629	BP	inflammatory response
e-CN-magenta	6,46E-28	1,17E-23	136	2511	BP	immune system process
e-CN-magenta	2,80E-27	5,09E-23	84	1051	BP	response to cytokine
e-CN-magenta	1,66E-25	3,02E-21	78	967	BP	cellular response to cytokine stimulus
e-CN-magenta	1,05E-24	1,91E-20	64	673	BP	cytokine-mediated signaling pathway
e-CN-magenta	2,30E-22	4,18E-18	129	2619	BP	cell surface receptor signaling pathway
e-CN-magenta	6,25E-22	1,14E-17	99	1689	BP	immune response
e-CN-magenta	8,93E-22	1,62E-17	74	1005	CC	extracellular space
e-CN-magenta	1,43E-21	2,59E-17	249	7667	BP	response to stimulus
e-CN-purple	2,86453E-08	0,000521	199	7667	BP	response to stimulus
e-CN-purple	1,28074E-06	0,023280	119	4125	CC	endomembrane system
e-CN-purple	1,57866E-06	0,028695	91	2910	BP	response to organic substance
e-CN-purple	1,97715E-06	0,035939	63	1776	CC	endoplasmic reticulum
e-CN-purple	4,95806E-06	0,090123	28	556	BP	small GTPase mediated signal transduction
e-CN-purple	1,47226E-05	0,267613	75	2384	BP	cellular response to organic substance
e-CN-purple	1,65165E-05	0,300221	23	435	BP	Ras protein signal transduction
e-CN-purple	1,87816E-05	0,341393	242	10564	CC	cytoplasm
e-CN-purple	5,56174E-05	1	5	22	BP	somatic stem cell division
e-CN-purple	6,13208E-05	1	16	262	BP	carboxylic acid catabolic process

Supplementary Table 3.S8 continued.
Enrichment of GO-terms for WGCNA modules in caudate nucleus.

module	enrichmentP	P adjusted	nModGenesInTerm	N	Term Ontology	termName
m-CN-red	7,98192E-10	1,520E-05	162,5	739	BP	cel activation
m-CN-red	2,1901E-09	2,086E-05	148,5	676	BP	leukocyte activation
m-CN-red	3,43562E-08	0,000218	279,3333333	1523	BP	immune system process
m-CN-red	1,42976E-07	0,000681	71,5	274	BP	regulation of cell activation
m-CN-red	1,83997E-07	0,000701	87	361	BP	lymphocyte activation
m-CN-red	2,7551E-07	0,000875	67,5	260	BP	regulation of leukocyte activation
m-CN-red	6,70338E-07	0,001824	59	223	BP	regulation of lymphocyte activation
m-CN-red	1,57389E-06	0,003748	66	261	CC	cell surface
m-CN-red	2,26239E-06	0,004315	48	170	BP	leukocyte migration
m-CN-red	2,49202E-06	0,004315	8	9	CC	uropod
m-CN-midnightblue	0,00098915	1	8	31	BP	positive regulation of myeloid leukocyte differentiation
m-CN-midnightblue	0,001010022	1	48	441	BP	innate immune response
m-CN-midnightblue	0,001387068	1	4	8	BP	positive regulation of monocyte differentiation
m-CN-midnightblue	0,003040319	1	3	5	BP	regulation of interleukin 8 biosynthetic process
m-CN-midnightblue	0,003110316	1	3	5	BP	regulation of chemokine secretion
m-CN-midnightblue	0,003110316	1	3	5	BP	positive regulation of chemokine secretion
m-CN-midnightblue	0,00437385	1	3	5	MF	angiotensin receptor binding
m-CN-midnightblue	0,00446208	1	3	5	BP	tail anchored membrane protein insertion into ER membrane
m-CN-midnightblue	0,004540139	1	2	2	BP	positive regulation of superoxide dismutase activity
m-CN-midnightblue	0,004540139	1	2	2	BP	positive regulation of removal of superoxide radicals

Supplementary Table 3.S9.
Enrichment of GO-terms for WGCNA modules in putamen.

module	EnrichmentP	P adjusted	nModGenes InTerm	N	Term Ontology	termName
e-PUT-black	2,15E-45	3,91E-41	147	1336	BP	defense response
e-PUT-black	1,48E-44	2,68E-40	100	621	BP	inflammatory response
e-PUT-black	4,25E-38	7,72E-34	193	2494	BP	immune system process
e-PUT-black	9,89E-34	1,80E-29	147	1675	BP	immune response
e-PUT-black	1,65E-33	3,01E-29	113	1043	BP	response to cytokine
e-PUT-black	5,82E-33	1,06E-28	89	667	BP	cytokine-mediated signaling pathway
e-PUT-black	1,34E-30	2,44E-26	358	7576	BP	response to stimulus
e-PUT-black	4,78E-30	8,69E-26	103	960	BP	cellular response to cytokine stimulus
e-PUT-black	1,65E-28	3,01E-24	102	984	BP	extracellular space
e-PUT-black	2,22E-27	4,04E-23	86	741	BP	response to other organism
e-PUT-cyan	1,60E-04	1	3	12	BP	neurotransmitter receptor localization to postsynaptic specialization membrane
e-PUT-cyan	3,34E-04	1	5	65	BP	regulation of postsynaptic membrane neurotransmitter receptor levels
e-PUT-cyan	4,75E-04	1	9	246	BP	negative regulation of cell adhesion
e-PUT-cyan	9,19E-04	1	4	47	BP	cellular response to nerve growth factor stimulus
e-PUT-cyan	1,16E-03	1	4	50	BP	response to nerve growth factor
e-PUT-cyan	1,24E-03	1	2	6	BP	maintenance of DNA methylation
e-PUT-cyan	1,24E-03	1	2	6	BP	branched-chain amino acid transport
e-PUT-cyan	1,24E-03	1	2	6	BP	maintenance of postsynaptic specialization structure
e-PUT-cyan	1,24E-03	1	2	6	BP	positive regulation of xenophagy
e-PUT-cyan	1,24E-03	1	2	6	CC	myelin sheath abaxonal region
e-PUT-turquoise	1,15E-13	2,08E-09	1174	4112	CC	nuclear lumen
e-PUT-turquoise	1,56E-13	2,83E-09	977	3352	CC	nucleoplasm
e-PUT-turquoise	1,88E-13	3,42E-09	149	358	BP	RNA splicing, via transesterification reactions
e-PUT-turquoise	1,93E-13	3,51E-09	148	355	BP	mRNA splicing, via spliceosome
e-PUT-turquoise	3,23E-13	5,87E-09	197	513	BP	mRNA processing

Supplementary Table 3.S9 continued.

Enrichment of GO-terms for WGCNA modules in putamen.

module	Enrich-mentP	P adjusted	nModGenes InTerm	N	Term Ontology	termName
e-PUT-turquoise	9,18E-12	1,67E-07	171	444	BP	RNA splicing
e-PUT-turquoise	8,63E-11	1,57E-06	1825	6810	CC	nucleus
e-PUT-turquoise	1,52E-10	2,76E-06	2623	10124	CC	intracellular membrane-bounded organelle
e-PUT-turquoise	2,76E-09	5,02E-05	80	181	CC	spliceosomal complex
e-PUT-turquoise	3,65E-08	6,63E-04	355	1144	BP	RNA processing
e-PUT-green	3,45E-19	6,26E-15	139	1130	CC	synapse
e-PUT-green	6,50E-18	1,18E-13	90	600	CC	postsynapse
e-PUT-green	8,68E-18	1,58E-13	72	418	CC	synaptic membrane
e-PUT-green	3,40E-17	6,17E-13	61	323	CC	postsynaptic density
e-PUT-green	4,90E-17	8,91E-13	63	344	CC	postsynaptic specialization
e-PUT-green	6,28E-17	1,14E-12	61	327	CC	asymmetric synapse
e-PUT-green	1,98E-16	3,60E-12	59	316	CC	postsynaptic membrane
e-PUT-green	2,89E-15	5,26E-11	60	344	CC	glutamatergic synapse
e-PUT-green	1,34E-13	2,44E-09	85	646	BP	chemical synaptic transmission
e-PUT-green	2,03E-13	3,68E-09	116	1027	CC	cell junction
m-PUT-plum	1,73E-03	1	5	113	BP	positive regulation of I-kappaB kinase/NF-kappaB signaling
m-PUT-plum	5,46E-03	1	5	147	BP	regulation of I-kappaB kinase/NF-kappaB signaling
m-PUT-plum	6,73E-03	1	6	217	CC	nuclear membrane
m-PUT-plum	6,96E-03	1	1	1	BP	pharynx development
m-PUT-plum	6,96E-03	1	1	1	BP	endothelin receptor signaling pathway
m-PUT-plum	7,30E-03	1	1	1	BP	error free postreplication DNA repair
m-PUT-plum	7,34E-03	1	10	522	BP	positive regulation of intracellular signal transduction
m-PUT-plum	7,59E-03	1	1	1	MF	high affinity inorganic phosphate:sodium symporter activity
m-PUT-plum	8,56E-03	1	1	1	BP	lymphocyte anergy
m-PUT-plum	8,56E-03	1	1	1	BP	regulation of T cell anergy

Supplementary Table 3.S10
Enrichment of GO-terms for WGCNA modules in ventral striatum.

module	Enrichment P	P adjusted	nModGenes InTerm	N	Term Ontology	termName
e-VS-pink	1,52E-31	2,77E-27	69	619	BP	inflammatory response
e-VS-pink	3,05E-28	5,55E-24	95	1327	BP	defense response
e-VS-pink	1,08E-27	1,96E-23	83	1039	BP	response to cytokine
e-VS-pink	2,97E-26	5,39E-22	130	2480	BP	immune system process
e-VS-pink	1,61E-24	2,93E-20	248	7578	BP	response to stimulus
e-VS-pink	9,22E-24	1,68E-19	74	955	BP	cellular response to cytokine stimulus
e-VS-pink	1,58E-22	2,87E-18	60	665	BP	cytokine-mediated signaling pathway
e-VS-pink	1,25E-21	2,27E-17	133	2885	BP	response to organic substance
e-VS-pink	1,50E-21	2,73E-17	96	1663	BP	immune response
e-VS-pink	8,14E-20	1,48E-15	121	2590	BP	cell surface receptor signaling pathway
e-VS-brown	3,75E-16	6,81E-12	40	128	BP	myelination
e-VS-brown	6,82E-16	1,24E-11	40	130	BP	axon ensheathment
e-VS-brown	4,67E-13	8,49E-09	47	205	BP	glial cell differentiation
e-VS-brown	3,87E-11	7,04E-07	52	271	BP	gliogenesis
e-VS-brown	2,07E-10	3,76E-06	29	107	BP	glial cell development
e-VS-brown	3,48E-10	6,32E-06	27	96	BP	oligodendrocyte differentiation
e-VS-brown	4,69E-10	8,52E-06	169	1496	BP	neurogenesis
e-VS-brown	8,36E-10	1,52E-05	117	933	MF	cytoskeletal protein binding
e-VS-brown	1,13E-09	2,06E-05	145	1243	BP	cytoskeleton organization
e-VS-brown	1,22E-09	2,22E-05	18	47	CC	myelin sheath
e-VS-salmon	4,46E-06	0,0810	35	2087	MF	enzyme binding
e-VS-salmon	9,26E-06	0,1684	4	18	BP	NLS-bearing protein import into nucleus
e-VS-salmon	2,73E-05	0,4969	6	77	BP	regulation of glycolytic process
e-VS-salmon	5,83E-05	1	2	2	MF	pyrimidine-specific mismatch base pair DNA N-glycosylase activity
e-VS-salmon	6,32E-05	1	8	176	BP	nucleotide catabolic process

Supplementary Table 3.S10 continued
Enrichment of GO-terms for WGCNA modules in ventral striatum.

module	Enrichment P	P adjusted	nModGenes InTerm	N	Term Ontology	termName
e-VS-salmon	7,49E-05	1	6	92	BP	regulation of ATP biosynthetic process
e-VS-salmon	8,00E-05	1	8	182	BP	nucleoside phosphate catabolic process
e-VS-salmon	0,0001	1	4	34	BP	positive regulation of heart contraction
e-VS-salmon	0,0002	1	6	111	BP	glycolytic process
e-VS-salmon	0,0002	1	4	39	MF	Ran GTPase binding
m-VS-lavender	0,0003	1	2	3	MF	natural killer cell lectin-like receptor binding
m-VS-lavender	0,0004	1	2	3	BP	susceptibility to natural killer cell mediated cytotoxicity
m-VS-lavender	0,0005	1	3	17	BP	negative regulation of lymphocyte mediated immunity
m-VS-lavender	0,0006	1	2	4	MF	protein binding, bridging involved in substrate recognition for ubiquitination
m-VS-lavender	0,0009	1	2	5	BP	gamma delta T cell activation
m-VS-lavender	0,0013	1	3	23	BP	negative regulation of leukocyte mediated immunity
m-VS-lavender	0,0013	1	5	80	BP	cellular glucose homeostasis
m-VS-lavender	0,0014	1	6	121	BP	glucose homeostasis
m-VS-lavender	0,0015	1	6	122	BP	carbohydrate homeostasis
m-VS-lavender	0,0015	1	3	23	BP	T cell mediated cytotoxicity
m-VS-salmon	0,0003	1	5	7	BP	cytoplasm organization
m-VS-salmon	0,0011	1	3	3	BP	regulation of mitochondrial membrane permeability involved in programmed necrotic cell death
m-VS-salmon	0,0012	1	3	3	MF	DNA/RNA helicase activity
m-VS-salmon	0,0020	1	7	18	BP	mitochondrial fusion
m-VS-salmon	0,0024	1	50	313	BP	protein targeting
m-VS-salmon	0,0025	1	11,5	38	CC	kinesin complex
m-VS-salmon	0,0035	1	14	59	BP	peroxisome organization
m-VS-salmon	0,0038	1	4	7	MF	aryl hydrocarbon receptor binding
m-VS-salmon	0,0043	1	3	4	MF	porin activity
m-VS-salmon	0,0044	1	8	26	BP	mRNA splice site selection

Supplementary Table 3.S11

Overlap between differentially expressed genes and CpG-sites in the caudate nucleus

| | | | | Expression | | | | | | Methylation | | | | |
Chr	Pos	Gene	Entrez GeneID	Base Mean	log2 FC	Lfc SE	stat	P_expr	FDR expr	cg	B	SE	P_meth	FDR meth
1	43283185	ERMAP	114625	500,22	0,07	0,03	2,40	1,64E-02	0,2425	cg01782487	0,30	0,08	8,19E-05	0,2724
3	48754518	IP6K2	51447	1590,73	-0,05	0,02	-2,39	1,69E-02	0,2470	cg07854244	0,20	0,06	4,01E-04	0,4361
6	32937414	BRD2	6046	2862,69	0,06	0,02	2,64	8,34E-03	0,1877	cg06071395	-7,69	2,12	2,94E-04	0,4088
6	112409342	FAM229B	619208	1095,64	0,09	0,04	2,47	1,36E-02	0,2252	cg15155408	-0,34	0,10	5,51E-04	0,4617
6	159066182	DYNLT1	6993	316,68	0,10	0,04	2,63	8,48E-03	0,1892	cg19483159	0,61	0,17	2,82E-04	0,4050
7	23145770	KLHL7	55975	1524,03	-0,05	0,01	-3,42	6,28E-04	0,0782	cg16493612	5,26	1,50	4,71E-04	0,4486
8	69246056	C8orf34	116328	907,62	0,22	0,08	2,87	4,15E-03	0,1426	cg03763300	-0,29	0,09	9,27E-04	0,5350
10	6244686	PFKFB3	5209	4744,38	0,13	0,04	3,01	2,58E-03	0,1204	cg14830402	3,03	0,92	9,72E-04	0,5439
11	33278681	HIPK3	10114	8005,36	0,05	0,02	2,55	1,07E-02	0,2052	cg23484383	0,39	0,12	8,90E-04	0,5307
11	64808285	SAC3D1	29901	98,09	-0,12	0,04	-2,95	3,18E-03	0,1295	cg04467611	-0,13	0,04	7,64E-04	0,5093
17	7339721	TMEM102	284114	21,73	-0,18	0,06	-3,02	2,50E-03	0,1192	cg14782678	-0,14	0,04	4,80E-04	0,4486
21	43429288	ZNF295-AS1	150142	18,62	0,33	0,09	3,81	1,36E-04	0,0511	cg15609935	0,19	0,05	1,34E-04	0,3190

Supplementary Table 3.S11 continued

Chr	Pos	Gene	Functional annotation (retrieved from UniProt)
1	43283185	ERMAP	Possible role as a cell-adhesion or receptor molecule of erythroid cells.
3	48754518	IP6K2	Converts inositol hexakisphosphate (InsP6) to diphosphoinositol pentakisphosphate (InsP7/PP-InsP5).
6	32937414	BRD2	May play a role in spermatogenesis or folliculogenesis (By similarity). Binds hyperacetylated chromatin and plays a role in the regulation of transcription, probably by chromatin remodeling. Regulates transcription of the CCND1 gene. Plays a role in nucleosome assembly.
6	112409342	FAM229B	?
6	159066182	DYNLT1	Acts as one of several non-catalytic accessory components of the cytoplasmic dynein 1 complex that are thought to be involved in linking dynein to cargos and to adapter proteins that regulate dynein function. Cytoplasmic dynein 1 acts as a motor for the intracellular retrograde motility of vesicles and organelles along microtubules. Binds to transport cargos and is involved in apical cargo transport such as rhodopsin-bearing vesicles in polarized epithelia. May also be a accessory component of axonemal dynein. Plays a role in neuronal morphogenesis; the function is independent of cytoplasmic dynein and seems to be coupled to regulation of the actin cytoskeleton by enhancing Rac1 activity. The function in neurogenesis may be regulated by association with a G-protein beta-gamma dimer. May function as a receptor-independent activator of heterotrimeric G-protein signaling; the activation appears to be independent of a nucleotide exchange. Plays a role in regulating neurogenesis; inhibits the genesis of neurons from precursor cells during cortical development presumably by antagonizing ARHGEF2. Involved in the regulation of mitotic spindle orientation (By similarity). Unrelated to the role in retrograde microtubule-associated movement may play a role in the dimerization of cytoplasmic proteins/domains such as for ACVR2B. Binds to the cytoplasmic domain of ACVR2B and, in vitro, inhibits ACVR2B signaling
7	23145770	KLHL7	Substrate-specific adapter of a BCR (BTB-CUL3-RBX1) E3 ubiquitin ligase complex. The BCR(KLHL7) complex acts by mediating ubiquitination and subsequent degradation of substrate proteins. Probably mediates 'Lys-48'-linked ubiquitination.
8	69246056	C8orf34	?
10	6244686	PFKFB3	Synthesis and degradation of fructose 2,6-bisphosphate.
11	33278681	HIPK3	Serine/threonine-protein kinase involved in transcription regulation, apoptosis and steroidogenic gene expression. Phosphorylates JUN and RUNX2. Seems to negatively regulate apoptosis by promoting FADD phosphorylation. Enhances androgen receptor-mediated transcription. May act as a transcriptional corepressor for NK homeodomain transcription factors. The phosphorylation of NR5A1 activates SF1 leading to increased steroidogenic gene expression upon cAMP signaling pathway stimulation. In osteoblasts, supports transcription activation: phosphorylates RUNX2 that synergizes with SPEN/MINT to enhance FGFR2-mediated activation of the osteocalcin FGF-responsive element (OCFRE).
11	64808285	SAC3D1	Involved in centrosome duplication and mitotic progression.
17	7339721	TMEM102	Selectively involved in CSF2 deprivation-induced apoptosis via a mitochondria-dependent pathway.
21	43429288	ZNF295-AS1	?

Supplementary Table 3.S12.
Results of GWAS Enrichment Analysis for WGCNA modules.

	PAU		AUD		CUD		OUD	
	N	p value	N	p value	N	p value	N	p value
Ventral Striatum	4	0,045	4	0,900	4	0,912	4	0,566
Caudate Nucleus	1141	0,422	1130	0,861	1132	0,131	1055	0,091
Putamen	77	0,247	77	0,467	77	0,845	72	0,025
VS-expr-pink	335	0,697	333	0,402	334	0,043	293	0,161
CN-expr-magenta	347	0,761	344	0,269	346	0,212	303	0,396
PUT-expr-black	505	0,883	502	0,559	504	0,112	448	0,459
VS-meth-lavender	94	0,497	93	0,071	93	0,961	88	0,471
CN-meth-red	1284	0,644	1277	0,084	1279	0,216	1209	0,120
PUT-meth-plum	74	0,110	74	0,548	74	0,353	71	0,619

PAU = Problematic Alcohol Use, AUD = Alcohol Use Disorder, CUD = Cannabis Use Disorder, OUD = Opioid Use Disorder, N = Number of overlapping genes between gene set and GWAS, p value = Enrichment p value

3.8.2 Supplementary Figures
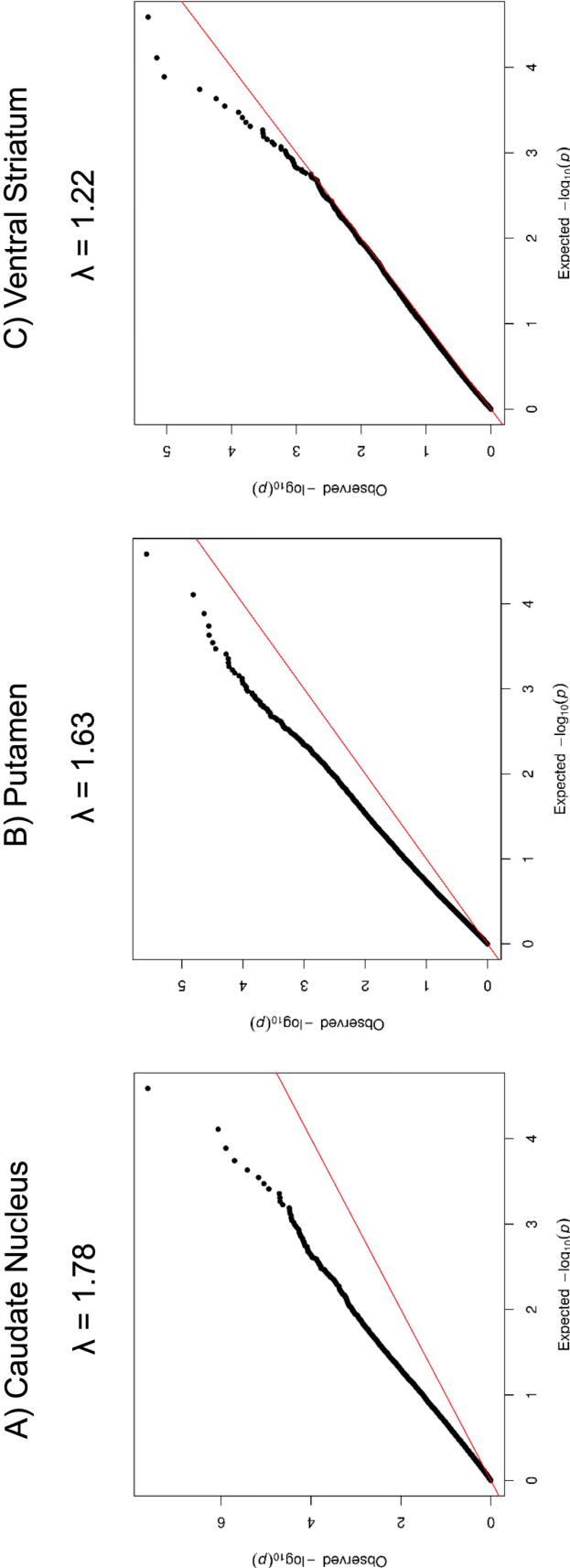
Supplementary Figure 3.S1. QQ-plots for the differential expression analysis in A) caudate nucleus, B) putamen and C) ventral striatum.
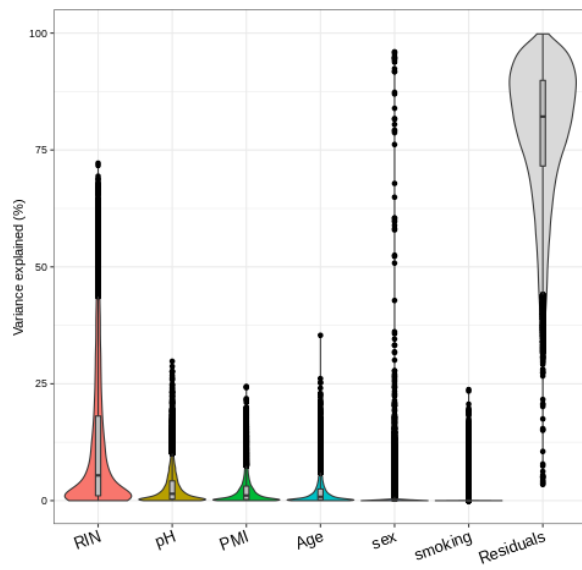
A) Caudate Nucleus
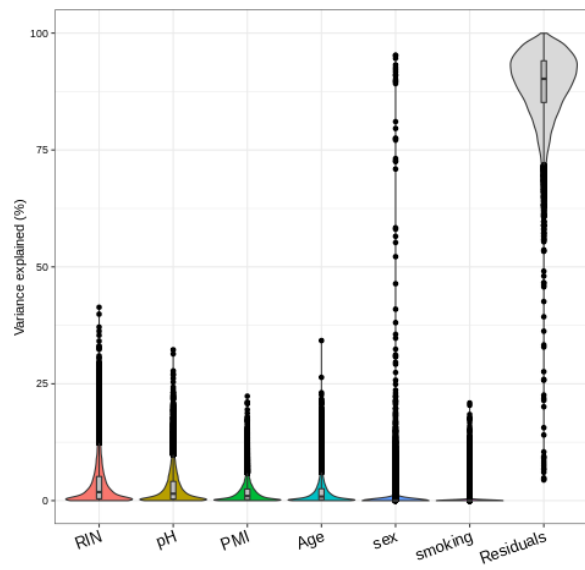
B) Ventral Striatum
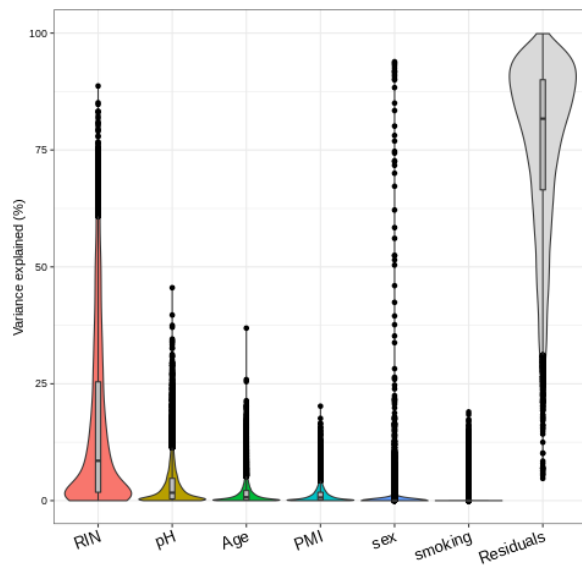
C) Putamen

Supplementary Figure 3.S2. Variance partition analysis of gene expression data from A) caudate nucleus, B) putamen and C) ventral striatum.
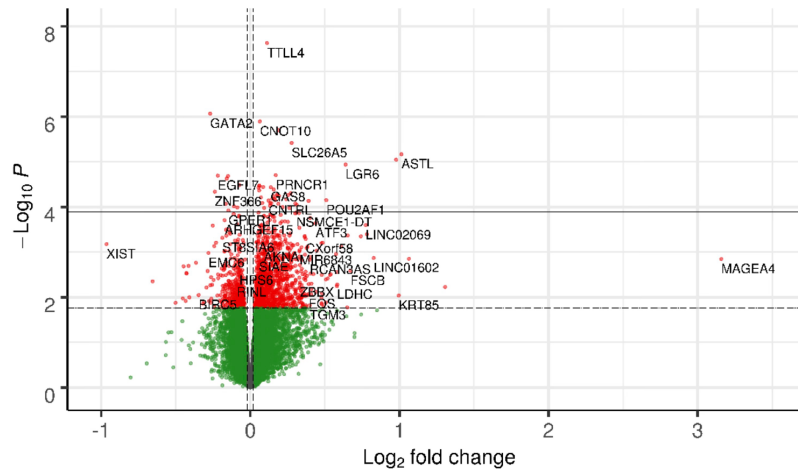
A) Caudate Nucleus
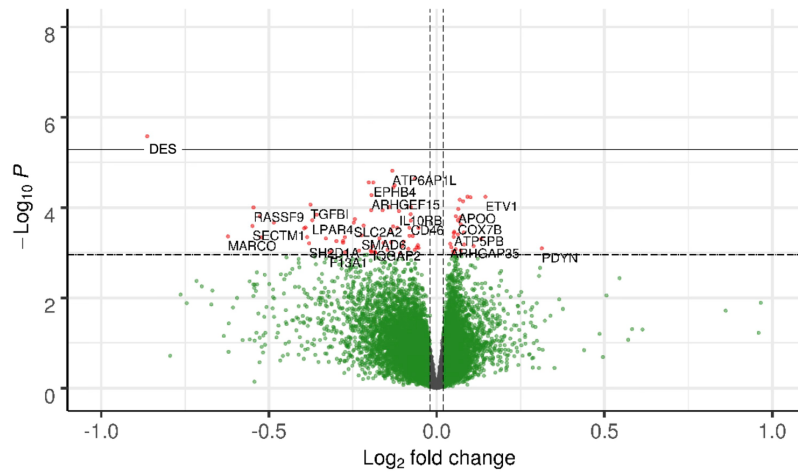
B) Putamen

C) Ventral Striatum
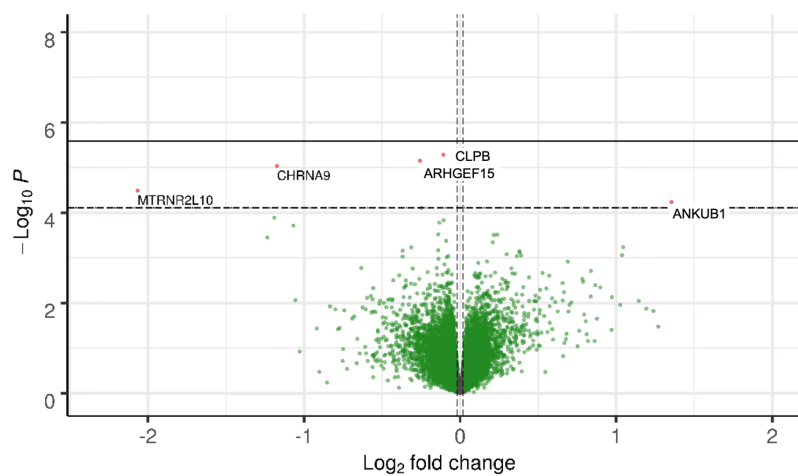
Supplementary Figure 3.S3. Volcano plots of the differential expression analysis in A) caudate nucleus, B) putamen and C) ventral striatum. Red dots indicate significance at FDR<0.25, green dots at log2(foldchange) > 0.2.

Supplementary Figure 3.S4. Heatmaps of the module trait relationships from WGCNA. A. displays data from caudate nucleus, B. from putamen and C. from ventral striatum. Methylation modules have the suffix 1 and expression modules suffix 2
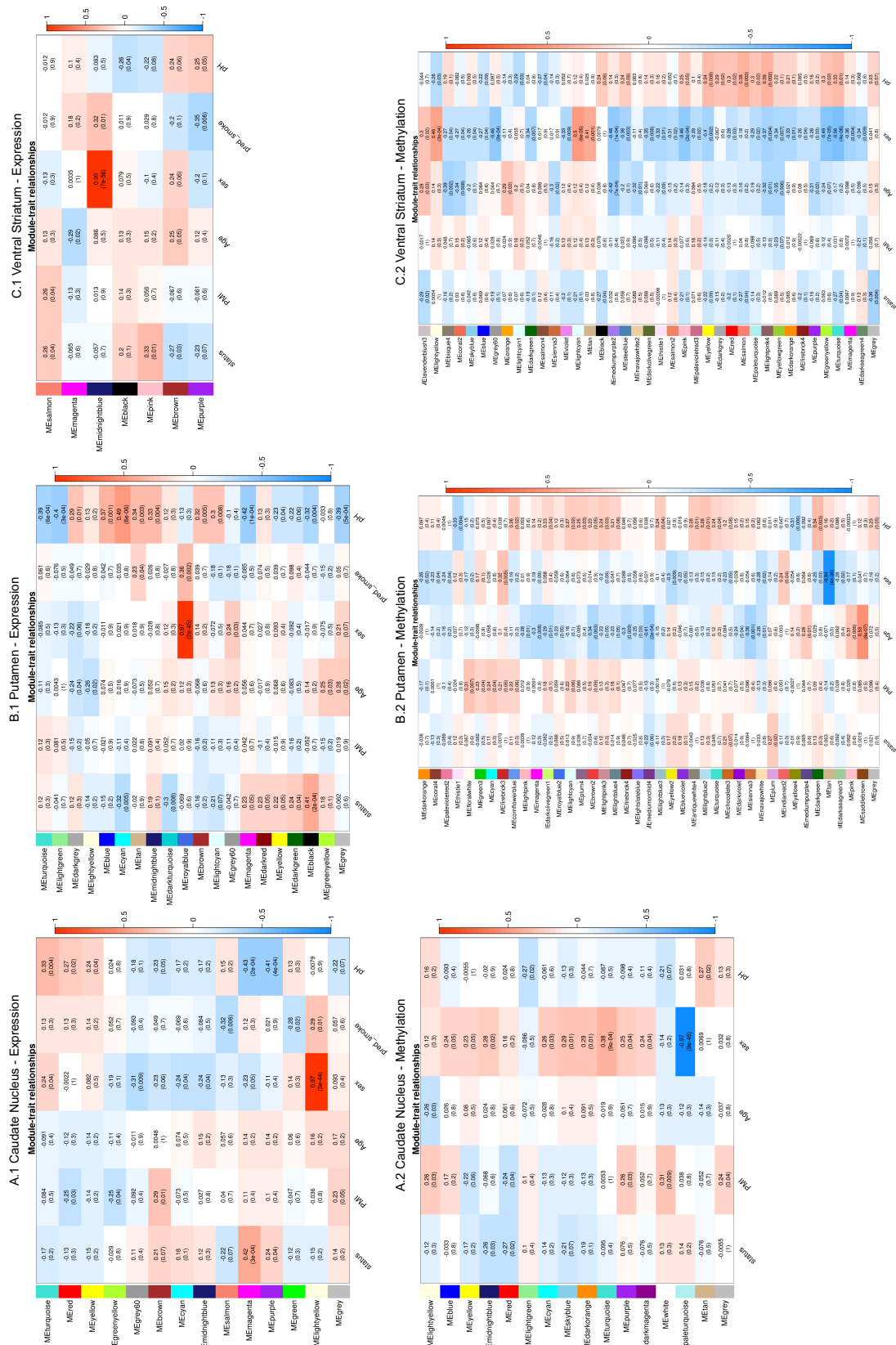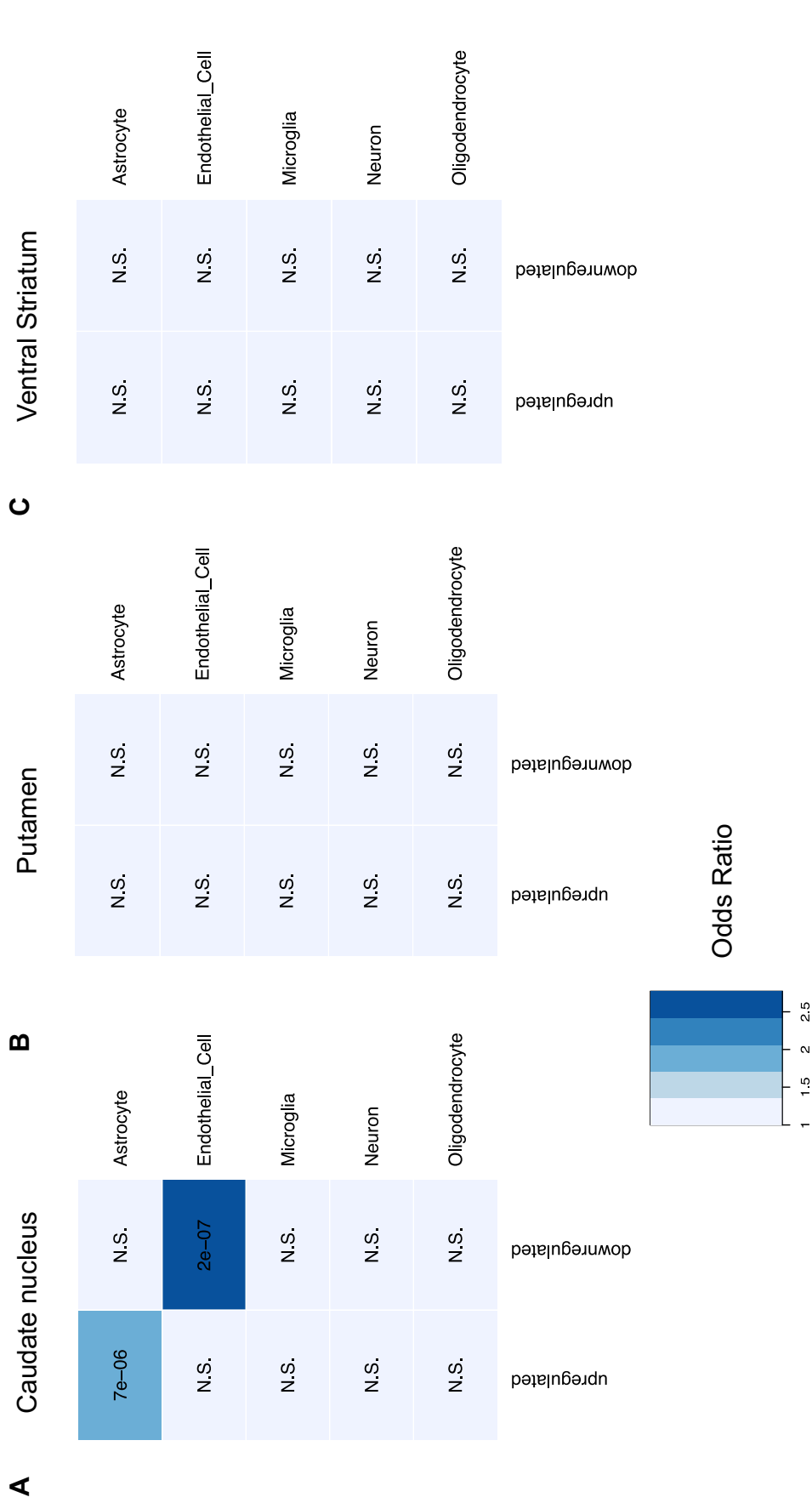
Supplementary Figure 3.S5. Heatmaps of cell-type enrichment of up- and downregulated genes in AUD (FDR<0.25) for A) caudate nucleus, B) putamen and C) ventral striatum
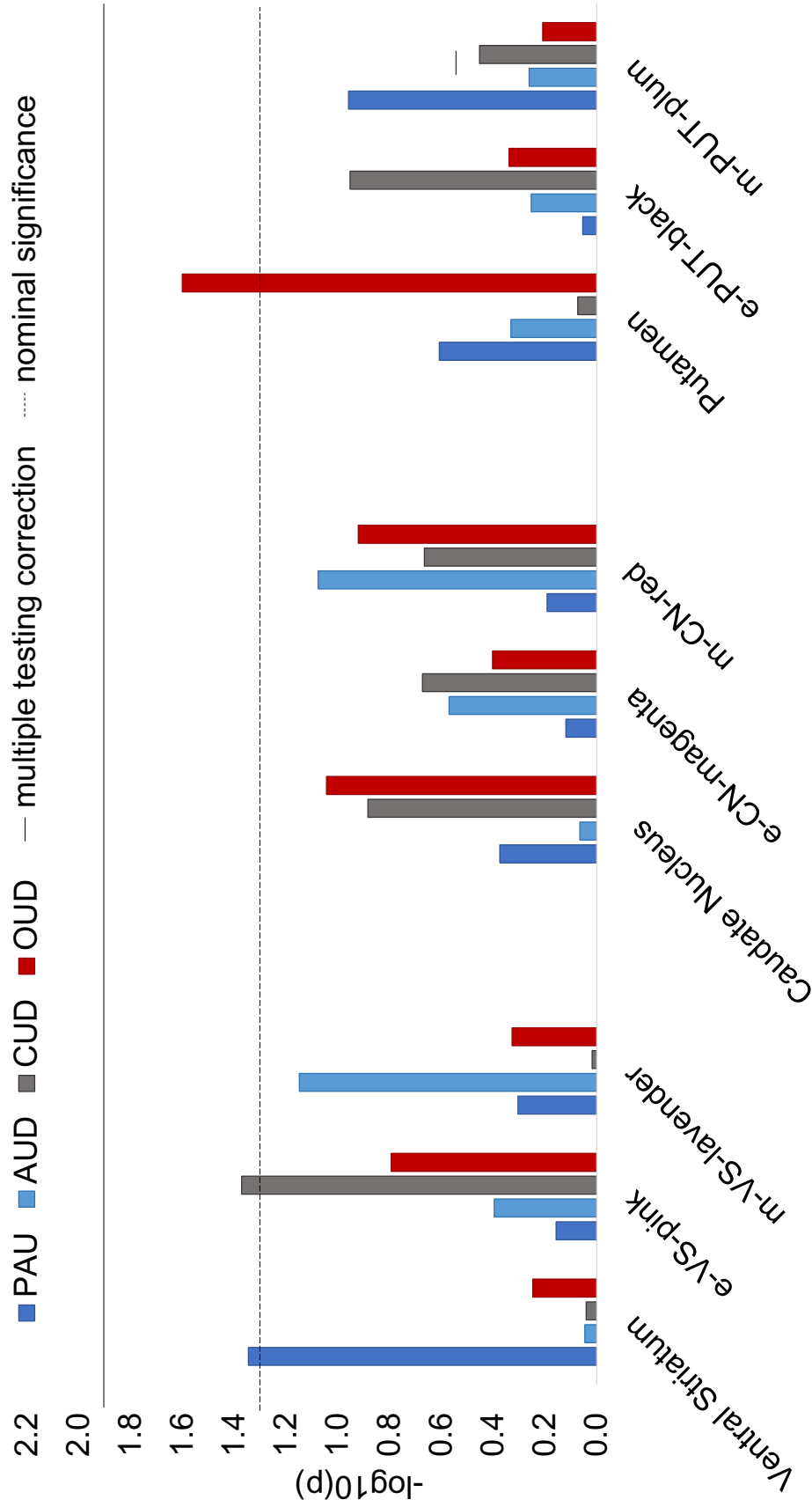
Supplementary Figure 3.S6. Bar plots depicting the –log10 transformed p values of GWAS enrichment analysis for DE genes and the WGCNA expression and methylation modules showing the strongest association with AUD in all three brain regions. Color represents the GWAS: dark blue = alcohol use disorder (AUD), light blue = problematic alcohol use (PAU), grey = Cannabis use disorder (CUD) and red = opioid use disorder (OUD). Dotted line represents nominal significance, solid line depicts significance threshold after multiple testing correction.

4   DISCUSSION

Multi-omics analyses represent an approach to gain a deeper understanding of AUD, paving the way towards novel and more targeted treatment approaches in the future. We identified differentially methylated positions and regions in the dorsal and ventral striatum of individuals with AUD compared to individuals without AUD. DMPs and DMRs were in genes previously associated with neurodegenerative diseases, cancer phenotypes and type 2 diabetes. The top hit in the ventral striatum could affect alcohol metabolization. While one of our top hits in the caudate nucleus, a DMR in *DDAH2* was replicated by pyrosequencing, we did not observe differential expression for this gene, neither with PCR nor by RNA-sequencing. Overall, there was little overlap on the single-gene level between the DNA methylation investigated in the first, and the gene expression in the second study. When we analyzed DNA methylation and gene expression together in the second study, we observed evidence for increased immune response and neuroinflammation in AUD. This main finding, as well as additional considerations, which emerge from the comparative analysis of both studies, are discussed in the following paragraphs.

4.1   Neuroinflammation

The main finding in these studies was the increased neuroinflammation associated with AUD. This is in line with previous studies, both in whole blood samples (Witt et al., 2020) and postmortem human brain tissue (Brenner et al., 2020; Kapoor et al., 2019). Alcohol consumption leads to increased inflammation and an activated immune response, which has been shown repeatedly: Witt et al. (2020) found differential DNA methylation between participants with and without AUD was enriched for inflammation-related pathways and that the differences between the groups were reduced after two weeks of withdrawal treatment. This also underlines the reversibility of AUD-associated DNA methylation changes. Evidence for (neuro-) inflammation in AUD further comes from a transcriptome-wide gene expression study in BA9. Here, network analyses revealed an AUD-associated module that was highly enriched for immune response processes (Kapoor et al., 2019). Also, in a snRNA-seq study of AUD in BA9, it was shown that the expression genes involved in neuroinflammation pathways differed between cell types, with astrocytes expressing the highest number (Brenner et al., 2020). Next to genome-wide approaches, candidate gene studies in postmortem human brain have investigated neuroinflammation in AUD (Crews et al., 2017).

In both the DNA methylation and gene expression data, we observed enrichment of immune- and inflammation-related pathways. In our network analysis, we identified *STAT3* as a conserved hub gene across all striatal brain regions and a similar gene network has been observed in the hippocampus in a rodent model of alcohol withdrawal (Chen et al., 2021). *STAT3* is a member of the JAK/STAT signaling pathway and is further known to play a role in the transcriptional activation of the C-reactive protein (Zhang et al., 1996), a key inflammatory protein, which is mainly synthesized by liver hepatocytes (Sproston & Ashworth, 2018). While STAT3 activation

promotes inflammation, it can also have a protective effect on liver injury (Zhao et al., 2021) and vice versa. For example, a knockout of *STAT3* in mice has been associated with increased alcohol-associated liver injuries (Miller et al., 2010). In light of this study and similar findings in rodents (Chen et al., 2021), the influence of *STAT3* knockout and overexpression on alcohol intake behavior and alcohol-associated organ damage should be investigated in a rodent model, which allows for harvesting both liver and brain from the animal.

At the same time, it is known that many solid tumors show increased STAT3 activation (Bharti et al., 2004; Kanda et al., 2004; Mora et al., 2002), which promotes cell survival and immune tolerance in tumor cells (Avalle et al., 2012). Further, STAT3 activation is required for tumorigenesis in a variety of cancers, e.g. in skin (Pedranzini et al., 2004) and thyroid cancer (Couto et al., 2012), and inhibition of STAT3 leads to growth arrest and apoptosis in tumor cell lines (Bharti et al., 2004; Mora et al., 2002). It is therefore important, that future studies not only explore further how knockout and overexpression of *STAT3* affect rodents with and without an AUD phenotype, but specifically investigate tumorigenesis in the animals as a potential side effect of *STAT3* overexpression.

4.2   Methodological Considerations

4.2.1   Methodological Differences between Study 1 and Study 2

In study 1, we performed an EWAS and a network analysis, WGCNA, in BA9, ACC, VS, CN and PUT. In the second study, the three striatal brain regions were additionally analyzed using RNA-sequencing and data integrated with DNA methylation. RNA-sequencing is much more cost intensive than analyzing DNA methylation on a microarray. Therefore, we focused on the brain regions for which we observed significant methylation differences in the EWAS. In addition, the Kapoor et al. (2019) study used samples from BA9 stemming from the same brain bank and we aimed to avoid sample overlap.

Another difference is the procedure of WGCNA network construction. Before performing WGCNA on DNA methylation data, a filtering step needs to be applied to reduce the number of CpG sites analyzed. In study 1, we filtered for AUD-associated CpG sites in the EWAS, following the example of a previous study (Liu et al., 2021). This approach enables the identification of co-methylated modules within the AUD-associated CpG sites. However, one of the strengths of WGCNA is related to its potential to identify regulatory networks based on the intercorrelation of features. By filtering for AUD-associated features, this ability is somewhat diminished, as other CpG sites that are not themselves associated with AUD could also be an important part of a module. Therefore, we repeated the WGCNA analysis in study 2 applying a less biased filtering approach. Here, quantile normalized beta values were filtered for promoter and enhancer associated CpG sites. The rationale was to select sites which are likely to influence on gene expression, while retaining the bottom-up approach of WGCNA.

4.2.2 Batch Effects and the Neurocircuitry of Addiction

The goal of this study was to investigate the molecular mechanisms of AUD in multiple brain regions belonging to the neurocircuitry of addiction. At the same time, we did not compare the different regions directly. One reason was because of confounding between sequencing batch and brain region. Batch is a very prominent driver of variation in both DNA methylation (Michels & Binder, 2018) and RNA sequencing studies (Conesa et al., 2016). To balance out batch effects, samples need to be randomized across processing plates. In our experiment we had several potential drivers of variance, such as AUD status, sex and smoking. Therefore, we decided to process each brain region on a separate plate and randomize samples on each plate for AUD status, sex, and smoking. While this approach provided us with a well-randomized balanced design within each brain region, it does not allow for a direct statistical comparison between the regions.

It also has to be noted that the entire set of five brain regions was not available for each donor. This has implications for within-subject testing, which is now possible in a multi-omics framework as discussed in the next section.

4.3 Multi-Omics Analyses

4.3.1 Overlap of DNA Methylation and Gene Expression

In the present studies, the investigation of multi-omics was not only able to show convergent evidence for neuroinflammation in AUD, but it also underlined that differential methylation does not necessarily lead to differential gene expression. Many of the CpG sites differentially methylated in study 1 were not associated with differential gene expression in study 2. There are several reasons for this observation. First, to impede transcription factor binding, several CpG sites in close proximity need to be methylated (CpG islands) and a single DMP might not have a direct impact on gene expression (Moore et al., 2013). Second, there is a variety of other epigenetic mechanisms, such as histone modifications and chromatin accessibility, but also hydroxymethylation of DNA, which also affect transcription (Gibney & Nolan, 2010). DNA methylation studies can have different trajectories, such as the discovery of biomarkers predicting diseases, which has been successfully done for smoking (Bollepalli et al., 2019). In our study, the aim was to identify functional mechanisms of DNA methylation differences in AUD using a microarray technology which is associated with several limitations. While the EPIC BeadChip covers about 850.000 CpG sites, the majority of probes are located in intergenic regions and in the gene body. When analyzing DNA methylation together with gene expression, DNA methylation in promoter and enhancer regions, which commonly harbor CpG islands, is of particular interest. These areas only represent a small percentage of the probes on the EPIC BeadChip and usually promoter regions are covered by not more than 2 or 3 CpG sites. As established in previous studies in the field of cancer research, drastic changes in DNA methylation are required to produce changes in gene expression. Yet, it can be argued that profound changes in DNA methylation should

be adequately represented by a small number of sites. When investigating functional mechanisms of phenotypes, which may have smaller effect sizes, a more detailed characterization of DNA methylation, such as using reduced representation or whole genome bisulfite sequencing may be advantageous.

4.3.2 Multi-Omics Integration Methods

There is a rapid increase in the number of multi-omics integration tools available. A recent publication presented MEFISTO, which allows for within and between subject comparisons in multi-omics data (Velten et al., 2022). This could have enabled direct statistical comparison of gene expression between the brain regions in study 2, but was released just after the manuscript was reviewed. MEFISTO is based on the multi-omics factor analysis (MOFA) tool representing the first dimensionality reduction multi-omics method (Argelaguet et al., 2018). Although we applied MOFA to our dataset, the results were not interpretable, because DNA methylation did not explain enough variance. This could be related to the microarray technology used, or because of the type and quality of tissue we investigated.

4.4 Tissue

Postmortem human brain tissue is a very valuable resource, but has several limitations that need be considered. One limitation that has an immediate impact on statistical procedures is the sample size, which has already been discussed. Even more important is tissue quality, which varies greatly between individuals as well as between tissue resources. As discussed in studies 1 and 2, this can be in part accounted for by controlling for RIN, postmortem interval and the pH value of the brain sample. Adding RIN, PMI and/or pH as covariates assumes that they affect the outcome, gene expression and DNA methylation, linearly. For gene expression, it has been shown that including RIN in the linear model is an adequate control, if RIN and the effect of interest are not associated (Gallego Romero et al., 2014). However, it is unclear how AUD status affects RIN.

Another major factor that has not been sufficiently described in the literature is how cause of death is related to DNA methylation and gene expression patterns in the brain. It is unknown whether the same biological processes occur independently of the cause of death or if a sudden death, e.g., traumatic brain injury after a car accident, and a prolonged phase of dying have differential impact on the molecular architecture of the brain. For peripheral blood it has been shown that the transcriptomic profile is more dependent on whether blood was taken pre- or postmortem than on cause of death (Ferreira et al., 2018). In our sample, cause of death is very heterogeneous between individuals, but also between groups. In addition, it is not clear how DNA methylation and gene expression might differ in living and postmortem brain tissue. In line with this, it must be noted that brain banks differ in their sampling procedures. Donors die not only due to different causes, but also in different environmental conditions, such as extreme heat, which can affect RNA quality.

In conclusion, while postmortem human brain tissue is the best available way to non-invasively study molecular mechanisms directly in the brain, it comes with many caveats.

4.5 Outlook

4.5.1 Translational Indications

Multi-omics analyses in postmortem human brain tissue inevitably investigate long term changes of AUD rather than mechanisms involved in the development. This can be seen as a limitation, but also as a chance to develop treatments that target the consequences of AUD instead of reversing the AUD status. For example, Lohoff et al. (2018) were able to identify PCSK9 inhibitors as a possible treatment for AUD-associated health consequences, such as liver fibrosis and increased stroke risk, through EWAS. Treatment with the PCSK9 inhibitor does not target abstinence, but aims to improve the quality of life for patients with AUD. A similar approach could be explored for inflammation-reducing drugs.

4.5.2 Meta-Analysis

By now, several studies of DNA methylation in AUD in postmortem human brain tissue have been published. Many of them had not been published prior to the presented studies 1 and 2. A meta-analysis of these datasets could significantly reduce noise and identify true signals. Of course, this proposes challenges, especially in harmonizing the data. Because technical effects and the correction for them heavily influences microarray and sequencing analyses, findings should not be compared exclusively based on summary statistics. Instead, a joint preprocessing of raw data is necessary to reduce technical variability between individual studies.

4.5.3 Extending Multi-Omics

The joint analysis of DNA methylation and gene expression is only one example of multi-omics. There are many other molecular features that can and should be integrated to deepen the understanding of molecular mechanisms in AUD. Just as differential DNA methylation does not necessarily lead to differential mRNA expression, differential mRNA expression does not necessarily result in differential protein expression. For now, it is not possible to accurately depict all molecular mechanisms in a tissue sample, but it might be sufficient to focus analyzes on a couple of -omics, which allow conclusions about other biological processes. For example, in single nuclei ATAC-seq enrichment for transcription factor binding motifs can be tested instead of having to analyze it in the wet lab. In any case, extending our efforts to proteomics and the study of small RNAs could help to get a more detailed picture of the molecular interplay that is associated with AUD.

In addition, DNA methylation and gene expression should be studied on the single-nuclei level, which enables a cell-type specific investigation. More importantly, single-

nuclei multiome analyses allow the characterization of DNA accessibility and gene expression in the same cell. Single-nuclei analyses could be a great asset to postmortem human brain studies, as quality metrics can be calculated for each cell enabling a more targeted correction and exclusion procedure than adding covariates to a linear model.

4.6   Conclusion

We identified epigenetic and transcriptomic signatures of AUD in postmortem human brain samples of individuals with and without AUD. We present convergent evidence for the importance of neuroinflammation in AUD and provide a basis for the functional validation of inflammation and immune response pathways in animal or iPSC models. It has been shown that multi-omics analysis is beneficial for interpreting findings from single-omics analyses. At the same time, our studies underline the rapid development of the field and analysis techniques that are consistently refined and extended.

5 SUMMARY

5.1 English Summary

Alcohol use disorder is characterized by a loss of control over alcohol intake and contributes to a large number of premature deaths worldwide by representing a strong risk factor for numerous diseases. Despite decade-long research on alcohol use disorder, treatment options are limited and relapse rates following withdrawal treatment are high. Currently, alcohol use disorder is understood as a brain disorder as neuroimaging studies have shown substantial alcohol use disorder-associated connectivity and activity alterations in the human brain. This led to the hypothesis of a neurocircuitry of addiction involving multiple brain regions such as the ventral and dorsal striatum, but also cortical regions that display aberrant functional connectivity patterns in alcohol use disorder. These profound brain changes in alcohol use disorder are assumed to be established by molecular processes such as aberrant DNA methylation and gene expression patterns. To investigate these processes in the human brain, postmortem brain tissue depicts a valuable resource. Previous studies have been published reporting on alcohol use disorder-associated differential methylation or differentially expressed genes mainly in the prefrontal cortex. So far, no analysis has integrated DNA methylation and gene expression data in a multi-Omics approach. Further, it remains unclear how alterations in DNA methylation and gene expression are related to each other in the alcohol use disorder brain. The overall aim of the presented studies was to identify functionally relevant molecular mechanisms of alcohol use disorder in the neurocircuitry of addiction.

To address these points, the first paper aimed to expand the epigenetic characterization of alcohol use disorder to the neurocircuitry of addiction by performing an epigenome-wide association study of DNA methylation in alcohol use disorder in five brain regions: the cortical regions anterior cingulate cortex and Brodmann Area 9, and the striatal regions caudate nucleus, putamen, and ventral striatum. In the second study, the gene expression profile of the striatal brain regions was investigated using RNA-Sequencing enabling the integration of DNA methylation and gene expression data in a multi-omics approach. The biological implication of alcohol use disorder-associated DNA methylation and expression signatures was investigated in both studies using a comprehensive set of bioinformatic tools including Gene Ontology- and gene-set enrichment analyses, weighted correlation network analyses, enrichment analyses of results from genome-wide association studies of substance use disorder phenotypes, and protein-protein interaction networks.

In the epigenome-wide association study of alcohol use disorder in five brain regions, 20 differentially methylated CpG sites were detected, two in caudate nucleus and 18 in the ventral striatum, that were associated with alcohol use disorder at epigenome-wide significance. Alcohol use disorder-associated DNA methylation signatures were strongest in the caudate nucleus, putamen, and ventral striatum and were enriched within immune-related cellular pathways. Gene expression analysis in the second

study suggested converging evidence for inflammatory and immunological signaling in alcohol use disorder. While the overlap of differential methylation and differential expression at the gene level was limited, it was evident on the network level. Consistent differential expression of the *ARHGEF15* gene was found in the caudate nucleus, putamen, and ventral striatum in alcohol use disorder. Further, the *STAT3* gene was identified as a conserved hub node in alcohol use disorder-associated gene networks and might be a promising candidate for further evaluation.

In conclusion, this is the first study that integrated DNA methylation and gene expression data from the same individuals in multiple brain regions in the context of alcohol use disorder. Converging evidence from this study supports the role of (neuro) inflammation in the pathophysiology of alcohol use disorder. Methods for multi-omics integration are rapidly emerging and the integration of multiple omics including epigenome-wide DNA Methylation, transcriptomics, proteomics, and non-coding RNAs enables the complementation, but also the prioritization of findings from single omics layers. In follow-up studies, functional validation of multi-omics-derived candidate genes and pathways should be performed using animal models and patient-derived brain organoids. Conducting such precision medicine approaches might lead to the discovery of novel therapeutic strategies in alcohol use disorder, which are urgently required.

5.2   German Summary – Zusammenfassung in deutscher Sprache

Die Alkoholkonsumstörung ist gekennzeichnet durch Kontrollverlust über den Alkoholkonsum und trägt in hohem Maße zur weltweiten Morbidität und Mortalität bei, da sie einen Risikofaktor für zahlreiche Erkrankungen darstellt. Trotz jahrzehntelanger Forschung auf dem Gebiet der Alkoholkonsumstörung sind die Behandlungsmöglichkeiten begrenzt, und die Rückfallquoten nach einer Entzugsbehandlung hoch. Gegenwärtig wird die Alkoholkonsumstörung als eine Störung des Gehirns verstanden, da Neuroimaging-Studien erhebliche, mit der Alkoholkonsumstörung zusammenhängende Konnektivitäts- und Aktivitätsveränderungen im menschlichen Gehirn nachgewiesen haben. Dies führte zu der Hypothese einer „neurocircuitry of addiction" (neuronaler Suchtschaltkreis), an der mehrere Hirnregionen, wie das ventrale und dorsale Striatum, aber auch kortikale Regionen beteiligt sind, die bei der Alkoholkonsumstörung abweichende funktionelle Konnektivitätsmuster aufweisen. Es wird angenommen, dass diese tiefgreifenden Veränderungen des Gehirns bei der Alkoholkonsumstörung durch molekulare Prozesse wie veränderte DNA-Methylierung und Genexpressionsmuster bedingt sind. Postmortales Hirngewebe stellt eine wertvolle Ressource dar, um diese Prozesse im menschlichen Gehirn zu untersuchen. In früheren Studien wurde über eine mit Alkoholkonsum assoziierte differentielle Methylierung oder differentielle Genexpression vor allem im präfrontalen Kortex berichtet. Bislang gibt es keine Studie im Feld der Alkoholkonsumstörung, die DNA-Methylierungs- und Genexpressionsdaten in einem Multi-Omics-Ansatz integriert. Darüber hinaus ist nach

wie vor unklar, wie Veränderungen der DNA-Methylierung und der Genexpression im Gehirn bei der Alkoholkonsumstörung zusammenhängen. Das übergeordnete Ziel der vorgestellten Studien bestand darin, funktionell relevante molekulare Mechanismen der Alkoholkonsumstörung in der neurocircuitry of addiction zu identifizieren.

Dazu wurde eine epigenomweite Assoziationsstudie zur DNA-Methylierung bei Alkoholkonsumstörung in fünf Hirnregionen durchgeführt: in den kortikalen Regionen anteriorer cingulärer Kortex und Brodmann Area 9 sowie in den striatalen Regionen Nucleus caudatus, Putamen und ventrales Striatum. In der zweiten Studie wurde das Genexpressionsprofil der striatalen Hirnregionen mittels RNA-Sequenzierung untersucht, was die Integration von DNA-Methylierungs- und Genexpressionsdaten in einem Multi-omics-Ansatz ermöglichte. Die biologische Bedeutung der mit Alkoholkonsum assoziierten DNA-Methylierungs- und Expressionssignaturen wurde in beiden Studien mit Hilfe einer umfassenden bioinformatischen Analyse-Sequenz untersucht, darunter Gene-Ontology- und Gene-set-Enrichment-Analysen, Netzwerk-analysen, Enrichment-Analysen von Ergebnissen aus genomweiten Assoziationsstudien zu Phänotypen von Substanzkonsumstörungen und Protein-Protein-Interaktions-Netzwerke.

In der epigenomweiten Assoziationsstudie zur Alkoholkonsumstörung in fünf Hirnregionen wurden 20 differentiell methylierte CpG-Sequenzen entdeckt, zwei im Nucleus caudatus und 18 im ventralen Striatum, die auf Ebene der epigenomweiten Signifikanz mit der Alkoholkonsumstörung in Verbindung gebracht wurden. Die mit der Alkoholkonsumstörung assoziierten DNA-Methylierungssignaturen waren im Nucleus caudatus, im Putamen und im ventralen Striatum am stärksten ausgeprägt und zeigten eine Anreicherung für immunbezogene Signalwege. Die Genexpressionsanalyse in der zweiten Studie wies in Zusammenhang mit den Ergebnissen der ersten Studie auf konvergierende Befunde für entzündliche und immunologische Signalwege bei der Alkoholkonsumstörung hin. Während die Überschneidung von differentieller Methylierung und differentieller Genexpression begrenzt war, zeigte sich eine Überschneidung der Befunde in der Netzwerkanalyse. Eine konsistente differentielle Expression des *ARHGEF15*-Gens wurde im Nucleus caudatus, im Putamen und im ventralen Striatum bei der Alkoholkonsumstörung festgestellt. Darüber hinaus wurde das *STAT3*-Gen als konservierter Knotenpunkt in Gennetzwerken identifiziert, die mit der Alkoholkonsumstörung in Verbindung stehen. *STAT3* stellt damit einen vielversprechenden Kandidaten für weitere Untersuchungen dar.

Zusammenfassend ist dies die erste Studie, in der DNA-Methylierungs- und Genexpressionsdaten von denselben Personen in mehreren Gehirnregionen im Zusammenhang mit der Alkoholkonsumstörung integriert wurden. Die konvergierenden Erkenntnisse aus dieser Studie unterstützen die Rolle der (Neuro-) Inflammation in der Pathophysiologie der Alkoholkonsumstörung. Die Methoden für die Datenintegration auf Basis eines Multi-Omics-Ansatzes entwickeln sich rasant, und die Integration mehrerer Omics-Ebenen, einschließlich epigenomweiter DNA-Methylierung, Transcriptomics, Proteomics und nicht-kodierender RNAs, ermöglicht

eine Erweiterung der Datenbasis und die Priorisierung von Erkenntnissen aus einzelnen Omics-Ebenen. In Folgestudien sollte eine funktionelle Validierung der aus der Multi-Omics-Analyse abgeleiteten Kandidatengene und Signalwege anhand von Tiermodellen und aus Patientengewebe generierten Hirnorganoiden durchgeführt werden. Die Durchführung solcher präzisionsmedizinischen Ansätze könnte zur Entdeckung dringend benötigter neuer therapeutischer Strategien bei der Alkoholkonsumstörung beitragen.

6   REFERENCES

Aberg, K. A., Chan, R. F., & van den Oord, E. J. C. G. (2020). MBD-seq - realities of a misunderstood method for high-quality methylome-wide association studies. *Epigenetics, 15*(4), 431-438. https://doi.org/10.1080/15592294.2019.1695339

Akkermans, S. E. A., Luijten, M., van Rooij, D., Franken, I. H. A., & Buitelaar, J. K. (2018). Putamen functional connectivity during inhibitory control in smokers and non-smokers. *Addiction Biology, 23*(1), 359-368. https://doi.org/10.1111/adb.12482

American Psychiatric Association. (1994). *Diagnostic and statistical manual of mental disorders DSM-IV*. American Psychiatric Association.

American Psychiatric Association. (2013). *Diagnostic and statistical manual of mental disorders: DSM-5*. American Psychiatric Association.

Andrews, S. (2010). *FastQC: A quality control tool for high throughput sequencing data.* In https://www.bioinformatics.babraham.ac.uk/projects/fastqc/.

Argelaguet, R., Velten, B., Arnol, D., Dietrich, S., Zenz, T., Marioni, J. C., Buettner, F., Huber, W., & Stegle, O. (2018). Multi-Omics Factor Analysis—a framework for unsupervised integration of multi-omics data sets. *Molecular Systems Biology, 14*(6), e8124. https://doi.org/10.15252/msb.20178124

Ashburner, M., Ball, C. A., Blake, J. A., Botstein, D., Butler, H., Cherry, J. M., Davis, A. P., Dolinski, K., Dwight, S. S., Eppig, J. T., Harris, M. A., Hill, D. P., Issel-Tarver, L., Kasarskis, A., Lewis, S., Matese, J. C., Richardson, J. E., Ringwald, M., Rubin, G. M., & Sherlock, G. (2000). Gene Ontology: tool for the unification of biology. *Nature Genetics, 25*(1), 25-29. https://doi.org/10.1038/75556

Astle, W. J., Elding, H., Jiang, T., Allen, D., Ruklisa, D., Mann, A. L., Mead, D., Bouman, H., Riveros-Mckay, F., Kostadima, M. A., Lambourne, J. J., Sivapalaratnam, S., Downes, K., Kundu, K., Bomba, L., Berentsen, K., Bradley, J. R., Daugherty, L. C., Delaneau, O., Freson, K., Garner, S. F., Grassi, L., Guerrero, J., Haimel, M., Janssen-Megens, E. M., Kaan, A., Kamat, M., Kim, B., Mandoli, A., Marchini, J., Martens, J. H. A., Meacham, S., Megy, K., O'Connell, J., Petersen, R., Sharifi, N., Sheard, S. M., Staley, J. R., Tuna, S., van der Ent, M., Walter, K., Wang, S. Y., Wheeler, E., Wilder, S. P., Iotchkova, V., Moore, C., Sambrook, J., Stunnenberg, H. G., Di Angelantonio, E., Kaptoge, S., Kuijpers, T. W., Carrillo-de-Santa-Pau, E., Juan, D., Rico, D., Valencia, A., Chen, L., Ge, B., Vasquez, L., Kwan, T., Garrido-Martín, D., Watt, S., Yang, Y., Guigo, R., Beck, S., Paul, D. S., Pastinen, T., Bujold, D., Bourque, G., Frontini, M., Danesh, J., Roberts, D. J., Ouwehand, W. H., Butterworth, A. S., & Soranzo, N. (2016). The Allelic Landscape of Human Blood Cell Trait Variation and Links to Common Complex Disease. *Cell, 167*(5), 1415-1429.e1419. https://doi.org/10.1016/j.cell.2016.10.042

Avalle, L., Pensa, S., Regis, G., Novelli, F., & Poli, V. (2012). STAT1 and STAT3 in tumorigenesis: A matter of balance. *JAK-STAT, 1*(2), 65-72. https://doi.org/10.4161/jkst.20045

Babor, T. F., Higgins-Biddle, J. C., Saunders, J. B., & Monteiro, M. G. (2001). *The alcohol use disorders identification test*. World Health Organization.

Bach, P., Kirsch, M., Hoffmann, S., Jorde, A., Mann, K., Frank, J., Charlet, K., Beck, A., Heinz, A., Walter, H., Rietschel, M., Kiefer, F., & Vollstädt-Klein, S. (2015). The effects of single nucleotide polymorphisms in glutamatergic neurotransmission genes on neural response to alcohol cues and craving. *Addiction Biology, 20*(6), 1022-1032. https://doi.org/10.1111/adb.12291

Baj, J., Flieger, W., Teresiński, G., Buszewicz, G., Sitarz, R., Forma, A., Karakuła, K., & Maciejewski, R. (2020). Magnesium, Calcium, Potassium, Sodium, Phosphorus, Selenium, Zinc, and Chromium Levels in Alcohol Use Disorder: A Review. *Journal of Clinical Medicine, 9*(6), 1901. https://doi.org/10.3390/jcm9061901

Baliunas, D. O., Taylor, B. J., Irving, H., Roerecke, M., Patra, J., Mohapatra, S., & Rehm, J. (2009). Alcohol as a risk factor for type 2 diabetes: A systematic review and meta-analysis. *Diabetes Care, 32*(11), 2123-2132. https://doi.org/10.2337/dc09-0227

Bazov, I., Kononenko, O., Watanabe, H., Kuntić, V., Sarkisyan, D., Taqi, M. M., Hussain, M. Z., Nyberg, F., Yakovleva, T., & Bakalkin, G. (2013). The endogenous opioid system in human alcoholics: molecular adaptations in brain areas involved in cognitive control of addiction. *Addiction Biology, 18*(1), 161-169. https://doi.org/10.1111/j.1369-1600.2011.00366.x

Benjamini, Y., & Hochberg, Y. (1995). Controlling the false discovery rate: a practical and powerful approach to multiple testing. *Journal of the Royal Statistical Society: Series B, 57*(1), 289-300. https://doi.org/10.1111/j.2517-6161.1995.tb02031.x

Bharti, A. C., Shishodia, S., Reuben, J. M., Weber, D., Alexanian, R., Raj-Vadhan, S., Estrov, Z., Talpaz, M., & Aggarwal, B. B. (2004). Nuclear factor-kappaB and STAT3 are constitutively active in CD138+ cells derived from multiple myeloma patients, and suppression of these transcription factors leads to apoptosis. *Blood, 103*(8), 3175-3184. https://doi.org/10.1182/blood-2003-06-2151

Biernacka, J. M., Coombes, B. J., Batzler, A., Ho, A. M.-C., Geske, J. R., Frank, J., Hodgkinson, C., Skime, M., Colby, C., Zillich, L., Pozsonyiova, S., Ho, M.-F., Kiefer, F., Rietschel, M., Weinshilboum, R., O'Malley, S. S., Mann, K., Anton, R., Goldman, D., & Karpyak, V. M. (2021). Genetic contributions to alcohol use disorder treatment outcomes: a genome-wide pharmacogenomics study. *Neuropsychopharmacology, 46*(12), 2132-2139. https://doi.org/10.1038/s41386-021-01097-0

Birdsill, A. C., Walker, D. G., Lue, L., Sue, L. I., & Beach, T. G. (2011). Postmortem interval effect on RNA and gene expression in human brain tissue. *Cell and Tissue Banking, 12*(4), 311-318. https://doi.org/10.1007/s10561-010-9210-8

Bollepalli, S., Korhonen, T., Kaprio, J., Anders, S., & Ollikainen, M. (2019). EpiSmokEr: a robust classifier to determine smoking status from DNA methylation data. *Epigenomics, 11*(13), 1469-1486. https://doi.org/10.2217/epi-2019-0206

Border, R., Johnson, E. C., Evans, L. M., Smolen, A., Berley, N., Sullivan, P. F., & Keller, M. C. (2019). No Support for Historical Candidate Gene or Candidate Gene-by-Interaction Hypotheses for Major Depression Across Multiple Large Samples. *American Journal of Psychiatry, 176*(5), 376-387. https://doi.org/10.1176/appi.ajp.2018.18070881

Brenner, E., Tiwari, G. R., Kapoor, M., Liu, Y., Brock, A., & Mayfield, R. D. (2020). Single cell transcriptome profiling of the human alcohol-dependent brain. *Human Molecular Genetics, 29*(7), 1144-1153. https://doi.org/10.1093/hmg/ddaa038

Cespuglio, R., Amrouni, D., Meiller, A., Buguet, A., & Gautier-Sauvigné, S. (2012). Nitric oxide in the regulation of the sleep-wake states. *Sleep Medicine Reviews, 16*(3), 265-279. https://doi.org/10.1016/j.smrv.2012.01.006

Chen, C., Zhang, C., Cheng, L., Reilly, J. L., Bishop, J. R., Sweeney, J. A., Chen, H. Y., Gershon, E. S., & Liu, C. (2014). Correlation between DNA methylation and gene expression in the brains of patients with bipolar disorder and schizophrenia. *Bipolar Disorders, 16*(8), 790-799. https://doi.org/https://doi.org/10.1111/bdi.12255

Chen, W.-Y., Chen, H., Hamada, K., Gatta, E., Chen, Y., Zhang, H., Drnevich, J., Krishnan, H. R., Maienschein-Cline, M., Grayson, D. R., Pandey, S. C., & Lasek, A. W. (2021). Transcriptomics identifies STAT3 as a key regulator of hippocampal gene expression and anhedonia during withdrawal from chronic alcohol exposure. *Translational Psychiatry, 11*(1), 298. https://doi.org/10.1038/s41398-021-01421-8

Clark, S. L., Chan, R. F., Zhao, M., Xie, L. Y., Copeland, W. E., Penninx, B. W. J. H., Aberg, K. A., & van den Oord, E. J. C. G. (2022). Dual methylation and hydroxymethylation study of alcohol use disorder. *Addiction Biology, 27*(2), e13114. https://doi.org/10.1111/adb.13114

Coleman, L. G., Jr., Zou, J., & Crews, F. T. (2017). Microglial-derived miRNA let-7 and HMGB1 contribute to ethanol-induced neurotoxicity via TLR7. *Journal of Neuroinflammation, 14*(1), 22. https://doi.org/10.1186/s12974-017-0799-4

Conesa, A., Madrigal, P., Tarazona, S., Gomez-Cabrero, D., Cervera, A., McPherson, A., Szcześniak, M. W., Gaffney, D. J., Elo, L. L., Zhang, X., & Mortazavi, A. (2016). A survey of best practices for RNA-seq data analysis. *Genome Biology, 17*(1), 13. https://doi.org/10.1186/s13059-016-0881-8

Cooper, M. S., Stark, Z., Lunke, S., Zhao, T., & Amor, D. J. (2019). IREB2-associated neurodegeneration. *Brain, 142*(8), e40. https://doi.org/10.1093/brain/awz183

Costain, G., Ghosh, M. C., Maio, N., Carnevale, A., Si, Y. C., Rouault, T. A., & Yoon, G. (2019). Absence of iron-responsive element-binding protein 2 causes a novel neurodegenerative syndrome. *Brain, 142*(5), 1195-1202. https://doi.org/10.1093/brain/awz072

Couto, J. P., Daly, L., Almeida, A., Knauf, J. A., Fagin, J. A., Sobrinho-Simões, M., Lima, J., Máximo, V., Soares, P., Lyden, D., & Bromberg, J. F. (2012). STAT3 negatively regulates thyroid tumorigenesis. *Proceedings of the National Academy of Sciences of the United States of America, 109*(35), E2361-2370. https://doi.org/10.1073/pnas.1201232109

Crews, F. T., Lawrimore, C. J., Walter, T. J., & Coleman, L. G. (2017). The role of neuroimmune signaling in alcoholism. *Neuropharmacology, 122*, 56-73. https://doi.org/10.1016/j.neuropharm.2017.01.031

Crews, F. T., Qin, L., Sheedy, D., Vetreno, R. P., & Zou, J. (2013). High mobility group box 1/Toll-like receptor danger signaling increases brain neuroimmune activation in alcohol dependence. *Biological Psychiatry, 73*(7), 602-612. https://doi.org/10.1016/j.biopsych.2012.09.030

Cui, C., Noronha, A., Morikawa, H., Alvarez, V. A., Stuber, G. D., Szumlinski, K. K., Kash, T. L., Roberto, M., & Wilcox, M. V. (2013). New insights on neurobiological mechanisms underlying alcohol addiction. *Neuropharmacology, 67*, 223-232. https://doi.org/10.1016/j.neuropharm.2012.09.022

Davis, R. L., & Syapin, P. J. (2005). Interactions of alcohol and nitric-oxide synthase in the brain. *Brain Research Reviews, 49*(3), 494-504. https://doi.org/10.1016/j.brainresrev.2005.01.008

de Leeuw, C. A., Mooij, J. M., Heskes, T., & Posthuma, D. (2015). MAGMA: Generalized Gene-Set Analysis of GWAS Data. *PLoS Computational Biology, 11*(4), e1004219. https://doi.org/10.1371/journal.pcbi.1004219

de Timary, P., Stärkel, P., Delzenne, N. M., & Leclercq, S. (2017). A role for the peripheral immune system in the development of alcohol use disorders? *Neuropharmacology, 122*, 148-160. https://doi.org/10.1016/j.neuropharm.2017.04.013

Deaton, A. M., & Bird, A. (2011). CpG islands and the regulation of transcription. *Genes & development, 25*(10), 1010-1022. https://doi.org/ 10.1101/gad.2037511

Degenhardt, L., Charlson, F., Ferrari, A., Santomauro, D., Erskine, H., Mantilla-Herrara, A., Whiteford, H., Leung, J., Naghavi, M., & Griswold, M. (2018). The global burden of disease attributable to alcohol and drug use in 195 countries and territories, 1990–2016: a systematic analysis for the Global Burden of Disease Study 2016. *The Lancet Psychiatry, 5*(12), 987-1012. https://doi.org/10.1016/S2215-0366(18)30337-7

DePoy, L., Daut, R., Brigman, J. L., MacPherson, K., Crowley, N., Gunduz-Cinar, O., Pickens, C. L., Cinar, R., Saksida, L. M., Kunos, G., Lovinger, D. M., Bussey, T. J., Camp, M. C., & Holmes, A. (2013). Chronic alcohol produces neuroadaptations to prime dorsal striatal learning. *Proceedings of the National Academy of Sciences of the United States of America, 110*(36), 14783-14788. https://doi.org/10.1073/pnas.1308198110

Dickinson, A., & Weiskrantz, L. (1985). Actions and habits: the development of behavioural autonomy. *Philosophical Transactions of the Royal Society of London. B, Biological Sciences, 308*(1135), 67-78. https://doi.org/doi:10.1098/rstb.1985.0010

Donnadieu-Rigole, H., Mura, T., Portales, P., Duroux-Richard, I., Bouthier, M., Eliaou, J. F., Perney, P., & Apparailly, F. (2016). Effects of alcohol withdrawal on monocyte subset defects in chronic alcohol users. *Journal of Leukocyte Biology, 100*(5), 1191-1199. https://doi.org/10.1189/jlb.5A0216-060RR

Donoghue, K., Elzerbi, C., Saunders, R., Whittington, C., Pilling, S., & Drummond, C. (2015). The efficacy of acamprosate and naltrexone in the treatment of alcohol dependence, Europe versus the rest of the world: a meta-analysis. *Addiction, 110*(6), 920-930. https://doi.org/https://doi.org/10.1111/add.12875

Du, P., Zhang, X., Huang, C. C., Jafari, N., Kibbe, W. A., Hou, L., & Lin, S. M. (2010). Comparison of Beta-value and M-value methods for quantifying methylation levels by microarray analysis. *BMC Bioinformatics, 11*, 587. https://doi.org/10.1186/1471-2105-11-587

Dugué, P.-A., Wilson, R., Lehne, B., Jayasekara, H., Wang, X., Jung, C.-H., Joo, J. E., Makalic, E., Schmidt, D. F., Baglietto, L., Severi, G., Gieger, C., Ladwig, K.-H., Peters, A., Kooner, J. S., Southey, M. C., English, D. R., Waldenberger, M., Chambers, J. C., Giles, G. G., & Milne, R. L. (2021). Alcohol consumption is associated with widespread changes in blood DNA methylation: Analysis of cross-sectional and longitudinal data. *Addiction Biology, 26*(1), e12855. https://doi.org/https://doi.org/10.1111/adb.12855

Duncan, L. E., & Keller, M. C. (2011). A Critical Review of the First 10 Years of Candidate Gene-by-Environment Interaction Research in Psychiatry. *American Journal of Psychiatry, 168*(10), 1041-1049. https://doi.org/10.1176/appi.ajp.2011.11020191

Durrenberger, P. F., Fernando, S., Kashefi, S. N., Ferrer, I., Hauw, J.-J., Seilhean, D., Smith, C., Walker, R., Al-Sarraj, S., Troakes, C., Palkovits, M., Kasztner, M., Huitinga, I., Arzberger, T., Dexter, D. T., Kretzschmar, H., & Reynolds, R. (2010). Effects of Antemortem and Postmortem Variables on Human Brain mRNA Quality: A BrainNet Europe Study. *Journal of Neuropathology & Experimental Neurology, 69*(1), 70-81. https://doi.org/10.1097/NEN.0b013e3181c7e32f

Edenberg, H. J. (2007). The genetics of alcohol metabolism: role of alcohol dehydrogenase and aldehyde dehydrogenase variants. *Alcohol Research & Health, 30*(1), 5-13.

Edgar, R., Jones, M., Meaney, M., Turecki, G., & Kobor, M. (2017). BECon: A tool for interpreting DNA methylation findings from blood in the context of brain. *Translational Psychiatry, 7*(8), e1187. https://doi.org/10.1038/tp.2017.171

Erickson, E. K., Grantham, E. K., Warden, A. S., & Harris, R. A. (2019). Neuroimmune signaling in alcohol use disorder. *Pharmacology Biochemistry and Behavior, 177*, 34-60. https://doi.org/10.1016/j.pbb.2018.12.007

Everitt, B. J., & Robbins, T. W. (2005). Neural systems of reinforcement for drug addiction: from actions to habits to compulsion. *Nature Neuroscience, 8*(11), 1481-1489. https://doi.org/10.1038/nn1579

Farris, S. P., Arasappan, D., Hunicke-Smith, S., Harris, R. A., & Mayfield, R. D. (2015). Transcriptome organization for chronic alcohol abuse in human brain. *Molecular Psychiatry, 20*(11), 1438-1447. https://doi.org/10.1038/mp.2014.159

Fatemi, M., Pao, M. M., Jeong, S., Gal-Yam, E. N., Egger, G., Weisenberger, D. J., & Jones, P. A. (2005). Footprinting of mammalian promoters: use of a CpG DNA methyltransferase revealing nucleosome positions at a single molecule level. *Nucleic Acids Research, 33*(20), e176. https://doi.org/10.1093/nar/gni180

Ferreira, P. G., Muñoz-Aguirre, M., Reverter, F., Sá Godinho, C. P., Sousa, A., Amadoz, A., Sodaei, R., Hidalgo, M. R., Pervouchine, D., Carbonell-Caballero, J., Nurtdinov, R., Breschi, A., Amador, R., Oliveira, P., Çubuk, C., Curado, J., Aguet, F., Oliveira, C., Dopazo, J., Sammeth, M., Ardlie, K. G., & Guigó, R. (2018). The effects of death and post-mortem cold ischemia on human tissue transcriptomes. *Nature Communications, 9*(1), 490. https://doi.org/10.1038/s41467-017-02772-x

Flanagan, J. M. (2015). Epigenome-wide association studies (EWAS): past, present, and future. *Methods in Molecular Biology, 1238*, 51-63. https://doi.org/10.1007/978-1-4939-1804-1_3

Frank, J., Cichon, S., Treutlein, J., Ridinger, M., Mattheisen, M., Hoffmann, P., Herms, S., Wodarz, N., Soyka, M., Zill, P., Maier, W., Mössner, R., Gaebel, W., Dahmen, N., Scherbaum, N., Schmäl, C., Steffens, M., Lucae, S., Ising, M., Müller-Myhsok, B., Nöthen, M. M., Mann, K., Kiefer, F., & Rietschel, M. (2012). Genome-wide significant association between alcohol dependence and a variant in the ADH gene cluster. *Addiction Biology, 17*(1), 171-180. https://doi.org/10.1111/j.1369-1600.2011.00395.x

Furberg, H., Kim, Y., Dackor, J., Boerwinkle, E., Franceschini, N., Ardissino, D., Bernardinelli, L., Mannucci, P. M., Mauri, F., Merlini, P. A., Absher, D., Assimes, T. L., Fortmann, S. P., Iribarren, C., Knowles, J. W., Quertermous, T., Ferrucci, L., Tanaka, T., Bis, J. C., Furberg, C. D., Haritunians, T., McKnight, B., Psaty, B. M., Taylor, K. D., Thacker, E. L., Almgren, P., Groop, L., Ladenvall, C., Boehnke, M., Jackson, A. U., Mohlke, K. L., Stringham, H. M., Tuomilehto, J., Benjamin, E. J., Hwang, S.-J., Levy, D., Preis, S. R., Vasan, R. S., Duan, J., Gejman, P. V., Levinson, D. F., Sanders, A. R., Shi, J., Lips, E. H., McKay, J. D., Agudo, A., Barzan, L., Bencko, V., Benhamou, S., Castellsagué, X., Canova,

C., Conway, D. I., Fabianova, E., Foretova, L., Janout, V., Healy, C. M., Holcátová, I., Kjaerheim, K., Lagiou, P., Lissowska, J., Lowry, R., Macfarlane, T. V., Mates, D., Richiardi, L., Rudnai, P., Szeszenia-Dabrowska, N., Zaridze, D., Znaor, A., Lathrop, M., Brennan, P., Bandinelli, S., Frayling, T. M., Guralnik, J. M., Milaneschi, Y., Perry, J. R. B., Altshuler, D., Elosua, R., Kathiresan, S., Lucas, G., Melander, O., O'Donnell, C. J., Salomaa, V., Schwartz, S. M., Voight, B. F., Penninx, B. W., Smit, J. H., Vogelzangs, N., Boomsma, D. I., de Geus, E. J. C., Vink, J. M., Willemsen, G., Chanock, S. J., Gu, F., Hankinson, S. E., Hunter, D. J., Hofman, A., Tiemeier, H., Uitterlinden, A. G., van Duijn, C. M., Walter, S., Chasman, D. I., Everett, B. M., Paré, G., Ridker, P. M., Li, M. D., Maes, H. H., Audrain-McGovern, J., Posthuma, D., Thornton, L. M., Lerman, C., Kaprio, J., Rose, J. E., Ioannidis, J. P. A., Kraft, P., Lin, D.-Y., Sullivan, P. F., The, T., & Genetics, C. (2010). Genome-wide meta-analyses identify multiple loci associated with smoking behavior. *Nature Genetics, 42*(5), 441-447. https://doi.org/10.1038/ng.571

Galandra, C., Basso, G., Cappa, S., & Canessa, N. (2018). The alcoholic brain: neural bases of impaired reward-based decision-making in alcohol use disorders. *Neurological Sciences, 39*(3), 423-435. https://doi.org/10.1007/s10072-017-3205-1

Gallego Romero, I., Pai, A. A., Tung, J., & Gilad, Y. (2014). RNA-seq: impact of RNA degradation on transcript quantification. *BMC Biology, 12*(1), 42. https://doi.org/10.1186/1741-7007-12-42

Gatta, E., Grayson, D. R., Auta, J., Saudagar, V., Dong, E., Chen, Y., Krishnan, H. R., Drnevich, J., Pandey, S. C., & Guidotti, A. (2021). Genome-wide methylation in alcohol use disorder subjects: implications for an epigenetic regulation of the cortico-limbic glucocorticoid receptors (NR3C1). *Molecular Psychiatry, 26*(3), 1029-1041. https://doi.org/10.1038/s41380-019-0449-6

Gibney, E. R., & Nolan, C. M. (2010). Epigenetics and gene expression. *Heredity, 105*(1), 4-13. https://doi.org/10.1038/hdy.2010.54

Glausier, J. R., Konanur, A., & Lewis, D. A. (2019). Factors Affecting Ultrastructural Quality in the Prefrontal Cortex of the Postmortem Human Brain. *Journal of Histochemistry & Cytochemistry, 67*(3), 185-202. https://doi.org/10.1369/0022155418819481

Goldman, D., Oroszi, G., & Ducci, F. (2005). The genetics of addictions: uncovering the genes. *Nature Reviews Genetics, 6*(7), 521-532. https://doi.org/10.1038/nrg1635

Goldstein, R. Z., & Volkow, N. D. (2011). Dysfunction of the prefrontal cortex in addiction: neuroimaging findings and clinical implications. *Nature Reviews Neuroscience, 12*(11), 652-669. https://doi.org/10.1038/nrn3119

Grant, B. F., Chou, S. P., Saha, T. D., Pickering, R. P., Kerridge, B. T., Ruan, W. J., Huang, B., Jung, J., Zhang, H., Fan, A., & Hasin, D. S. (2017). Prevalence of 12-Month Alcohol Use, High-Risk Drinking, and DSM-IV Alcohol Use Disorder in the United States, 2001-2002 to 2012-2013: Results From the National

Epidemiologic Survey on Alcohol and Related Conditions. *JAMA Psychiatry, 74*(9), 911-923. https://doi.org/10.1001/jamapsychiatry.2017.2161

Grodin, E. N., Bujarski, S., Towns, B., Burnette, E., Nieto, S., Lim, A., Lin, J., Miotto, K., Gillis, A., Irwin, M. R., Evans, C., & Ray, L. A. (2021). Ibudilast, a neuroimmune modulator, reduces heavy drinking and alcohol cue-elicited neural activation: a randomized trial. *Translational Psychiatry, 11*(1), 355. https://doi.org/10.1038/s41398-021-01478-5

Gu, H. F. (2017). Genetic, Epigenetic and Biological Effects of Zinc Transporter (SLC30A8) in Type 1 and Type 2 Diabetes. *Current diabetes reviews, 13*(2), 132-140. https://doi.org/10.2174/1573399812666151123104540

Hagens, G. v., Whalley, A., Maschke, R., & Kriz, W. (1990). Längs-und Querschnitte durch den Hirnstamm. In *Schnittanatomie des menschlichen Gehirns* (pp. 65-76). Springer.

Hagerty, S. L., Bidwell, L. C., Harlaar, N., & Hutchison, K. E. (2016). An Exploratory Association Study of Alcohol Use Disorder and DNA Methylation. *Alcoholism: Clinical and Experimental Research, 40*(8), 1633-1640. https://doi.org/10.1111/acer.13138

Heinz, A., Kiefer, F., Smolka, M. N., Endrass, T., Beste, C., Beck, A., Liu, S., Genauck, A., Romund, L., Banaschewski, T., Bermpohl, F., Deserno, L., Dolan, R. J., Durstewitz, D., Ebner-Priemer, U., Flor, H., Hansson, A. C., Heim, C., Hermann, D., Kiebel, S., Kirsch, P., Kirschbaum, C., Koppe, G., Marxen, M., Meyer-Lindenberg, A., Nagel, W. E., Noori, H. R., Pilhatsch, M., Priller, J., Rietschel, M., Romanczuk-Seiferth, N., Schlagenhauf, F., Sommer, W. H., Stallkamp, J., Ströhle, A., Stock, A. K., Winterer, G., Winter, C., Walter, H., Witt, S., Vollstädt-Klein, S., Rapp, M. A., Tost, H., & Spanagel, R. (2020). Addiction Research Consortium: Losing and regaining control over drug intake (ReCoDe)-From trajectories to mechanisms and interventions. *Addict Biol, 25*(2), e12866. https://doi.org/10.1111/adb.12866

Hoffman, G. E., & Schadt, E. E. (2016). variancePartition: interpreting drivers of variation in complex gene expression studies. *BMC Bioinformatics, 17*(1), 483. https://doi.org/10.1186/s12859-016-1323-z

Hormozdiari, F., Gazal, S., van de Geijn, B., Finucane, H. K., Ju, C. J. T., Loh, P.-R., Schoech, A., Reshef, Y., Liu, X., O'Connor, L., Gusev, A., Eskin, E., & Price, A. L. (2018). Leveraging molecular quantitative trait loci to understand the genetic architecture of diseases and complex traits. *Nature Genetics, 50*(7), 1041-1047. https://doi.org/10.1038/s41588-018-0148-2

Horvath, S. (2013). DNA methylation age of human tissues and cell types. *Genome biology, 14*(10), 3156. https://doi.org/10.1186/gb-2013-14-10-r115

Houseman, E. A., Accomando, W. P., Koestler, D. C., Christensen, B. C., Marsit, C. J., Nelson, H. H., Wiencke, J. K., & Kelsey, K. T. (2012). DNA methylation arrays as surrogate measures of cell mixture distribution. *BMC Bioinformatics, 13*, 86. https://doi.org/10.1186/1471-2105-13-86

Houseman, E. A., Molitor, J., & Marsit, C. J. (2014). Reference-free cell mixture adjustments in analysis of DNA methylation data. *Bioinformatics, 30*(10), 1431-1439. https://doi.org/10.1093/bioinformatics/btu029

Howell, W. M., Carter, V., & Clark, B. (2010). The HLA system: immunobiology, HLA typing, antibody screening and crossmatching techniques. *Journal of Clinical Pathology, 63*(5), 387-390. https://doi.org/10.1136/jcp.2009.072371

Ikeda, M., Takahashi, A., Kamatani, Y., Okahisa, Y., Kunugi, H., Mori, N., Sasaki, T., Ohmori, T., Okamoto, Y., Kawasaki, H., Shimodera, S., Kato, T., Yoneda, H., Yoshimura, R., Iyo, M., Matsuda, K., Akiyama, M., Ashikawa, K., Kashiwase, K., Tokunaga, K., Kondo, K., Saito, T., Shimasaki, A., Kawase, K., Kitajima, T., Matsuo, K., Itokawa, M., Someya, T., Inada, T., Hashimoto, R., Inoue, T., Akiyama, K., Tanii, H., Arai, H., Kanba, S., Ozaki, N., Kusumi, I., Yoshikawa, T., Kubo, M., & Iwata, N. (2018). A genome-wide association study identifies two novel susceptibility loci and trans population polygenicity associated with bipolar disorder. *Molecular Psychiatry, 23*(3), 639-647. https://doi.org/10.1038/mp.2016.259

Irizarry, R. A., Ladd-Acosta, C., Wen, B., Wu, Z., Montano, C., Onyango, P., Cui, H., Gabo, K., Rongione, M., & Webster, M. (2009). The human colon cancer methylome shows similar hypo-and hypermethylation at conserved tissue-specific CpG island shores. *Nature Genetics, 41*(2), 178-186. https://doi.org/10.1038/ng.298

Jaffe, A. E., & Kaminsky, Z. A. (2018). *FlowSorted. DLPFC. 450k: Illumina HumanMethylation data on sorted frontal cortex cell populations.* In (Version 1.24.0) R package.

Johnson, E. C., Demontis, D., Thorgeirsson, T. E., Walters, R. K., Polimanti, R., Hatoum, A. S., Sanchez-Roige, S., Paul, S. E., Wendt, F. R., Clarke, T.-K., Lai, D., Reginsson, G. W., Zhou, H., He, J., Baranger, D. A. A., Gudbjartsson, D. F., Wedow, R., Adkins, D. E., Adkins, A. E., Alexander, J., Bacanu, S.-A., Bigdeli, T. B., Boden, J., Brown, S. A., Bucholz, K. K., Bybjerg-Grauholm, J., Corley, R. P., Degenhardt, L., Dick, D. M., Domingue, B. W., Fox, L., Goate, A. M., Gordon, S. D., Hack, L. M., Hancock, D. B., Hartz, S. M., Hickie, I. B., Hougaard, D. M., Krauter, K., Lind, P. A., McClintick, J. N., McQueen, M. B., Meyers, J. L., Montgomery, G. W., Mors, O., Mortensen, P. B., Nordentoft, M., Pearson, J. F., Peterson, R. E., Reynolds, M. D., Rice, J. P., Runarsdottir, V., Saccone, N. L., Sherva, R., Silberg, J. L., Tarter, R. E., Tyrfingsson, T., Wall, T. L., Webb, B. T., Werge, T., Wetherill, L., Wright, M. J., Zellers, S., Adams, M. J., Bierut, L. J., Boardman, J. D., Copeland, W. E., Farrer, L. A., Foroud, T. M., Gillespie, N. A., Grucza, R. A., Harris, K. M., Heath, A. C., Hesselbrock, V., Hewitt, J. K., Hopfer, C. J., Horwood, J., Iacono, W. G., Johnson, E. O., Kendler, K. S., Kennedy, M. A., Kranzler, H. R., Madden, P. A. F., Maes, H. H., Maher, B. S., Martin, N. G., McGue, M., McIntosh, A. M., Medland, S. E., Nelson, E. C., Porjesz, B., Riley, B. P., Stallings, M. C., Vanyukov, M. M., Vrieze, S., Walters, R., Polimanti, R., Johnson, E., McClintick, J., Hatoum, A., He, J., Wendt, F., Zhou, H., Adams, M., Adkins, A., Aliev, F., Bacanu, S.-A., Batzler, A., Bertelsen, S., Biernacka, J., Bigdeli, T., Chen, L.-S., Clarke, T.-K., Chou, Y.-L., Degenhardt, F., Docherty,

A., Edwards, A., Fontanillas, P., Foo, J., Fox, L., Frank, J., Giegling, I., Gordon, S., Hack, L., Hartmann, A., Hartz, S., Heilmann-Heimbach, S., Herms, S., Hodgkinson, C., Hoffman, P., Hottenga, J., Kennedy, M., Alanne-Kinnunen, M., Konte, B., Lahti, J., Lahti-Pulkkinen, M., Lai, D., Ligthart, L., Loukola, A., Maher, B., Mbarek, H., McIntosh, A., McQueen, M., Meyers, J., Milaneschi, Y., Palviainen, T., Pearson, J., Peterson, R., Ripatti, S., Ryu, E., Saccone, N., Salvatore, J., Sanchez-Roige, S., Schwandt, M., Sherva, R., Streit, F., Strohmaier, J., Thomas, N., Wang, J.-C., Webb, B., Wedow, R., Wetherill, L., Wills, A., Boardman, J., Chen, D., Choi, D.-S., Copeland, W., Culverhouse, R., Dahmen, N., Degenhardt, L., Domingue, B., Elson, S., Frye, M., Gäbel, W., Hayward, C., Ising, M., Keyes, M., Kiefer, F., Kramer, J., Kuperman, S., Lucae, S., Lynskey, M., Maier, W., Mann, K., Männistö, S., Müller-Myhsok, B., Murray, A., Nurnberger, J., Palotie, A., Preuss, U., Räikkönen, K., Reynolds, M., Ridinger, M., Scherbaum, N., Schuckit, M., Soyka, M., Treutlein, J., Witt, S., Wodarz, N., Zill, P., Adkins, D., Boden, J., Boomsma, D., Bierut, L., Brown, S., Bucholz, K., Cichon, S., Costello, E. J., de Wit, H., Diazgranados, N., Dick, D., Eriksson, J., Farrer, L., Foroud, T., Gillespie, N., Goate, A., Goldman, D., Grucza, R., Hancock, D., Harris, K. M., Heath, A., Hesselbrock, V., Hewitt, J., Hopfer, C., Horwood, J., Iacono, W., Johnson, E., Kaprio, J., Karpyak, V., Kendler, K., Kranzler, H., Krauter, K., Lichtenstein, P., Lind, P., McGue, M., MacKillop, J., Madden, P., Maes, H., Magnusson, P., Martin, N., Medland, S., Montgomery, G., Nelson, E., Nöthen, M., Palmer, A., Pederson, N., Penninx, B., Porjesz, B., Rice, J., Rietschel, M., Riley, B., Rose, R., Rujescu, D., Shen, P.-H., Silberg, J., Stallings, M., Tarter, R., Vanyukov, M., Vrieze, S., Wall, T., Whitfield, J., Zhao, H., Neale, B., Gelernter, J., Edenberg, H., Agrawal, A., Davis, L. K., Bogdan, R., Gelernter, J., Edenberg, H. J., Stefansson, K., Børglum, A. D., & Agrawal, A. (2020). A large-scale genome-wide association study meta-analysis of cannabis use disorder. *The Lancet Psychiatry, 7*(12), 1032-1045. https://doi.org/10.1016/S2215-0366(20)30339-4

Kanai, M., Akiyama, M., Takahashi, A., Matoba, N., Momozawa, Y., Ikeda, M., Iwata, N., Ikegawa, S., Hirata, M., & Matsuda, K. (2018). Genetic analysis of quantitative traits in the Japanese population links cell types to complex human diseases. *Nature Genetics, 50*(3), 390-400. https://doi.org/10.1038/s41588-018-0047-6

Kanda, N., Seno, H., Konda, Y., Marusawa, H., Kanai, M., Nakajima, T., Kawashima, T., Nanakin, A., Sawabu, T., Uenoyama, Y., Sekikawa, A., Kawada, M., Suzuki, K., Kayahara, T., Fukui, H., Sawada, M., & Chiba, T. (2004). STAT3 is constitutively activated and supports cell survival in association with survivin expression in gastric cancer cells. *Oncogene, 23*(28), 4921-4929. https://doi.org/10.1038/sj.onc.1207606

Kapoor, M., Chao, M. J., Johnson, E. C., Novikova, G., Lai, D., Meyers, J. L., Schulman, J., Nurnberger, J. I., Porjesz, B., Liu, Y., Hesselbrock, V., Kuperman, S., Kramer, J., Kamarajan, C., Pandey, A., Bierut, L., Rice, J. P., Bucholz, K. K., Schuckit, M., Tischfield, J., Brooks, A., Hart, R. P., Almasy, L., Dick, D., Salvatore, J., Slesinger, P., Foroud, T., Edenberg, H. J., Marcora, E., Agrawal, A., Goate, A., & The Collaborative Study on the Genetics of, A. (2021). Multi-omics integration analysis identifies novel genes for alcoholism with potential

overlap with neurodegenerative diseases. *Nature Communications, 12*(1), 5071. https://doi.org/10.1038/s41467-021-25392-y

Kapoor, M., Wang, J. C., Farris, S. P., Liu, Y., McClintick, J., Gupta, I., Meyers, J. L., Bertelsen, S., Chao, M., Nurnberger, J., Tischfield, J., Harari, O., Zeran, L., Hesselbrock, V., Bauer, L., Raj, T., Porjesz, B., Agrawal, A., Foroud, T., Edenberg, H. J., Mayfield, R. D., & Goate, A. (2019). Analysis of whole genome-transcriptomic organization in brain to identify genes associated with alcoholism. *Translational Psychiatry, 9*(1), 89. https://doi.org/10.1038/s41398-019-0384-y

Kim, D., Paggi, J. M., Park, C., Bennett, C., & Salzberg, S. L. (2019). Graph-based genome alignment and genotyping with HISAT2 and HISAT-genotype. *Nature Biotechnology, 37*(8), 907-915. https://doi.org/10.1038/s41587-019-0201-4

Koob, G. F., & Colrain, I. M. (2020). Alcohol use disorder and sleep disturbances: a feed-forward allostatic framework. *Neuropsychopharmacology, 45*(1), 141-165. https://doi.org/10.1038/s41386-019-0446-0

Koob, G. F., & Volkow, N. D. (2010). Neurocircuitry of Addiction. *Neuropsychopharmacology, 35*(1), 217-238. https://doi.org/10.1038/npp.2009.110

Kranzler, H. R., Zhou, H., Kember, R. L., Vickers Smith, R., Justice, A. C., Damrauer, S., Tsao, P. S., Klarin, D., Baras, A., Reid, J., Overton, J., Rader, D. J., Cheng, Z., Tate, J. P., Becker, W. C., Concato, J., Xu, K., Polimanti, R., Zhao, H., & Gelernter, J. (2019, 2019/04/02). Genome-wide association study of alcohol consumption and use disorder in 274,424 individuals from multiple populations. *Nature Communications, 10*(1), 1499. https://doi.org/10.1038/s41467-019-09480-8

Kukurba, K. R., & Montgomery, S. B. (2015). RNA Sequencing and Analysis. *Cold Spring Harbor Protocols, 2015*(11), 951-969. https://doi.org/10.1101/pdb.top084970

Kwon, J. M., & Goate, A. M. (2000). The candidate gene approach. *Alcohol Research & Health, 24*(3), 164-168.

Lai, D., Wetherill, L., Bertelsen, S., Carey, C. E., Kamarajan, C., Kapoor, M., Meyers, J. L., Anokhin, A. P., Bennett, D. A., Bucholz, K. K., Chang, K. K., De Jager, P. L., Dick, D. M., Hesselbrock, V., Kramer, J., Kuperman, S., Nurnberger, J. I., Jr., Raj, T., Schuckit, M., Scott, D. M., Taylor, R. E., Tischfield, J., Hariri, A. R., Edenberg, H. J., Agrawal, A., Bogdan, R., Porjesz, B., Goate, A. M., & Foroud, T. (2019). Genome-wide association studies of alcohol dependence, DSM-IV criterion count and individual criteria. *Genes Brain and Behavior, 18*(6), e12579. https://doi.org/10.1111/gbb.12579

Lake, B. B., Ai, R., Kaeser, G. E., Salathia, N. S., Yung, Y. C., Liu, R., Wildberg, A., Gao, D., Fung, H. L., Chen, S., Vijayaraghavan, R., Wong, J., Chen, A., Sheng, X., Kaper, F., Shen, R., Ronaghi, M., Fan, J. B., Wang, W., Chun, J., & Zhang, K. (2016). Neuronal subtypes and diversity revealed by single-nucleus RNA

sequencing of the human brain. *Science, 352*(6293), 1586-1590. https://doi.org/10.1126/science.aaf1204

Langfelder, P., & Horvath, S. (2008). WGCNA: an R package for weighted correlation network analysis. *BMC bioinformatics, 9*(1), 559. https://doi.org/10.1186/1471-2105-9-559

Lehne, B., Drong, A. W., Loh, M., Zhang, W., Scott, W. R., Tan, S. T., Afzal, U., Scott, J., Jarvelin, M. R., Elliott, P., McCarthy, M. I., Kooner, J. S., & Chambers, J. C. (2015). A coherent approach for analysis of the Illumina HumanMethylation450 BeadChip improves data quality and performance in epigenome-wide association studies. *Genome Biology, 16*(1), 37. https://doi.org/10.1186/s13059-015-0600-x

Levy, S. E., & Myers, R. M. (2016). Advancements in Next-Generation Sequencing. *Annual Review of Genomics and Human Genetics, 17*(1), 95-115. https://doi.org/10.1146/annurev-genom-083115-022413

Li, G., Liu, Y., Zhang, Y., Kubo, N., Yu, M., Fang, R., Kellis, M., & Ren, B. (2019). Joint profiling of DNA methylation and chromatin architecture in single cells. *Nature Methods, 16*(10), 991-993. https://doi.org/10.1038/s41592-019-0502-z

Liao, Y., Smyth, G. K., & Shi, W. (2019). The R package Rsubread is easier, faster, cheaper and better for alignment and quantification of RNA sequencing reads. *Nucleic Acids Research, 47*(8), e47. https://doi.org/10.1093/nar/gkz114

Liberzon, A., Birger, C., Thorvaldsdóttir, H., Ghandi, M., Mesirov, Jill P., & Tamayo, P. (2015). The Molecular Signatures Database Hallmark Gene Set Collection. *Cell Systems, 1*(6), 417-425. https://doi.org/10.1016/j.cels.2015.12.004

Lim, Y., Beane-Ebel, J. E., Tanaka, Y., Ning, B., Husted, C. R., Henderson, D. C., Xiang, Y., Park, I.-H., Farrer, L. A., & Zhang, H. (2021). Exploration of alcohol use disorder-associated brain miRNA–mRNA regulatory networks. *Translational Psychiatry, 11*(1), 504. https://doi.org/10.1038/s41398-021-01635-w

Lin, H., Wang, F., Rosato, A. J., Farrer, L. A., Henderson, D. C., & Zhang, H. (2020). Prefrontal cortex eQTLs/mQTLs enriched in genetic variants associated with alcohol use disorder and other diseases. *Epigenomics, 12*(9), 789-800. https://doi.org/10.2217/epi-2019-0270

Listabarth, S., König, D., Vyssoki, B., & Hametner, S. (2020). Does thiamine protect the brain from iron overload and alcohol-related dementia? *Alzheimer's & Dementia, 16*(11), 1591-1595. https://doi.org/10.1002/alz.12146

Litten, R. Z., Falk, D. E., Ryan, M. L., & Fertig, J. B. (2016). Discovery, Development, and Adoption of Medications to Treat Alcohol Use Disorder: Goals for the Phases of Medications Development. *Alcoholism: Clinical and Experimental Research, 40*(7), 1368-1379. https://doi.org/10.1111/acer.13093

Liu, A., Dai, Y., Mendez, E. F., Hu, R., Fries, G. R., Najera, K. E., Jiang, S., Meyer, T. D., Stertz, L., Jia, P., Walss-Bass, C., & Zhao, Z. (2021). Genome-Wide Correlation of DNA Methylation and Gene Expression in Postmortem Brain Tissues of Opioid Use Disorder Patients. *International Journal of Neuropsychopharmacology, 24*(11), 879–891. https://doi.org/10.1093/ijnp/pyab043

Liu, J., Lewohl, J. M., Dodd, P. R., Randall, P. K., Harris, R. A., & Mayfield, R. D. (2004). Gene expression profiling of individual cases reveals consistent transcriptional changes in alcoholic human brain. *Journal of Neurochemistry, 90*(5), 1050-1058. https://doi.org/10.1111/j.1471-4159.2004.02570.x

Liu, J., Lewohl, J. M., Harris, R. A., Iyer, V. R., Dodd, P. R., Randall, P. K., & Mayfield, R. D. (2006). Patterns of gene expression in the frontal cortex discriminate alcoholic from nonalcoholic individuals. *Neuropsychopharmacology, 31*(7), 1574-1582. https://doi.org/10.1038/sj.npp.1300947

Lohoff, F. W., Clarke, T.-K., Kaminsky, Z. A., Walker, R. M., Bermingham, M. L., Jung, J., Morris, S. W., Rosoff, D., Campbell, A., Barbu, M., Charlet, K., Adams, M., Lee, J., Howard, D. M., O'Connell, E. M., Whalley, H., Porteous, D. J., McIntosh, A. M., & Evans, K. L. (2022). Epigenome-wide association study of alcohol consumption in N = 8161 individuals and relevance to alcohol use disorder pathophysiology: identification of the cystine/glutamate transporter SLC7A11 as a top target. *Molecular Psychiatry, 27*(3), 1754-1764. https://doi.org/10.1038/s41380-021-01378-6

Lohoff, F. W., Roy, A., Jung, J., Longley, M., Rosoff, D. B., Luo, A., O'Connell, E., Sorcher, J. L., Sun, H., & Schwandt, M. (2020). Epigenome-wide association study and multi-tissue replication of individuals with alcohol use disorder: evidence for abnormal glucocorticoid signaling pathway gene regulation. *Molecular Psychiatry, 26*(6), 2224-2237. https://doi.org/10.1038/s41380-020-0734-4

Lohoff, F. W., Sorcher, J. L., Rosen, A. D., Mauro, K. L., Fanelli, R. R., Momenan, R., Hodgkinson, C. A., Vendruscolo, L. F., Koob, G. F., & Schwandt, M. (2018). Methylomic profiling and replication implicates deregulation of PCSK9 in alcohol use disorder. *Molecular psychiatry, 23*(9), 1900-1910. https://doi.org/10.1038/mp.2017.168

Lokk, K., Modhukur, V., Rajashekar, B., Märtens, K., Mägi, R., Kolde, R., Koltšina, M., Nilsson, T. K., Vilo, J., Salumets, A., & Tõnisson, N. (2014). DNA methylome profiling of human tissues identifies global and tissue-specific methylation patterns. *Genome Biology, 15*(4), r54. https://doi.org/10.1186/gb-2014-15-4-r54

Longley, M. J., Lee, J., Jung, J., & Lohoff, F. W. (2021). Epigenetics of alcohol use disorder—A review of recent advances in DNA methylation profiling. *Addiction biology, 26*(6), e13006. https://doi.org/10.1111/adb.13006

Love, M. I., Huber, W., & Anders, S. (2014). Moderated estimation of fold change and dispersion for RNA-seq data with DESeq2. *Genome Biology, 15*(12), 550. https://doi.org/10.1186/s13059-014-0550-8

Lövkvist, C., Dodd, I. B., Sneppen, K., & Haerter, J. O. (2016). DNA methylation in human epigenomes depends on local topology of CpG sites. *Nucleic Acids Research, 44*(11), 5123-5132. https://doi.org/10.1093/nar/gkw124

Maas, S. C. E., Vidaki, A., Wilson, R., Teumer, A., Liu, F., van Meurs, J. B. J., Uitterlinden, A. G., Boomsma, D. I., de Geus, E. J. C., Willemsen, G., van Dongen, J., van der Kallen, C. J. H., Slagboom, P. E., Beekman, M., van Heemst, D., van den Berg, L. H., Duijts, L., Jaddoe, V. W. V., Ladwig, K. H., Kunze, S., Peters, A., Ikram, M. A., Grabe, H. J., Felix, J. F., Waldenberger, M., Franco, O. H., Ghanbari, M., & Kayser, M. (2019). Validated inference of smoking habits from blood with a finite DNA methylation marker set. *European Journal of Epidemiology, 34*(11), 1055-1074. https://doi.org/10.1007/s10654-019-00555-w

Margolis, S. S., Salogiannis, J., Lipton, D. M., Mandel-Brehm, C., Wills, Z. P., Mardinly, A. R., Hu, L., Greer, P. L., Bikoff, J. B., Ho, H.-Y. H., Soskis, M. J., Sahin, M., & Greenberg, M. E. (2010). EphB-Mediated Degradation of the RhoA GEF Ephexin5 Relieves a Developmental Brake on Excitatory Synapse Formation. *Cell, 143*(3), 442-455. https://doi.org/10.1016/j.cell.2010.09.038

Martino, D., & Saffery, R. (2015). Characteristics of DNA methylation and gene expression in regulatory features on the Infinium 450k Beadchip. *bioRxiv*. https://doi.org/10.1101/032862

Maze, I., & Nestler, E. J. (2011). The epigenetic landscape of addiction. *Annals of the New York Academy of Sciences, 1216*, 99-113. https://doi.org/10.1111/j.1749-6632.2010.05893.x

McClintick, J. N., Tischfield, J. A., Deng, L., Kapoor, M., Xuei, X., & Edenberg, H. J. (2019). Ethanol activates immune response in lymphoblastoid cells. *Alcohol, 79*, 81-91. https://doi.org/10.1016/j.alcohol.2019.01.001

McKenzie, A. T., Wang, M., Hauberg, M. E., Fullard, J. F., Kozlenkov, A., Keenan, A., Hurd, Y. L., Dracheva, S., Casaccia, P., Roussos, P., & Zhang, B. (2018). Brain Cell Type Specific Gene Expression and Co-expression Network Architectures. *Scientific Reports, 8*(1), 8868. https://doi.org/10.1038/s41598-018-27293-5

Meng, W., Sjöholm, L. K., Kononenko, O., Tay, N., Zhang, D., Sarkisyan, D., Geske, J. R., Qiu, W., Watanabe, H., & Almamoun, R. (2021). Genotype-dependent epigenetic regulation of DLGAP2 in alcohol use and dependence. *Molecular Psychiatry, 26*(8), 4367-4382. https://doi.org/10.1038/s41380-019-0588-9

Michels, K. B., & Binder, A. M. (2018). Considerations for Design and Analysis of DNA Methylation Studies. In J. Tost (Ed.), *DNA Methylation Protocols* (pp. 31-46). Springer New York. https://doi.org/10.1007/978-1-4939-7481-8_2

Miller, A. M., Wang, H., Park, O., Horiguchi, N., Lafdil, F., Mukhopadhyay, P., Moh, A., Fu, X. Y., Kunos, G., Pacher, P., & Gao, B. (2010). Anti-Inflammatory and Anti-Apoptotic Roles of Endothelial Cell STAT3 in Alcoholic Liver Injury. *Alcoholism:*

Clinical and Experimental Research, 34(4), 719-725. https://doi.org/10.1111/j.1530-0277.2009.01141.x

Moore, L. D., Le, T., & Fan, G. (2013). DNA Methylation and Its Basic Function. *Neuropsychopharmacology, 38*(1), 23-38. https://doi.org/10.1038/npp.2012.112

Mora, L. B., Buettner, R., Seigne, J., Diaz, J., Ahmad, N., Garcia, R., Bowman, T., Falcone, R., Fairclough, R., Cantor, A., Muro-Cacho, C., Livingston, S., Karras, J., Pow-Sang, J., & Jove, R. (2002). Constitutive activation of Stat3 in human prostate tumors and cell lines: direct inhibition of Stat3 signaling induces apoptosis of prostate cancer cells. *Cancer Research, 62*(22), 6659-6666.

Moran, S., Arribas, C., & Esteller, M. (2016). Validation of a DNA methylation microarray for 850,000 CpG sites of the human genome enriched in enhancer sequences. *Epigenomics, 8*(3), 389-399. https://doi.org/10.2217/epi.15.114

Nagel, M., Jansen, P. R., Stringer, S., Watanabe, K., de Leeuw, C. A., Bryois, J., Savage, J. E., Hammerschlag, A. R., Skene, N. G., Muñoz-Manchado, A. B., Agee, M., Alipanahi, B., Auton, A., Bell, R. K., Bryc, K., Elson, S. L., Fontanillas, P., Furlotte, N. A., Hinds, D. A., Hromatka, B. S., Huber, K. E., Kleinman, A., Litterman, N. K., McIntyre, M. H., Mountain, J. L., Noblin, E. S., Northover, C. A. M., Pitts, S. J., Sathirapongsasuti, J. F., Sazonova, O. V., Shelton, J. F., Shringarpure, S., Tian, C., Tung, J. Y., Vacic, V., Wilson, C. H., White, T., Tiemeier, H., Linnarsson, S., Hjerling-Leffler, J., Polderman, T. J. C., Sullivan, P. F., van der Sluis, S., Posthuma, D., & andMe Research, T. (2018). Meta-analysis of genome-wide association studies for neuroticism in 449,484 individuals identifies novel genetic loci and pathways. *Nature Genetics, 50*(7), 920-927. https://doi.org/10.1038/s41588-018-0151-7

Nicolas, C. S., Amici, M., Bortolotto, Z. A., Doherty, A., Csaba, Z., Fafouri, A., Dournaud, P., Gressens, P., Collingridge, G. L., & Peineau, S. (2013). The role of JAK-STAT signaling within the CNS. *JAK-STAT, 2*(1), e22925-e22925. https://doi.org/10.4161/jkst.22925

Noori, H. R., Spanagel, R., & Hansson, A. C. (2012). Neurocircuitry for modeling drug effects. *Addiction Biology, 17*(5), 827-864. https://doi.org/10.1111/j.1369-1600.2012.00485.x

O'Tousa, D., & Grahame, N. (2014). Habit formation: implications for alcoholism research. *Alcohol, 48*(4), 327-335. https://doi.org/10.1016/j.alcohol.2014.02.004

Pardiñas, A. F., Holmans, P., Pocklington, A. J., Escott-Price, V., Ripke, S., Carrera, N., Legge, S. E., Bishop, S., Cameron, D., & Hamshere, M. L. (2018). Common schizophrenia alleles are enriched in mutation-intolerant genes and in regions under strong background selection. *Nature Genetics, 50*(3), 381-389. https://doi.org/10.1038/s41588-018-0059-2

Park, S. Q., Kahnt, T., Beck, A., Cohen, M. X., Dolan, R. J., Wrase, J., & Heinz, A. (2010). Prefrontal cortex fails to learn from reward prediction errors in alcohol

dependence. *The Journal of Neuroscience, 30*(22), 7749-7753. https://doi.org/10.1523/JNEUROSCI.5587-09.2010

Pasala, S., Barr, T., & Messaoudi, I. (2015). Impact of alcohol abuse on the adaptive immune system. *Alcohol research: current reviews, 37*(2), 185.

Pedersen, B. S., Schwartz, D. A., Yang, I. V., & Kechris, K. J. (2012). Comb-p: software for combining, analyzing, grouping and correcting spatially correlated P-values. *Bioinformatics, 28*(22), 2986-2988. https://doi.org/10.1093/bioinformatics/bts545

Pedranzini, L., Leitch, A., & Bromberg, J. (2004). Stat3 is required for the development of skin cancer. *The Journal of Clinical Investigation, 114*(5), 619-622. https://doi.org/10.1172/jci22800

Petrakis, I. L., Ralevski, E., Gueorguieva, R., Sloan, M. E., Devine, L., Yoon, G., Arias, A. J., & Sofuoglu, M. (2019). Targeting neuroinflammation with minocycline in heavy drinkers. *Psychopharmacology, 236*(10), 3013-3021. https://doi.org/10.1007/s00213-019-05205-3

Phipson, B., Maksimovic, J., & Oshlack, A. (2016). missMethyl: an R package for analyzing data from Illumina's HumanMethylation450 platform. *Bioinformatics, 32*(2), 286-288. https://doi.org/10.1093/bioinformatics/btv560

Polimanti, R., Walters, R. K., Johnson, E. C., McClintick, J. N., Adkins, A. E., Adkins, D. E., Bacanu, S. A., Bierut, L. J., Bigdeli, T. B., Brown, S., Bucholz, K. K., Copeland, W. E., Costello, E. J., Degenhardt, L., Farrer, L. A., Foroud, T. M., Fox, L., Goate, A. M., Grucza, R., Hack, L. M., Hancock, D. B., Hartz, S. M., Heath, A. C., Hewitt, J. K., Hopfer, C. J., Johnson, E. O., Kendler, K. S., Kranzler, H. R., Krauter, K., Lai, D., Madden, P. A. F., Martin, N. G., Maes, H. H., Nelson, E. C., Peterson, R. E., Porjesz, B., Riley, B. P., Saccone, N., Stallings, M., Wall, T. L., Webb, B. T., Wetherill, L., Edenberg, H. J., Agrawal, A., & Gelernter, J. (2020). Leveraging genome-wide data to investigate differences between opioid use vs. opioid dependence in 41,176 individuals from the Psychiatric Genomics Consortium. *Molecular Psychiatry, 25*(8), 1673-1687. https://doi.org/10.1038/s41380-020-0677-9

Ponomarev, I., Wang, S., Zhang, L., Harris, R. A., & Mayfield, R. D. (2012). Gene coexpression networks in human brain identify epigenetic modifications in alcohol dependence. *The Journal of Neuroscience, 32*(5), 1884-1897. https://doi.org/10.1523/jneurosci.3136-11.2012

Rakyan, V. K., Down, T. A., Balding, D. J., & Beck, S. (2011). Epigenome-wide association studies for common human diseases. *Nature Reviews Genetics, 12*(8), 529-541. https://doi.org/https://doi.org/10.1038/nrg3000

Ramasamy, A., Curjuric, I., Coin, L. J., Kumar, A., McArdle, W. L., Imboden, M., Leynaert, B., Kogevinas, M., Schmid-Grendelmeier, P., Pekkanen, J., Wjst, M., Bircher, A. J., Sovio, U., Rochat, T., Hartikainen, A.-L., Balding, D. J., Jarvelin, M.-R., Probst-Hensch, N., Strachan, D. P., & Jarvis, D. L. (2011). A genome-wide meta-analysis of genetic variants associated with allergic rhinitis and grass

sensitization and their interaction with birth order. *Journal of Allergy and Clinical Immunology, 128*(5), 996-1005. https://doi.org/10.1016/j.jaci.2011.08.030

Robertson, N. J., Chai, J.-G., Millrain, M., Scott, D., Hashim, F., Manktelow, E., Lemonnier, F., Simpson, E., & Dyson, J. (2007). Natural regulation of immunity to minor histocompatibility antigens. *The Journal of Immunology, 178*(6), 3558-3565. https://doi.org/10.4049/jimmunol.178.6.3558

Robison, A. J., & Nestler, E. J. (2011). Transcriptional and epigenetic mechanisms of addiction. *Nature Reviews Neuroscience, 12*(11), 623-637. https://doi.org/10.1038/nrn3111

Ruderfer, D. M., Ripke, S., McQuillin, A., Boocock, J., Stahl, E. A., Pavlides, J. M. W., Mullins, N., Charney, A. W., Ori, A. P., & Loohuis, L. M. O. (2018). Genomic dissection of bipolar disorder and schizophrenia, including 28 subphenotypes. *Cell, 173*(7), 1705-1715. e1716. https://doi.org/10.1016/j.cell.2018.05.046

Sanchez-Roige, S., Palmer, A. A., Fontanillas, P., Elson, S. L., Adams, M. J., Howard, D. M., Edenberg, H. J., Davies, G., Crist, R. C., Deary, I. J., McIntosh, A. M., & Clarke, T.-K. (2018). Genome-Wide Association Study Meta-Analysis of the Alcohol Use Disorders Identification Test (AUDIT) in Two Population-Based Cohorts. *American Journal of Psychiatry, 176*(2), 107-118. https://doi.org/10.1176/appi.ajp.2018.18040369

Saunders, C., Smith, L., Wibrand, F., Ravn, K., Bross, P., Thiffault, I., Christensen, M., Atherton, A., Farrow, E., Miller, N., Kingsmore, Stephen F., & Ostergaard, E. (2015). CLPB Variants Associated with Autosomal-Recessive Mitochondrial Disorder with Cataract, Neutropenia, Epilepsy, and Methylglutaconic Aciduria. *The American Journal of Human Genetics, 96*(2), 258-265. https://doi.org/10.1016/j.ajhg.2014.12.020

Schultz, W. (2007). Multiple dopamine functions at different time courses. *Annual Review of Neuroscience, 30*, 259-288. https://doi.org/10.1146/annurev.neuro.28.061604.135722

Sergushichev, A. A. (2016). An algorithm for fast preranked gene set enrichment analysis using cumulative statistic calculation. *bioRxiv*. https://doi.org/10.1101/060012

Shabalin, A. A., Aberg, K. A., & van den Oord, E. J. (2015). Candidate gene methylation studies are at high risk of erroneous conclusions. *Epigenomics, 7*(1), 13-15. https://doi.org/10.2217/epi.14.70

Shen, L. (2021). *GeneOverlap: Test and visualize gene overlaps.* In R package version 1.28.0.

Shigeta, Y., Ishii, H., Takagi, S., Yoshitake, Y., Hirano, T., Takata, H., Kohno, H., & Tsuchiya, M. (1980). HLA antigens as immunogenetic markers of alcoholism and alcoholic liver disease. *Pharmacology Biochemistry and Behavior, 13 Suppl 1*, 89-94. https://doi.org/10.1016/s0091-3057(80)80014-1

Sjoerds, Z., van den Brink, W., Beekman, A. T., Penninx, B. W., & Veltman, D. J. (2014). Cue reactivity is associated with duration and severity of alcohol dependence: an FMRI study. *PLoS One, 9*(1), e84560. https://doi.org/10.1371/journal.pone.0084560

Sladek, R., Rocheleau, G., Rung, J., Dina, C., Shen, L., Serre, D., Boutin, P., Vincent, D., Belisle, A., Hadjadj, S., Balkau, B., Heude, B., Charpentier, G., Hudson, T. J., Montpetit, A., Pshezhetsky, A. V., Prentki, M., Posner, B. I., Balding, D. J., Meyre, D., Polychronakos, C., & Froguel, P. (2007). A genome-wide association study identifies novel risk loci for type 2 diabetes. *Nature, 445*(7130), 881-885. https://doi.org/10.1038/nature05616

Spanagel, R., Siegmund, S. V., Cowen, M. S., Schroff, K. C., Schumann, G., Fiserová, M., Sillaber, I., Wellek, S., Singer, M., & Putzke, J. (2002). The Neuronal Nitric Oxide Synthase Gene Is Critically Involved in Neurobehavioral Effects of Alcohol. *The Journal of Neuroscience, 22*, 8676 - 8683. https://doi.org/10.1523/JNEUROSCI.22-19-08676.2002

Sproston, N. R., & Ashworth, J. J. (2018, 2018-April-13). Role of C-Reactive Protein at Sites of Inflammation and Infection [Review]. *Frontiers in Immunology, 9*, 754. https://doi.org/10.3389/fimmu.2018.00754

Sugden, K., Hannon, E. J., Arseneault, L., Belsky, D. W., Broadbent, J. M., Corcoran, D. L., Hancox, R. J., Houts, R., Moffitt, T. E., Poulton, R., Prinz, J. A., Thomson, W. M., Williams, B. S., Wong, C. C. Y., Mill, J., & Caspi, A. (2019). Establishing a generalized polyepigenetic biomarker for tobacco smoking. *Translational Psychiatry, 9*(1), 92. https://doi.org/10.1038/s41398-019-0430-9

Szabo, G., & Saha, B. (2015). Alcohol's Effect on Host Defense. *Alcohol research: current reviews, 37*(2), 159-170.

Szklarczyk, D., Gable, A. L., Nastou, K. C., Lyon, D., Kirsch, R., Pyysalo, S., Doncheva, N. T., Legeay, M., Fang, T., Bork, P., Jensen, L. J., & von Mering, C. (2021). The STRING database in 2021: customizable protein–protein networks, and functional characterization of user-uploaded gene/measurement sets. *Nucleic Acids Research, 49*(D1), D605-D612. https://doi.org/10.1093/nar/gkaa1074

Taber, K. H., Black, D. N., Porrino, L. J., & Hurley, R. A. (2012). Neuroanatomy of dopamine: reward and addiction. *The Journal of Neuropsychiatry and Clinical Neurosciences, 24*(1), 1-4. https://doi.org/10.1176/appi.neuropsych.24.1.1

Tang, Y.-Y., Posner, M. I., Rothbart, M. K., & Volkow, N. D. (2015). Circuitry of self-control and its role in reducing addiction. *Trends in Cognitive Sciences, 19*(8), 439-444. https://doi.org/10.1016/j.tics.2015.06.007

Team, R. C. (2013). R: A language and environment for statistical computing.

Thakkar, M. M., Sharma, R., & Sahota, P. (2015). Alcohol disrupts sleep homeostasis. *Alcohol, 49*(4), 299-310. https://doi.org/10.1016/j.alcohol.2014.07.019

Tóth, M. E., Vígh, L., & Sántha, M. (2014). Alcohol stress, membranes, and chaperones. *Cell Stress and Chaperones, 19*(3), 299-309. https://doi.org/10.1007/s12192-013-0472-5

Trabzuni, D., Ryten, M., Walker, R., Smith, C., Imran, S., Ramasamy, A., Weale, M. E., & Hardy, J. (2011). Quality control parameters on a large dataset of regionally dissected human control brains for whole genome expression studies. *Journal of Neurochemistry, 119*(2), 275-282. https://doi.org/10.1111/j.1471-4159.2011.07432.x

Velten, B., Braunger, J. M., Argelaguet, R., Arnol, D., Wirbel, J., Bredikhin, D., Zeller, G., & Stegle, O. (2022). Identifying temporal and spatial patterns of variation from multimodal data using MEFISTO. *Nature Methods, 19*(2), 179-186. https://doi.org/10.1038/s41592-021-01343-9

Verhulst, B., Neale, M. C., & Kendler, K. S. (2015). The heritability of alcohol use disorders: a meta-analysis of twin and adoption studies. *Psychological Medicine, 45*(5), 1061-1072. https://doi.org/10.1017/S0033291714002165

Vetreno, R. P., Qin, L., Coleman Jr, L. G., & Crews, F. T. (2021). Increased Toll-like Receptor-MyD88-NFκB-Proinflammatory neuroimmune signaling in the orbitofrontal cortex of human alcohol use disorder. *Alcoholism: Clinical and Experimental Research, 45*(9), 1747-1761. https://doi.org/10.1111/acer.14669

Volkow, N. D., Koob, G. F., & McLellan, A. T. (2016). Neurobiologic Advances from the Brain Disease Model of Addiction. *New England Journal of Medicine, 374*(4), 363-371. https://doi.org/10.1056/NEJMra1511480

Volkow, N. D., & Morales, M. (2015). The Brain on Drugs: From Reward to Addiction. *Cell, 162*(4), 712-725. https://doi.org/10.1016/j.cell.2015.07.046

Vollstädt-Klein, S., Wichert, S., Rabinstein, J., Bühler, M., Klein, O., Ende, G., Hermann, D., & Mann, K. (2010). Initial, habitual and compulsive alcohol use is characterized by a shift of cue processing from ventral to dorsal striatum. *Addiction, 105*(10), 1741-1749. https://doi.org/10.1111/j.1360-0443.2010.03022.x

Walters, R. K., Polimanti, R., Johnson, E. C., McClintick, J. N., Adams, M. J., Adkins, A. E., Aliev, F., Bacanu, S.-A., Batzler, A., Bertelsen, S., Biernacka, J. M., Bigdeli, T. B., Chen, L.-S., Clarke, T.-K., Chou, Y.-L., Degenhardt, F., Docherty, A. R., Edwards, A. C., Fontanillas, P., Foo, J. C., Fox, L., Frank, J., Giegling, I., Gordon, S., Hack, L. M., Hartmann, A. M., Hartz, S. M., Heilmann-Heimbach, S., Herms, S., Hodgkinson, C., Hoffmann, P., Jan Hottenga, J., Kennedy, M. A., Alanne-Kinnunen, M., Konte, B., Lahti, J., Lahti-Pulkkinen, M., Lai, D., Ligthart, L., Loukola, A., Maher, B. S., Mbarek, H., McIntosh, A. M., McQueen, M. B., Meyers, J. L., Milaneschi, Y., Palviainen, T., Pearson, J. F., Peterson, R. E., Ripatti, S., Ryu, E., Saccone, N. L., Salvatore, J. E., Sanchez-Roige, S., Schwandt, M., Sherva, R., Streit, F., Strohmaier, J., Thomas, N., Wang, J.-C., Webb, B. T., Wedow, R., Wetherill, L., Wills, A. G., Agee, M., Alipanahi, B., Auton, A., Bell, R. K., Bryc, K., Elson, S. L., Fontanillas, P., Furlotte, N. A., Hinds, D. A., Huber, K. E., Kleinman, A., Litterman, N. K., McCreight, J. C.,

McIntyre, M. H., Mountain, J. L., Noblin, E. S., Northover, C. A. M., Pitts, S. J., Sathirapongsasuti, J. F., Sazonova, O. V., Shelton, J. F., Shringarpure, S., Tian, C., Tung, J. Y., Vacic, V., Wilson, C. H., Boardman, J. D., Chen, D., Choi, D.-S., Copeland, W. E., Culverhouse, R. C., Dahmen, N., Degenhardt, L., Domingue, B. W., Elson, S. L., Frye, M. A., Gäbel, W., Hayward, C., Ising, M., Keyes, M., Kiefer, F., Kramer, J., Kuperman, S., Lucae, S., Lynskey, M. T., Maier, W., Mann, K., Männistö, S., Müller-Myhsok, B., Murray, A. D., Nurnberger, J. I., Palotie, A., Preuss, U., Räikkönen, K., Reynolds, M. D., Ridinger, M., Scherbaum, N., Schuckit, M. A., Soyka, M., Treutlein, J., Witt, S., Wodarz, N., Zill, P., Adkins, D. E., Boden, J. M., Boomsma, D. I., Bierut, L. J., Brown, S. A., Bucholz, K. K., Cichon, S., Costello, E. J., de Wit, H., Diazgranados, N., Dick, D. M., Eriksson, J. G., Farrer, L. A., Foroud, T. M., Gillespie, N. A., Goate, A. M., Goldman, D., Grucza, R. A., Hancock, D. B., Harris, K. M., Heath, A. C., Hesselbrock, V., Hewitt, J. K., Hopfer, C. J., Horwood, J., Iacono, W., Johnson, E. O., Kaprio, J. A., Karpyak, V. M., Kendler, K. S., Kranzler, H. R., Krauter, K., Lichtenstein, P., Lind, P. A., McGue, M., MacKillop, J., Madden, P. A. F., Maes, H. H., Magnusson, P., Martin, N. G., Medland, S. E., Montgomery, G. W., Nelson, E. C., Nöthen, M. M., Palmer, A. A., Pedersen, N. L., Penninx, B. W. J. H., Porjesz, B., Rice, J. P., Rietschel, M., Riley, B. P., Rose, R., Rujescu, D., Shen, P.-H., Silberg, J., Stallings, M. C., Tarter, R. E., Vanyukov, M. M., Vrieze, S., Wall, T. L., Whitfield, J. B., Zhao, H., Neale, B. M., Gelernter, J., Edenberg, H. J., Agrawal, A., & andMe Research, T. (2018). Transancestral GWAS of alcohol dependence reveals common genetic underpinnings with psychiatric disorders. *Nature Neuroscience, 21*(12), 1656-1669. https://doi.org/10.1038/s41593-018-0275-1

Wang, F., Xu, H., Zhao, H., Gelernter, J., & Zhang, H. (2016). DNA co-methylation modules in postmortem prefrontal cortex tissues of European Australians with alcohol use disorders. *Scientific reports, 6,* 19430. https://doi.org/10.1038/srep19430

Watanabe, K., Stringer, S., Frei, O., Umićević Mirkov, M., de Leeuw, C., Polderman, T. J. C., van der Sluis, S., Andreassen, O. A., Neale, B. M., & Posthuma, D. (2019). A global overview of pleiotropy and genetic architecture in complex traits. *Nature Genetics, 51*(9), 1339-1348. https://doi.org/10.1038/s41588-019-0481-0

Willer, C. J., Li, Y., & Abecasis, G. R. (2010). METAL: fast and efficient meta-analysis of genomewide association scans. *Bioinformatics, 26*(17), 2190-2191. https://doi.org/10.1093/bioinformatics/btq340

Wirth, A. (2010). Rho kinase and hypertension. *Biochimica et Biophysica Acta (BBA) - Molecular Basis of Disease, 1802*(12), 1276-1284. https://doi.org/10.1016/j.bbadis.2010.05.002

Witt, S. H., Frank, J., Frischknecht, U., Treutlein, J., Streit, F., Foo, J. C., Sirignano, L., Dukal, H., Degenhardt, F., Koopmann, A., Hoffmann, S., Koller, G., Pogarell, O., Preuss, U. W., Zill, P., Adorjan, K., Schulze, T. G., Nöthen, M., Spanagel, R., Kiefer, F., & Rietschel, M. (2020). Acute alcohol withdrawal and recovery in men lead to profound changes in DNA methylation profiles: a longitudinal

clinical study. *Addiction, 115*(11), 2034-2044. https://doi.org/10.1111/add.15020

World Health Organization. (2019). *Global status report on alcohol and health 2018*. World Health Organization.

Yen, C. H., Ho, P. S., Yeh, Y. W., Liang, C. S., Kuo, S. C., Huang, C. C., Chen, C. Y., Shih, M. C., Ma, K. H., Sung, Y. F., Lu, R. B., & Huang, S. Y. (2017). Differential cytokine levels between early withdrawal and remission states in patients with alcohol dependence. *Psychoneuroendocrinology, 76*, 183-191. https://doi.org/10.1016/j.psyneuen.2016.10.015

Zeilinger, S., Kühnel, B., Klopp, N., Baurecht, H., Kleinschmidt, A., Gieger, C., Weidinger, S., Lattka, E., Adamski, J., Peters, A., Strauch, K., Waldenberger, M., & Illig, T. (2013). Tobacco Smoking Leads to Extensive Genome-Wide Changes in DNA Methylation. *PLoS One, 8*(5), e63812. https://doi.org/10.1371/journal.pone.0063812

Zhang, D., Sun, M., Samols, D., & Kushner, I. (1996, Apr 19). STAT3 participates in transcriptional activation of the C-reactive protein gene by interleukin-6. *Journal of Biological Chemistry, 271*(16), 9503-9509. https://doi.org/10.1074/jbc.271.16.9503

Zhao, J., Qi, Y.-F., & Yu, Y.-R. (2021). STAT3: A key regulator in liver fibrosis. *Annals of Hepatology, 21*, 100224. https://doi.org/https://doi.org/10.1016/j.aohep.2020.06.010

Zhen, L., Shao, T., Luria, V., Li, G., Li, Z., Xu, Y., & Zhao, X. (2018). EphB2 Deficiency Induces Depression-Like Behaviors and Memory Impairment: Involvement of NMDA 2B Receptor Dependent Signaling [Original Research]. *Frontiers in Pharmacology, 9*, 862. https://doi.org/10.3389/fphar.2018.00862

Zhou, H., Sealock, J. M., Sanchez-Roige, S., Clarke, T.-K., Levey, D. F., Cheng, Z., Li, B., Polimanti, R., Kember, R. L., Smith, R. V., Thygesen, J. H., Morgan, M. Y., Atkinson, S. R., Thursz, M. R., Nyegaard, M., Mattheisen, M., Børglum, A. D., Johnson, E. C., Justice, A. C., Palmer, A. A., McQuillin, A., Davis, L. K., Edenberg, H. J., Agrawal, A., Kranzler, H. R., & Gelernter, J. (2020). Genome-wide meta-analysis of problematic alcohol use in 435,563 individuals yields insights into biology and relationships with other traits. *Nature Neuroscience, 23*(7), 809-818. https://doi.org/10.1038/s41593-020-0643-5

Zhou, Z., Yuan, Q., Mash, D. C., & Goldman, D. (2011). Substance-specific and shared transcription and epigenetic changes in the human hippocampus chronically exposed to cocaine and alcohol. *Proceedings of the National Academy of Sciences of the United States of America, 108*(16), 6626-6631. https://doi.org/10.1073/pnas.1018514108

Zillich, L., Frank, J., Streit, F., Friske, M. M., Foo, J. C., Sirignano, L., Heilmann-Heimbach, S., Dukal, H., Degenhardt, F., Hoffmann, P., Hansson, A. C., Nöthen, M. M., Rietschel, M., Spanagel, R., & Witt, S. H. (2022). Epigenome-wide association study of alcohol use disorder in five brain regions.

Neuropsychopharmacology, 47(4), 832-839. https://doi.org/10.1038/s41386-021-01228-7

7 RELATED PUBLICATIONS

Zillich, L., Poisel, E., Frank, J., Foo, J. C., Friske, M. M., Streit, F., Sirignano, L., Heilmann-Heimbach, S., Heimbach, A., Hoffmann, P., Degenhardt, F., Hansson, A. C., Bakalkin, G., Nöthen, M. M., Rietschel, M., Spanagel, R., & Witt, S. H. (2022). Multi-omics signatures of alcohol use disorder in the dorsal and ventral striatum. Transl Psychiatry, 12(1), 190. https://doi.org/10.1038/s41398-022-01959-1

Zillich, L.*, Poisel, E.*, Streit, F., Frank, J., Fries, G. R., Foo, J. C., Friske, M. M., Sirignano, L., Hansson, A. C., Nöthen, M. M., Witt, S. H., Walss-Bass, C., Spanagel, R., & Rietschel, M. (2022). Epigenetic Signatures of Smoking in Five Brain Regions. J Pers Med, 12(4). https://doi.org/10.3390/jpm12040566

Zillich, L., Frank, J., Streit, F., Friske, M. M., Foo, J. C., Sirignano, L., Heilmann-Heimbach, S., Dukal, H., Degenhardt, F., Hoffmann, P., Hansson, A. C., Nöthen, M. M., Rietschel, M., Spanagel, R., & Witt, S. H. (2022). Epigenome-wide association study of alcohol use disorder in five brain regions. Neuropsychopharmacology, 47(4), 832-839. https://doi.org/10.1038/s41386-021-01228-7

Wedemeyer, F.*, Kaminski, J. A.*, **Zillich, L.,** Hall, A. S. M., Friedel, E., & Witt, S. H. (2020). Prospects of Genetics and Epigenetics of Alcohol Use Disorder. Current Addiction Reports, 7(4), 446-452. https://doi.org/10.1007/s40429-020-00331-x

*shared first authorship

8 CURRICULUM VITAE

PERSONALIEN

Name und Vorname: Lea Sigrid Silke Zillich

Geburtsdatum: 30.09.1994

Geburtsort: Heidelberg

SCHULISCHER WERDEGANG

(2004) – (2012)	Alexander-von-Humboldt Gymnasium Konstanz
19.06.2012	Abitur

UNIVERSITÄRER WERDEGANG

WS2013/14	Beginn des Bachelorstudiums Theaterwissenschaft an der Ludwig-Maximilians-Universität München
WS2014/2015	Beginn des Bachelorstudiums Psychologie an der Universität Mannheim Bachelorarbeit: *Entwicklung und Validierung des Identitätsfragebogens bei Depressionen*
WS2016/2017	Auslandssemester an der Drexel University Philadelphia, PA, USA
19.06.2017	Bachelor of Science, Note: 1,8
WS2017/2018	Beginn des Masterstudiums Kognitive und Klinische Psychologie an der Universität Mannheim Masterarbeit: *Changes in Internalized Stigma during Cognitive-Behavioral-Therapy*
17.07.2019	Master of Science, Note: 1,4

BERUFLICHER WERDEGANG

08/2022 – 12/2022	Forschungsaufenthalt am National Institute on Alcohol Abuse and Alcoholism (NIAAA) in Bethesda, MD, USA
Seit 09/2019	Wissenschaftliche Mitarbeiterin (Doktorandin) in der Abteilung für Genetische Epidemiologie in der Psychiatrie am Zentralinstitut für Seelische Gesundheit
09/2017-09/2019	Studentische Hilfskraft in der Abteilung für Genetische Epidemiologie in der Psychiatrie am Zentralinstitut für Seelische Gesundheit
03/2015-07/2017	Studentische Hilfskraft am Zentrum für Psychologische Psychotherapie Mannheim

9   DANKSAGUNG